UNIVERSITY OF OKLAHOMA

GRADUATE COLLEGE

OPTIMIZING WETTABILITY TO MAXIMIZE PRODUCTION FROM RETROGRADE CONDENSATE RESERVOIRS – A SIMULATION APPROACH

A THESIS

SUBMITTED TO THE GRADUATE FACULTY

in partial fulfillment of the requirements for the

Degree of

MASTER OF SCIENCE

By

MAXINE WEISS
Norman, Oklahoma
2017

OPTIMIZING WETTABILITY TO MAXIMIZE PRODUCTION FROM RETROGRADE CONDENSATE RESERVOIRS – A SIMULATION APPROACH

A THESIS APPROVED FOR THE
MEWBOURNE SCHOOL OF PETROLEUM AND GEOLOGICAL ENGINEERING

BY

_____
Dr. Mashhad Fahs, Chair

_____
Dr. Catalin Teodoriu

_____
Dr. Ahmad Jamili

For Heather and Max,

Dawson, Isabelle and Eden,

Ian, Colin, Dylan and Natalie,

Gilderoy, Wally and Oma.

Acknowledgements

I would like to express my deepest gratitude to my committee chair and mentor, Dr. Mashhad Fahs, for three years of guidance and friendship over the course of my undergraduate and graduate research at this amazing University. Words cannot adequately describe how inspirational it has been for me to work under such a fabulous female role model in a program and industry where numbers overwhelmingly favor the opposite sex. I couldn't have asked for a more understanding individual to collaborate with or a more similarly dispositioned person that shared and respected my work habits, thought processes, and professional goals.

I would also like to acknowledge my committee members, Dr. Jamili and Dr. Teodoriu, for their patience and expertise, as well as the other world-class professors across numerous departments that I've had the benefit of working with over the course of the past five years.

Finally, I would like to thank the many friends I have made here who allowed this native Floridian to fall in love with the oil business and Oklahoma. We arrived here from different states, with different backgrounds, but our passion for this industry and regard for one another will remain a commonality between us for many years to come.

Table of Contents

List of Tables

List of Figures

Abstract

It is well documented that significant production loss can be expected when regions of a retrograde condensate reservoir fall below the dew point, leading to liquid banking around the wellbore. Several methods have been utilized in industry for quite some time that can alleviate this productivity loss for a temporary period, but the viability of permanent wettability alteration in the near-wellbore region has been steadily improving in recent years. Through these treatments, the affected zone around the wellbore can adopt a more favorable relative permeability schema than the natural liquid-wetting nature of most reservoir rocks. A simulation study of the effect of wettability alteration in retrograde condensate reservoirs was undertaken in order to understand the relative economic and total recovery benefits of strongly gas-wetting treatments and intermediate gas-wetting treatments over this undesirable natural state.

A radial reservoir model was built using CMG Builder and three different retrograde condensate reservoir fluid models were created using WINPROP. Numerous simulation runs were conducted on each of the fluid-reservoir model combinations to assess the impact of absolute permeability and treatment zone wettability. Aside from these primary cases, other facets of production were examined for specific permeability-fluid combinations to understand the interplay of time step size, treatment radius and rate of return on the outcome of the simulation case. Of the 27 primary cases analyzed in this study, the intermediate gas-wetting treatment was found to be the optimal option regardless of absolute permeability or fluid composition. Treatment radius was also shown to have a significant impact on production improvement but the added cost of these larger treatments is often not worth the incremental production gains.

Chapter 1: Introduction

1.1 Problem Overview

Though the oil and gas industry typically conjures images of thick, black oil or simple, dry gas to the layman, the petroleum engineer knows that hydrocarbon reservoir fluids comprise a spectrum with near-infinite combinations of liquids, gases and impurities. The following study was undertaken to understand reservoir conditions that affect production from a specific compositional range of these hydrocarbon fluids known as 'retrograde condensates', so named for their tendency to revert from the gas phase to the oil phase and back to gas under conditions of isothermal pressure depletion.

The characteristic "condensate banking" phenomenon that typifies this type of reservoir fluid presents an obstacle to production in most cases that can only be solved with pressure support or chemical injection of fluids into the near-wellbore region. There are a variety of chemicals that can transform the natural wettability state of a reservoir to water-wetting from oil-wetting or from liquid-wetting to gas-wetting depending on the desired effect. Reservoir rock is completely liquid-wetting by nature, which explains the production issues that arise in a gas reservoir with a ring of condensate around the wellbore. When the fluid saturation increases, the permeability to gas decreases, thus having a negative impact on the well's overall production. One might think that a treatment resulting in a completely gas-wet system would allow for the passage of the condensate bank and promote the optimal production, but past research in this area suggests that the actual optimal scenario is an intermediate-wetting state between gas and liquid. The study in question, Zoghbi et al. (2010), utilized a reservoir model created in

CMG and a retrograde fluid composition in WINPROP to understand the best wettability conditions for different values of initial reservoir pressure, treatment radius, and permeability. It concluded that, not only was the intermediate-wetting phase more desirable in terms of production over the gas-wetting phase, but that the benefits of the treatment were more pronounced in reservoirs with relatively low permeability and lower reservoir pressure. The impact of an increased treatment radius was not as pronounced.

The fact that it is possible to "over-treat" a reservoir by making it too gas-wetting is particularly significant in this economic climate because operators are seeking to minimize the cost of any sort of treatment to their wells. Exceeding the ideal injection threshold of any type of wellbore wettability-altering treatment would not only reduce the ultimate production from the reservoir but the excess chemical costs would certainly be an additional waste of capital. The simulation study discussed in the subsequent chapters expands upon previous work in this area by evaluating multiple retrograde fluid compositions ranging from rich condensates to lean condensates. Based on the physics of the differing reservoir fluids it was anticipated that the intermediate wettability scenario would show the most production improvement for the rich case and the least improvement for the lean case. The radial CMG reservoir model depicted in Zoghbi et al. (2010) was the basis for the study described here so that there would be an equivalent metric for comparison. Simulation studies, though they have some drawbacks, are ideal for this type of work because they allow the engineer a level of control which is simply impossible in the field, or even a secure laboratory setting. All reservoir properties, save the desired variable, can remain constant to develop a firm grasp on the scale of the impact that a single factor can have on production volumes. Lastly, the study always seeks to place

every outcome in the context of industry, because academic revelations that are never put into practice in the field are of little benefit to society.

1.2 Significance to Industry

In a booming industry where WTI oil is priced at $100/bbl, short term gains are often made at the expense of cost-saving methods and procedural efficiencies. In such prosperous times it is not uncommon to drill unnecessary wells in producing fields simply to keep a rig occupied until its contracted term has expired. Poor engineering practices and inattention to detail are acceptable modes of operation because even a marginal well drilled in a mediocre geological prospect can result in a net profit for the company when oil price is high. Projects presenting higher risk are also acceptable with the associated potential for significant gains or significant losses, because in the end, elevated oil prices are capable of recouping the occasional failed endeavor.

However, ours is a cyclical industry and the $50/bbl oil price that the market is currently experiencing following the downturn of mid-2014 is not nearly as forgiving; new ventures are frequently passed over in favor of tried-and-true methods and safer investments. More care is taken with each and every decision, from casing design to landing zone because lower activity levels and slashed budgets create the time and sense of urgency that is crucial for success. Success, in this case, being defined as the execution of the development strategy that will result in the highest ultimate recovery and long-term financial gain.

This explains the importance of understanding the impact of wettability alteration on the productivity and profit garnered from retrograde condensate reservoirs, where the

economics are all the more formidable. Oil products are often used to create fuel for transportation, but natural gas, along with coal, is the primary driver of the generation of electricity in power plants. Population growth and urbanization will ensure that global electric requirements will rise for many generations to come. That being said, current natural gas prices in the domestic market are approximately $3.20/MSCF while condensate prices typically run between 40 and 50 percent of the price of oil. Yet despite this historic trend, the value gap between natural gas liquids and oil has begun to shrink recently, in large part due to our increased ability to export propane and butane (NGI 2017). Liquefied natural gas (LNG), formed from methane and ethane, is another important subset of production from dry gas and gas condensate wells which only occupies about $1/600^{th}$ of the volume as those same compounds in the gas phase (Shell 2015). As technology transportation continues to develop, LNGs too will increase in price as international markets, primarily in Asia, become available to American product. Unlike the oil market, which has a fairly unified price internationally, the natural gas and LNG markets are much more localized due to the difficulty of transportation. So, while the gas price may not be conducive to a condensate well in the United States at a particular point in time, the Russians sell natural gas to Europe at a price that is 10 times higher than that of the United States, and Indonesian LNG prices in Japan are currently almost 20 times higher than the domestic price (Egypt Data Portal 2017). We can gather from this data that gas condensate wells have tremendous potential to be profitable in multiple areas of the globe.

Understanding reduces risk and uncertainty and allows projects to be considered that might previously have been passed over for other prospects, and a diversified

portfolio composed of all manner of fluid types is paramount to business health; take the Eagle Ford Shale for example. Reservoir fluid type is tied to thermal maturity. Higher thermal maturity is associated with higher gas content and greater depth. In a low-permeability reservoir, fluids remain stratified in their locations of formation (oil at the top and gas at the bottom), whereas in a more permeable formation fluid types tend to align themselves by specific gravity (gas at the top and oil at the bottom).

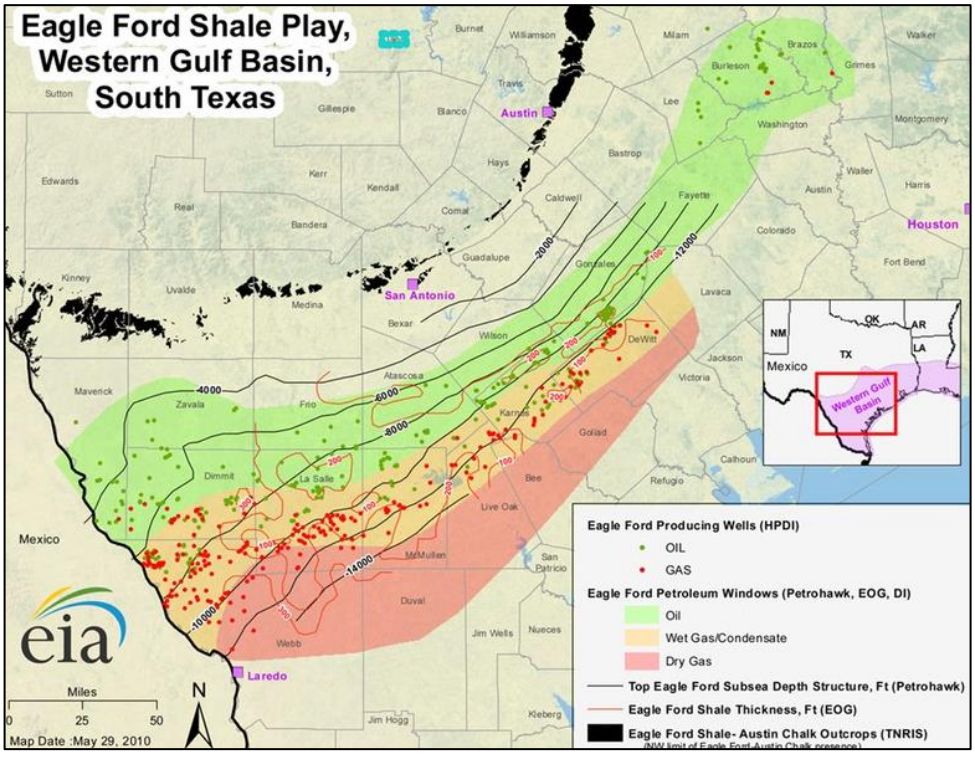

Figure 1. Map of Eagle Ford Shale play (Western Gulf Basin, South Texas) highlighting various fluid windows and well types (EIA 2010)

The Eagle Ford's low permeability has preserved three well-defined fluid windows, with an oil window up-dip followed by a condensate window and a gas window in its deepest location as seen in **Fig. 1**. In order for valuable condensate to be extracted from that window, the rock-fluid interactions that govern production must be thoroughly

described and predictable. Then again, our domestic, low-permeability oil systems represent only one piece of the puzzle. The Middle East is typified by particularly high permeability systems, which have very different flow characteristics than low permeability reservoirs. This discrepancy underscores the need for careful consideration when planning oilfield operations.

1.3 Chapter Summaries

Chapter 2 begins with a detailed introduction to the terminology used throughout the study and continues with a discussion of the literature pertaining to the various advances that have been made in this subject in the past. Chapter 3 then beings with an overview of the reservoir and fluid models, simulation input parameters and the methods followed for the execution of the simulation runs. It ends with a note on the various assumptions made over the course of the study so that the limitations are made clear. Chapter 4 contains the analysis portion of the study and the bulk of the figures which serve to illustrate the relationship between the numerous variables that have been assessed, including fluid composition, time step size, treatment radius, reservoir radius, and a discussion of economics. Finally, Chapter 5 summarizes the main conclusions that can be drawn from the study and makes suggestions for future work in this area. Appendices A and B include additional tables and figures respectively. Also, Appendices C and D include a description of some of the nomenclature and abbreviations used throughout the work for quick reference.

Chapter 2: Fundamental Concepts

2.1 Background Information

One of the most basic ways in which a petroleum reservoir can be classified is by its fluid type. Regardless of rock type, reservoir fluids are often described by two inextricably linked properties: chemical composition and phase behavior. The chemical composition often involves hydrocarbons chains (such as alkanes and alkenes), aromatics (like benzene), impurities (like hydrogen sulfide, brine, nitrogen, and carbon dioxide), as well as resins and asphaltenes. On the other hand, phase behavior describes the PVT (pressure, volume and temperature) relations that affect the physical state of the chemical compounds, namely the solid, liquid and gaseous phases. Petroleum engineers are primarily concerned with the manner in which the isothermal decreases in pressure that a fluid experiences, from reservoir to wellbore, and wellbore to surface, will affect the production of liquid and gas from the well. These relationships are not entirely intuitive because phase changes of multi-component systems are path-dependent. Though two petroleum systems may contain identical fluids and initial pressures and temperatures, if they reach the same endpoint pressure at different rates they may conclude with different fluid compositions.

2.1.1 Phase Behavior

A common visual used to describe the phase behavior of a particular fluid composition is the PT (pressure-temperature) phase diagram; an example for a retrograde condensate reservoir is shown in **Fig. 2** on the following page.

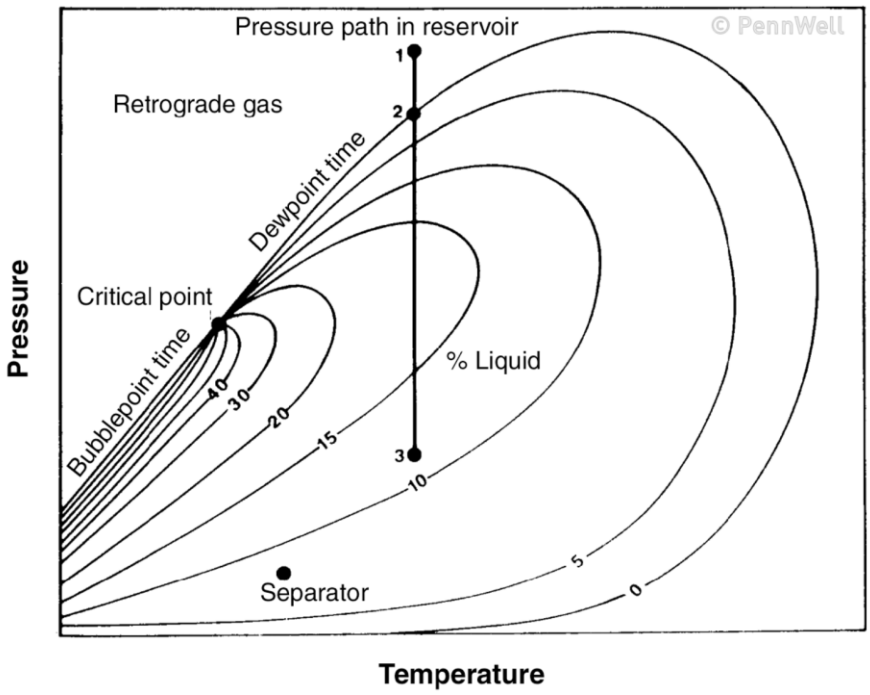

Figure 2. Phase diagram for retrograde condensate reservoir fluid (McCain 1990)

The critical point labeled above is located at the specific temperature and pressure at which the liquid and gaseous phases of the fluid are indistinguishable. Fluids outside of the curved envelope are at a single phase, and those inside are a mixture of liquid and gas phases. Reservoir processes are essentially isothermal, meaning constant temperature, so the path of a fluid from reservoir to wellbore can be represented by a vertical line, say from point 1 to point 3 in the Fig. 2. An isothermal process that crossed the bubble point line would mean that the fluid began as a liquid, and after crossing the bubble point line into the 2-phase envelope, it would begin to experience the emergence of gas from the solution. An isothermal process that crossed the dew point line (point 2) would mean that the fluid began as a gas, and after crossing the dew point line into the 2-phase envelope, liquid would begin to condense from the vapor. The result, in both cases, is a reservoir with more than one phase of hydrocarbons, which can prove to b e a complication to

production. The curved lines within the 2-phase envelope can be used to approximate the relative proportions of liquid and gas.

The transition from reservoir temperature and pressure to surface temperature and pressure is not isothermal, and involves a reduction in both properties which is evident in Fig. 2 at the point labeled ‘separator’ (which is a type of surface equipment). The curved lines within the phase envelope represent different fluid fractions, and because the isothermal pathway from reservoir PT to wellbore PT (point 1 to point 3) crosses the 15% fluid line more than once, this suggests that the liquid fraction shifts from increasing to decreasing. This explains the relevance of the term “retrograde” in the retrograde condensate classification.

Aside from their unique phase behavior, gas condensates may also be characterized by fluid properties such as the yield (ratio of produced oil volume to produced gas volume), density (API gravity), and C^{7+} fraction (percent weight of fluid attributed to hydrocarbons at least as heavy as heptane). The variability in condensate properties is compounded by the fact that the composition is actually a dynamic characteristic; the gas produced from condensate reservoirs becomes leaner and less valuable as time passes. The complexities in phase behavior that this fluid type can exhibit often lead to their exclusion from oil and gas operations. However, in-situ fluid samples obtained via well-testing can be analyzed in petrophysical labs using flash vaporization tests or differential liberation tests to better understand phase behavior relationships and make informed engineering decisions.

2.1.2 Condensate Banking

Before a well has been drilled, a reservoir with consistent elevation can usually be assumed to have a uniform reservoir pressure. However, as soon as the wellbore has been drilled and completed there exists a locus of pressure reduction that has an impact on every part of the reservoir with which it has hydraulic communication. Generally, reservoir pressure is constant at points of equal distance from the wellbore. This phenomenon can be conceptualized as a ring of constant pressure for a vertical well or parallels of constant pressure for a horizontal well. Fluid flow occurs in the direction from areas of high pressure (reservoir periphery) to areas of low pressure (wellbore). For simplification purposes the reservoir engineer often represents the reservoir pressure as a constant average pressure rather than as a function of distance.

Figure 3 portrays the reservoir pressure trend at a single point in time, with r_w representing the radius of the wellbore at left and r_e representing the effective radius of the reservoir at right. In the case of condensate reservoirs, the pressure at the reservoir boundary may place that portion of fluid in the gas phase, but as the fluid moves towards the wellbore it passes below the dew point pressure in red and forms a 2-phase region of radius r_{CD} known as a "condensate bank".

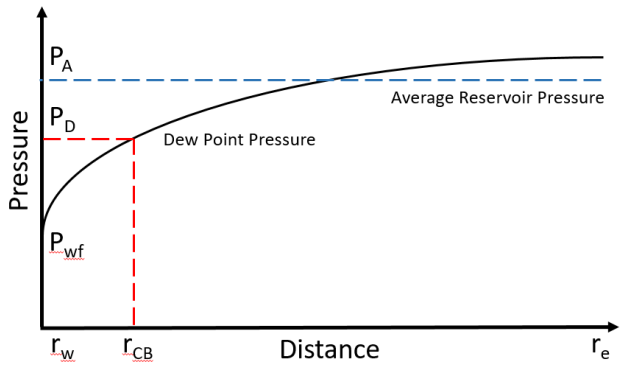

Figure 3. Reservoir pressure as a function of distance from wellbore

Phase behavior is important to retrograde condensates because of the reservoir's proximity to the dew point line. Single phase oil or gas reservoirs are much simpler to model and quantify reserves from, whereas condensates have a composition that actually varies with distance. The severity of this effect can increase as the permeability of the reservoir decreases because less fluid dropout is required to block the pore throats.

2.1.3 Relevant Reservoir Properties

The absolute permeability of a reservoir is a measure of the rock's flow capacity and is most closely correlated to the size of the pore throats, which act as a "bottleneck" of sorts to the flow of fluid from pore to pore. Pore throat size is a function of numerous rock properties including, but not limited to: mineral composition, diagenesis, lateral stresses, and compaction. All else remaining constant, a reservoir with a higher permeability will result in a well with a higher flow rate than a reservoir with lower permeability. The presence of natural or induced fractures can enhance reservoir permeability by providing additional, larger conduits for fluid flow.

Darcy's law is a common equation in petroleum engineering that is often used to calculate permeability, from a core sample for example, if certain other parameters are known. **Equation 1** relates Darcy's law, with flow rate (q) in cm^3/s, cross-sectional area (A) in cm^2, permeability (k) in darcies, viscosity (μ) in cp, pressure change (dP) in atm, and length (dl) in cm.

$$v = \frac{q}{A} = \frac{k}{\mu}\left(\frac{dP}{dl}\right) \quad (1)$$

An important distinction is made between absolute permeability and effective permeability, the former used in the context of a single-phase system, the latter used with

regards to multi-phase systems. The effective permeability of a fluid is always lower than its absolute permeability would be in a single-phase situation. More common than the effective permeability is the relative permeability, which is the ratio of the effective permeability to the absolute permeability. These ratios can be described in terms of fluid relationships, such as oil to gas or oil to water, or in terms of state relationships, such as liquid to gas.

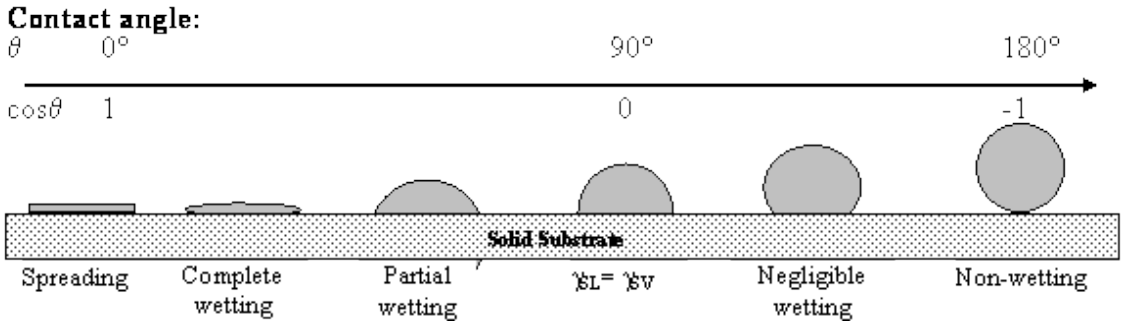

Figure 4. The full spectrum of wettability relationships (Njobuenwu 2016)

In order to fully comprehend the concept of relative permeability, a discussion of wettability and capillary pressure is required. The term wettability is used to express the relative affinity or adhesion a certain fluid or gas may have with a solid surface. It is a function of the molecular forces between the surface and liquid. If a rock is called 'water-wetting', then a drop of water placed on that surface will tend to spread onto that surface and form an acute contact angle while a drop of oil may form a bead of liquid on that surface with an obtuse contact angle, as shown in **Fig. 4**. To complicate matters further, fluids flowing to a well are not stationary, which means that a fluid droplet will then have both an advancing and receding contact angle. These properties can be studied in combination imbibition-drainage experiments on core. Most reservoirs can be considered water-wetting over oil-wetting (with the exception of some carbonate reservoirs), and

liquid-wetting over gas-wetting. Gas-wetting surfaces in this context are always the result of chemical additives. Wettability forces are partially responsible for dictating the flow of fluids through porous media because they tend to impede the flow of the wetting phase by trapping it against the rock surface, and likewise tend to promote the flow of the non-wetting phase through the reservoir.

This phenomenon leads to a consideration of the capillary forces acting in a reservoir. Capillary pressure is a function of the complex interactions between the physical structure of the reservoir rock and geochemistry of its components. It may be defined as the difference between the pressure of the non-wetting and wetting phases, such as in **Eq. 2**, where capillary pressure (P_{cog}), oil phase pressure (p_o), and gas phase pressure (p_g) carry the same pressure units.

$$P_{cgo} = p_g - p_o \tag{2}$$

The labyrinthine network of pores and pore throats that make up a reservoir rock are irregular and tortuous, but they may be simplified conceptually to a set of many capillary tubes, in which case the capillary pressure can be expressed using **Eq. 3**. Equation 3 states that capillary pressure (p_c) in dynes, is a function of the interfacial tension (γ) in dynes/cm^2, contact angle (θ) in radians, and the radius of the capillary tube (r_c) in cm.

$$p_c = \frac{2\gamma \cos(\theta)}{r_c} \tag{3}$$

Lab measurements using mercury injection are the most common method of determining the capillary pressure characteristics of a rock sample, though the centrifuge and porous-plate methods can be used as well. Mercury is injected into the core at increasing pressure, invading the larger passageways first and the smallest passageways

last. Furthermore, steady-state laboratory measurements of relative permeability involve the simultaneous injection of the two fluids or phases in question at constant rates, and the measurement of the resultant proportions of produced fluids.

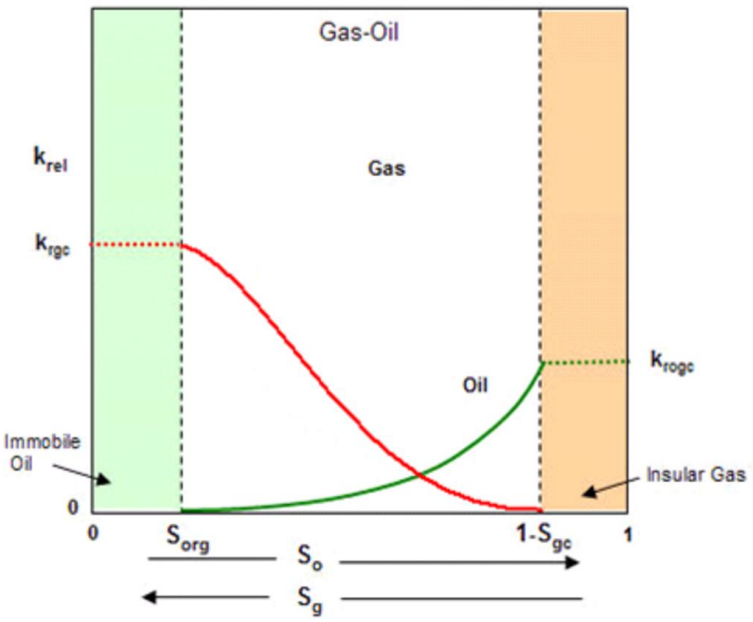

Figure 5. Oil-gas relative permeability curves (Fekete 2016)

Figure 5 includes a sample set of relative permeability curves, a concise synthesis of the information obtained from relative permeability (k_{rel}) and capillary pressure data. The y-axis is in units of fluid saturation, a dimensionless value used to describe the relative proportion of the pore spaces occupied by a certain fluid. The critical gas saturation (S_{cg}) represents the minimum gas saturation required for gas flow while the residual oil saturation (S_{rog}) is the lowest possible saturation of oil that can be obtained from the rock. A lower residual oil saturation means that a higher proportion of the oil volume at least has the potential to be recovered. These end-point saturation values are particularly vital to the execution of secondary recovery methods, such as water-flooding,

or WAG-flooding, which are implemented when the reservoir pressure is no longer sufficient to lift the fluid to the surface.

Equations 4 and 5 are known as the Brooks-Corey power law correlations for a two-phase oil and gas system, with dimensionless relative permeability (k_{rg}, k_{ro}), dimensionless maximum relative permeability (k_{rg}^{max}, k_{ro}^{max}), and oil and gas saturation (S_o, S_g) expressed as fractions, critical oil and gas saturation (S_{oc}, S_{gc}) expressed as fractions, and the dimensionless oil and gas Corey exponents (n_o, n_g). These equations are used by simulation software to interpolate a curve between a given set of endpoint saturations. The exponents range from n = 1 to 6, with an exponent of 1 resulting in a straight-line relationship and an exponent of 6 resulting in the most curvature (Corey 1954).

$$k_{rg} = k_{rg}^{max}\left(\frac{S_g - S_{gc}}{1 - S_{gc} - S_{oc}}\right)^{n_g} \quad (4)$$

$$k_{ro} = k_{ro}^{max}\left(\frac{S_o - S_{oc}}{1 - S_{gc} - S_{oc}}\right)^{n_o} \quad (5)$$

Both the red and green lines in Fig. 5 illustrate that as the saturation of a phase decreases, so does the relative permeability of that phase. In a retrograde condensate reservoir, the formation is initially entirely saturated with gas, but as soon as the condensate bank forms around the wellbore, there exists an increased liquid saturation that intensifies the longer production lasts. It follows that the relative permeability of the gas to the oil will decrease with increasing proximity to the wellbore, which may or may not pose challenges to production and economics. These facts demonstrate the significance of rock-fluid interactions in a retrograde condensate reservoir.

2.1.4 Methods of Altering Wettability and Mitigating Condensate Blockage

Condensate formation in the near-wellbore region can certainly impede production by causing formation damage, ultimately constraining flow and harming well productivity. The pseudo-skin caused by the banking effect can also result in further economic loss because the heavier liquid fraction may be permanently trapped in the reservoir because its permeability to gas is too low. An ideal scenario would likely involve producing the entire reservoir in the gas phase and allowing the liquid fraction to drop out in the surface equipment to avoid trapping it down hole. One must also consider that a large amount of water is involved in the hydraulic fracturing process that has become commonplace for moderate to low-permeability reservoirs. Liquid-wetting reservoir rock likely means that a significant fraction of this fluid will fail to flow back.

There are a number of methods that an engineer can implement to postpone the onset of condensate banking by supporting the reservoir pressure at a value above the dew point, or by periodically removing the liquid after its formation. The cases in this study will focus on one variation of the above methods. Given that reservoir rock tends to be liquid-wetting over gas-wetting, the downhole situation is not naturally conducive to this desire to remove the condensate barrier. Thus, a need arises to alter the natural wettability state of the reservoir.

A state of super gas-wetting alteration is more difficult to achieve than intermediate gas-wetting, but can be achieved with the use of fluorosurfactant-modified nano-silica, which forms a coarse structure on the rock surface, which acts as a gas adsorption layer (Jin and Wang 2016). In general, a surfactant works by reducing the surface tension between the relevant phases. Our study seeks to understand the relative

merits of different degrees of wettability alteration and how they vary with condensate richness. A vast array of properties, in particular the severity of water salinity, can negatively impact the efficacy of a wettability-altering treatment, but the treatment to the model used in this study is considered completely effective for the purpose of simplification.

2.1.5 Simulations

In recent decades, the visualization of reservoir geometry and accuracy of production forecasting has been dramatically improved upon with the introduction of elaborate computer simulation software. A reservoir model design may be as simple as a monolayer with a single well or as complex as an amalgamation of numerous stratigraphic intervals, each with its own unique reservoir properties, spatial configurations, fluid saturations, and well completion characteristics. Models essentially work by converting the reservoir structure into a grid composed of many cells. A predetermined model duration is divided into many small times steps, and for each time step the pressure, saturation, and other flow properties of each cell are evaluated by the program based on the well's production constraints. Simple models are important tools for reservoir engineers because they allow the individual to explore the effect of any number of variables on production outcome. More complex models may allow for greater intricacy but this is usually at the expense of the desired, short run time.

While a production output value from a certain model may not be of the level of accuracy required to book reserves for the formation, it does allow the engineer to semi-quantitatively assess the impact of say, a ten percent reduction in porosity versus a five

percent reduction in permeability. Different methods of obtaining reservoir property data include well-logging, well-testing, core measurements, outcrop analysis, and data extrapolation from offset wells. Each technique and data type has an associated range of error. For example, one engineer might claim that a certain project is economic based on a well log interpretation. Be that as it may, a second engineer might use modeling and sensitivity analysis to conclude that even a two percent decrease in certain well-log parameters will render the project uneconomic. The error attributed to certain types of well-logs can often exceed the narrow two percent range determined by the second engineer, which suggests that the error associated with this project could be too high to risk an investment. For any project evaluation endeavor, once variable sensitivity has been established, a substantial amount of risk may be mitigated. In the case of this study, the sensitivity of production to variables such as fluid composition, absolute permeability, and wettability is explored in detail.

Nevertheless, renowned statistician George Box once said, "essentially all models are wrong, but some are useful" (Box 1976). Some engineers may be tempted to be distrustful of all modeling methods while others will overstate the applicability of their results. The conscientious engineer must take care to appropriately stress the benefits and limitations of their work. Even a seemingly insignificant model attribute such as grid type and cell size can have an appreciable effect on the model outcome when all other factors are held constant. Grid size is controlled by the level of refinement required for the modeling objective; in areas where pressure changes are very rapid, greater refinement is necessary for model stability (Hamoodi et al. 2001).

If the properties in one cell vary too dramatically from one time step to the next, the model will likely break or the results will be non-physical. Likewise, the selection of the minimum and maximum time step size is critical to model stability. Composition changes from cell to cell may be quite large in the early life of the well, requiring a small time step size, but after several months of production the rate of decline in production will likely decrease, meaning a larger minimum time step size will be adequate.

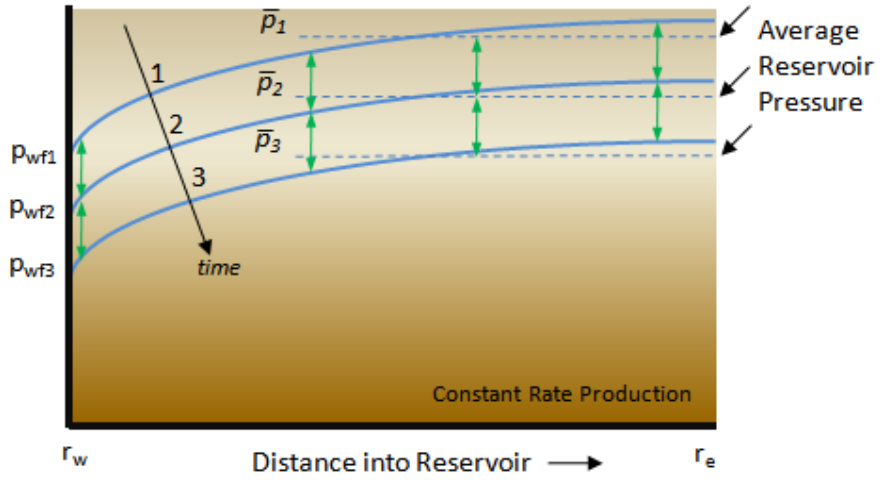

Figure 6. Pressure profile as a function of radius in a steady-state reservoir with a vertical well (Fekete 2016)

Take the pressure distribution in **Fig. 6** for example. The average reservoir pressure ($\bar{p}$) decreases with each successive time step because the reservoir becomes less charged as the volume of fluids removed increases. The time step lines are parallel because the reservoir has reached steady-state flow, where each reduction in bottomhole flowing pressure, p_{wf}, is instantaneously "felt" at every point in the reservoir. The pressure profile has the greatest curvature (largest change in pressure per unit distance) closest to the wellbore (r_w at left denotes the wellbore radius), which would require a smaller grid size to adequately portray in a modeling scenario.

2.2 Literature Review

The volume of literature on wettability optimization for a gas-condensate well is quite limited as it is a relatively new area of study, though information on methods of altering wettability and the impact of condensate banking on well productivity is abundant. Simulation studies are also fairly uncommon for a number of reasons. Modeling complex phase behavior interactions requires a great deal of processing power, but beyond this, production and condensate banking behavior varies dramatically from fluid to fluid, meaning that one cannot simply extrapolate the results of one model to the results of many other field cases. This uniqueness can be costly to operators because they may lack the time and capital to model cases for each variant of fluid they receive.

We are also beginning to understand that phase behavior in nano-porous media, the "shales" that have become the backbone of domestic oil production, deviates from the phase behavior we have come to expect from conventional reservoir rock. Because this shift in phase behavior due to ultra-confinement is not completely understood, it has yet to be applied to many commercial reservoir simulators. The tight permeability also creates a challenge in the laboratory setting. Without appropriate laboratory measurements, engineers have no reliable way to calibrate their model's specific rock-fluid interactions. Odusina et al. (2011) conducted a shale wettability study using nuclear magnetic resonance (NMR) to monitor the imbibition of brine and decane into Eagle Ford, Barnett, Floyd and Woodford core samples. The study concluded that shale wettability is affected by complex mineralogical content, tortuous pore structure, and the quantity and maturity of the organic content (TOC). NMR results suggested that both the

brine and decane phases exhibited surface relaxation after injection, which implies a state of mixed wettability supported by the oil-wetting organics and largely water-wetting mineral grains (Odusina et al. 2011).

Rock with permeability on the order of shales must be hydraulically fractured in order to be economic. Odusina et al. (2011) goes on to demonstrate that these shale samples, in a reservoir setting, would contribute to the loss of hydraulic fracturing fluid. This level of intricacy and complexity is not typically conducive to modeling in a business setting and explains why lower permeabilities were not explored in the modeling study detailed in later chapters.

2.2.1 Alleviation of Condensate Banking

Many condensate reservoirs are located in deep, hot, low-permeability reservoir rock which contributes to higher well cost. A typical corporate workflow in the evaluation of a condensate field might include five techniques to predict deliverability loss: laboratory testing, conversion of laboratory data to a relative permeability model, spreadsheet tools, single-well models and full-field models (Kamath 2007). Though laboratory studies may be plentiful in literature, studies that integrate laboratory, simulation and field results are scarce. Productivity improvement as a result of large slugs of CO_2 injection, "huff-n-puff" style, or even hydraulic fracturing, late in the life of the well can sometimes lead to positive economics but there is a great deal of uncertainty in the modeling of these treatment techniques. The composition of the in-situ fluid is constantly evolving, which means that the thermodynamic properties are likewise variable, so the simulation of gas injection would have to make some fairly substantial

assumptions. Hydraulic fracturing treatments can be designed prior to their execution with a specific goal of fracture dimensions in mind, but the engineer is rarely aware of their true geometry (Kamath 2007). Unlike these methods, permanent wettability alteration via the injection of fluoropolymers is a fairly straightforward process that would only involve the designation of different relative permeability curves to different sectors of the model.

Solvent injection, which works by multi-contact miscible displacement, has an added benefit over pressure support through gas cycling or hydraulic fracturing because there is little to no damage associated with this method (Sayed and Al-Muntasheri 2016). Hydraulic fracturing can increase the contact area between reservoir fluids and solids, which can postpone the problem of condensate dropout but often incurs formation damage in the form of skin (Noh and Firoozabadi 2008). This increased liquid saturation in the near-wellbore region leads to a larger two-phase high-velocity coefficient (β), which coincides with more restrictive flow; liquid-wetting rocks tend to have higher two-phase high-velocity coefficients as do rocks with higher immobile liquid fractions.

Wettability alteration to intermediate gas-wetting was shown by Noh and Firoozabadi (2008) to reduce the high-velocity coefficient. Rather than hamper the productivity of the near-wellbore zone with water-based frac fluid that reduces the relative permeability to oil and gas and increases the two-phase high-velocity coefficient, a fluoropolymer surfactant can be injected that permanently alters the wettability of the treatment zone and makes the effect of the increased near-wellbore condensate saturation on β less pronounced (Noh and Firoozabadi 2008). The effects of this method of wettability alteration will be modeled in the study that follows.

2.2.2 Permanent Wettability Alteration

While the improvement in core wettability from liquid- to intermediate gas-wetting is definitive from core measurements, correlating this positive change to new relative permeability curves poses some challenges. Gilani et al. (2011) has shown that wettability measurements can be quantitatively characterized through imbibition tests, drop tests, brine-compatibility tests, contact angle measurements, and x-ray photoelectron spectroscopy (XPS). Nevertheless, only qualitative interpretations of relative permeability changes can be adapted from these results so their use is best relegated to the realm of screening tools so that improper chemicals can be removed from consideration before expensive, high-pressure, high-temperature (HPHT) core-flooding is performed. Gilani et al. (2011) concluded that empirically derived correlations were the best method of predicting relative permeability changes based on laboratory measurements of wettability improvement; it was also determined that the change in wettability is directly related to the concentration of fluorine, which decreases as the distance from the core inlet increases.

Though surfactant usage has an enormous potential for wettability alteration, this category is so large and diverse that proper chemical selection is imperative for successful recovery. Polymeric fluorinated surfactants are effective at lowering the interfacial tension between water and condensate and water and gas, but are less effective at reducing this value in condensate-gas systems (Zheng et al. 2010). In a study of sandstone wettability that measured spreading coefficients (S) at ambient conditions, Zheng et al. (2010) found that productivity could be improved through the use of anionic surfactants,

but not nonionic surfactants. The spreading coefficient, simply another manner in which liquid-to-solid adhesion can be measured, lowers with the use of anionic surfactants.

Interestingly enough, Fahimpour and Jamiolahmady (2015) also compared the capabilities of both anionic and nonionic fluorinated wettability modifiers, but rather on carbonate rock samples, which are tested much less frequently than clastic samples. Based on contact angle measurements, unsteady state flow tests and brine compatibility tests, it was determined that the nonionic variant was most stable in brine and the anionic variant proved most apt at repelling the liquid phase. The study proffered that an ideal treatment would contain some optimal weight percentage of both of these chemicals. Though in some cases, filtration was required to prevent large chemical aggregates from plugging the core and reducing the permeability (Fahimpour and Jamiolahmady 2015).

Chemical suitability is dictated by both the rock and the fluid in question. Fahimpour et al. (2013) used outcrop rock samples and various synthetic, binary fluid systems to test the efficacy of a chemical on wettability alteration with varying fluid components. Contact angle measurements were able to show that the chemical under scrutiny was less oil-repellant against leaner gas compositions, which has major implications for the potential use of the chemical with low-yield condensates. Further evaluation determined that the interfacial tension, unique to a fluid composition, has a significant impact on the viability of surfactant treatment, with a reduction in the stability and effectiveness of chemical treatments to fluids with lower interfacial tension (Fahimpour et al. 2013).

Another factor of note is the impact of reservoir temperature on treatment success. The so-called “condensate window” in terms of hydrocarbon generation potential falls at

intermediate temperatures and pressures when compared with the cooler “oil window” and hotter “dry gas window”. This calls into question the appropriateness of ambient condition tests for fluorosurfactants when the actual reservoir environment will exhibit much more extreme temperatures and pressures. While many previous tests were limited to approximately 200°F, Fahes and Firoozabadi (2007) conducted tests at roughly 290°F on eight polymers composed of functional groups that adhere to rock surfaces as a result of acid-base interactions, which promote low free surface energy on the rock face. At higher temperatures, wettability treatments can become ineffective due to thermal decomposition, but this study demonstrated that permanent wettability alteration could be achieved through irreversible adsorption of the chemical onto the rock surface. Not only that, but the absolute permeability of the rock was not perceptibly affected by the chemical adsorption (Fahes and Firoozabadi 2007).

Finally, Jahanbakhsh et al. (2016) neatly summarizes the influence of fluid saturation and saturation history, pore structure and distribution, absolute permeability, and interfacial tension over wettability alteration. Tests are typically conducted on higher permeability rock because they are faster and therefore less expensive, but a problem emerges when one attempts to normalize these results to low permeability rock. The study concludes that relative permeability data from high permeability rock can be normalized to remove the effect of irreducible saturation. The relative permeabilities are then de-normalized and assigned to a rock type that is specific to the irreducible saturation of the low permeability rock (Jahanbakhsh 2016). The fact that this down-scaling method is possible is beneficial in that it may allow low permeability models to be simulated more accurately, but it does call into question the validity of such empirical workflows.

2.2.3 Simulation Studies of Condensate Fluids

Modeling is so beneficial to industry because it integrates diverse data types and simultaneously allows the engineer to simplify the behavior of systems that would otherwise be too complex to anticipate. An excellent example of this is the fact that the composition and marketability of produced gas tends to change over time, which makes a compositional simulator an ideal vehicle for predicting cash flows in a condensate well (Coskuner 1999). Composition varies not only with time but with distance from the wellbore because the fractions of liquid and gas phases are based on pressure, which likewise varies with distance from the wellbore. When the condensate drops out after the pressure falls below the dew point it spreads as a monolayer across the mineral surfaces while the excess forms into liquid lenses. Capillary number and relative permeability thus vary on a microscale (Coskuner 1999).

It follows that a fine grid and fully or adaptive implicit formulation may be required to adequately model the system, the cost of which may effectively remove it from the realm of possibility for many operators. Coskuner (1999) enumerates the challenges that the modeler of a retrograde condensate formation faces: the competing forces of inertia, viscosity, capillarity and gravity. The best results ensue when experimental data is used to create relative permeability curves and full-field scale models are calibrated using the results of single-well models, which are upscaled using pseudo-functions (Coskuner 1999).

The narrow economic margins of shale condensate reservoirs require further specifications. Flow in these environments deviates from Darcy flow to Knudsen flow, which describes the micro-flow through bundles of capillary tubes with a distribution of

pore sizes (Labed 2015). Knudsen flow is more impactful at low permeabilities and reservoir pressures and ignoring its effects in these situations can lead to an underestimation of well production, and likewise net present value (NPV), by up to 30%. This study is invaluable to the modeling of condensate behavior because it is one of few that factors in the impact of economics. Fracture spacing optimization can be very different depending on whether the end goal is to maximize profit or ultimate recovery, which may seem counter-intuitive. In general, higher gas prices lead to shorter fracture spacing design and higher NPV (Labed 2015).

The lower pressures exhibited in the fractures of these hydraulically stimulated wells are prone to condensate accumulation (Ganjdanesh et al. 2016). The lower productivity that results from this blockage is compounded by the residual water that fails to flow back from the hydraulic fracturing fluid. Ganjdanesh et al. (2016) performed a compositional modeling study that assessed the effectiveness of dimethyl ether (DME) as a temporary treatment method for condensate banking as opposed to methanol (MeOH) and ethanol (EtOH). DME was shown to be superior to the other options, not only in the speed of flow back but in gas recovery, improving the relative permeability in the treated zone by a factor of 2.5 (Ganjdanesh et al. 2016).

Delavarmoghaddam et al. (2009) acknowledges that the aforementioned solvent treatments and hydraulic fracturing are temporary fixes to a larger problem. This unique study is one of the first to simulate the effects of permanent wettability alteration on production from condensate reservoirs. The study uses a set of liquid-wetting relative permeability curves for the reservoir and an intermediate gas-wetting set of curves for the treatment zone. Two very similar sets of fluid compositions are compared, as well as

different connate water saturations and permeabilities including 1, 10 and 50 md. The study concludes that the treatment is somewhat effective in the relatively leaner case, has little to no effect on the richer case, and is most effective when there is no connate water saturation. It goes on to describe the contradictory trends that emerge in higher permeability reservoirs. In these cases, the larger pressure drop leads to a greater accumulation of condensate in the near-wellbore region. Higher permeability also leads to a high flow velocity which tends to sweep the area of fluid, leading to a reduction in fluid saturation near the wellbore. These two trends are obviously at odds and suggest that careful consideration must be taken in high permeability reservoirs that are more prone to blockage (Delavarmoghaddam et al. 2016).

Zoghbi et al. (2010) predates Delavarmoghaddam et al. (2016), but runs along a very similar vein and is the primary catalyst for the inception and design of this study. Though it only uses one, fairly intermediate fluid composition, it includes a set of relative permeability curves that correspond to a strong gas-wetting state which is mostly absent in the literature. The reservoir dimensions and properties for the majority of the runs conducted in this study were taken from Zoghbi et al. (2010). The paper concludes that the intermediate gas-wetting treatment leads to greater ultimate recovery than the strong gas-wetting and liquid-wetting curves in all permeability cases (1, 10, and 100 md). It continues by stating that initial reservoir pressure essentially has no effect on the performance of the different treatments, and a treatment radius of 30 ft is only slightly more effective than a treatment radius of 15 ft. Finally, the effect of the treatment is more pronounced in lower permeability reservoirs than in higher ones.

However, neither Zoghbi et al. (2010) nor Delavarmoghaddam et al. (2016) combine the analysis of multiple reservoir fluid compositions with differing degrees of wettability alteration and absolute permeability. A wider range of fluid compositions would prove more applicable to a greater variety of fields and enhance our knowledge of the interactions between the thermodynamic properties of hydrocarbons and their fluid mechanical characteristics. Economic considerations are also not factored into the determination of the optimal treatment in either study. The economic variables associated with the development of a well can be split into two main categories: expenses and credits. Expenses include drilling and completions costs, lease-operating expenses (LOE), production costs, taxes, and recurring transportation fees. Credits are more loosely defined as profit-promoting factors like the prices of the various hydrocarbon components, tax breaks, efficiencies, and reductions in service company prices. This study attempts to fill the aforementioned gaps in understanding.

Chapter 3: Methodology

3.1 Input Parameters

3.1.1 Reservoir Model

CMG software was used to create both the reservoir model and the fluid models, using the Builder module and Winprop module respectively. GEM served as the EOS compositional simulator. Parameters such as wellbore radius, reservoir radius, formation compressibility and porosity were taken from Zoghbi et al. (2010) in an effort to match the preliminary results from that paper to some test runs on the newly created model. A summary of the reservoir model input parameters is included in **Table 1**.

Table 1. CMG model reservoir properties

Property	Value
Reservoir Radius, ft	15,000
Wellbore Radius (Innermost Grid Radius), ft	0.33
Reservoir Top Depth, ft	8,000
Reservoir Thickness, ft	70
Initial Reservoir Pressure, psi	5,500
Porosity, %	12
Water Saturation, %	0
Formation Compressibility, psi^{-1}	$1x10^{-6}$
Minimum Allowable Bottomhole Pressure, psi	2,000

A radial model with a radius of 15,000 ft was created with a vertical well at the center; a minimum bottomhole flowing pressure (p_{wf}) constraint of 2,000 psi was chosen

to be imposed on the well in order to ensure that at least some of the fluid in each fluid-type case would fall below the dew point at some time during the production period. Surface gas rate constraints were imposed on each case run, but varied by permeability and fluid type because both leaner fluids and higher permeabilities would lend themselves to higher rate constraints. An image of the reservoir model construction is included in **Fig. 7**. It is comprised of one layer that is 70 ft thick. The entire thickness is considered net pay. Essentially, pressure differentials drive the flow of fluids from one place to another. A minimum bottomhole pressure must be maintained because, gas wells in particular, typically tie into pipeline transportation systems that can operate at pressures upwards of 1,000 psi.

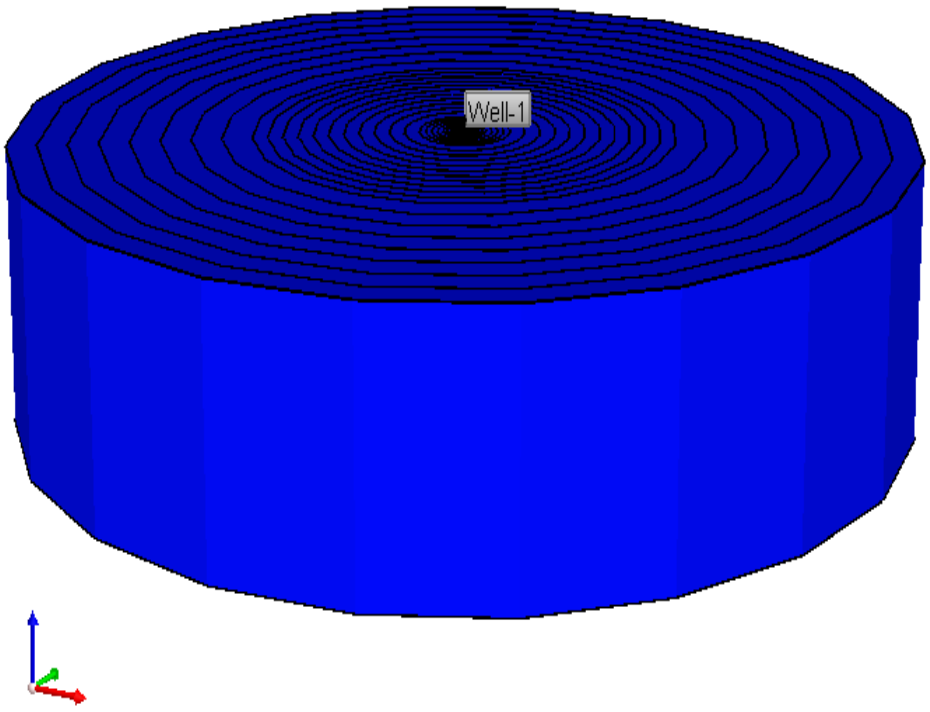

Figure 7. 3D representation with exaggerated thickness of CMG reservoir model used in the study

Figure 7 also displays the variation in grid size present in the reservoir model. **Table 2** includes the thickness of each of the 78 "shell-like" cells ranging from nearest to the wellbore at the top to furthest from the wellbore at the bottom. Cell width is smallest nearest to the wellbore because this is where the pressure change is most abrupt from one time step to the next.

Table 2. Grid cell dimensions

Cell Number	Number of Cells	Thickness, ft	Distance of Outer Cell Edge from Wellbore, ft
1	1	0.1	0.1
2	1	0.2	0.3
3	1	0.3	0.6
4	1	0.4	1
5 – 8	4	0.5	3
9 – 15	7	1	10
16 – 25	10	2	30
26 – 35	10	3	60
36 – 43	8	5	100
44 – 45	2	30	160
46 – 51	6	40	400
52 – 53	2	50	500
54 – 55	2	100	700
56 – 59	4	200	1,500
60 – 70	11	500	7,000
71 – 78	8	1,000	15,000

In order to create a zone of modified relative permeability to represent the treatment radius of the wettability alteration, a sector was created. In the context of CMG, a 'sector' is simply defined as a grouping of cells that can be activated, if desired, to adopt certain values. The treatment sector contained the innermost 18 cells, which is equivalent

to a treatment radius of 16 ft. While running the different cases, the sector could be assigned a different set of relative permeability curves than the reservoir, which remained strongly liquid-wetting for every simulation case. **Figure 8** includes the three sets of relative permeability curves used in the study: strong liquid-wetting, strong gas-wetting, and intermediate gas-wetting. Endpoint saturations are consistent with literature as well as the Corey exponents that were used to influence the curvature (Corey 1954). For the intermediate gas-wetting and strong gas-wetting cases the Corey exponents were 2 and 2.5 for liquid and gas respectively. For the strong-liquid wetting case the exponents were 4 and 2.5 for liquid and gas respectively (Zoghbi et al. 2010). The magnitude of the exponents is tied to the strength of the wettability of the phase in question. The strength of the wettability of the phase is also tied to the end-point saturation. For example, if a system is more strongly gas-wetting, the residual oil saturation will be lower.

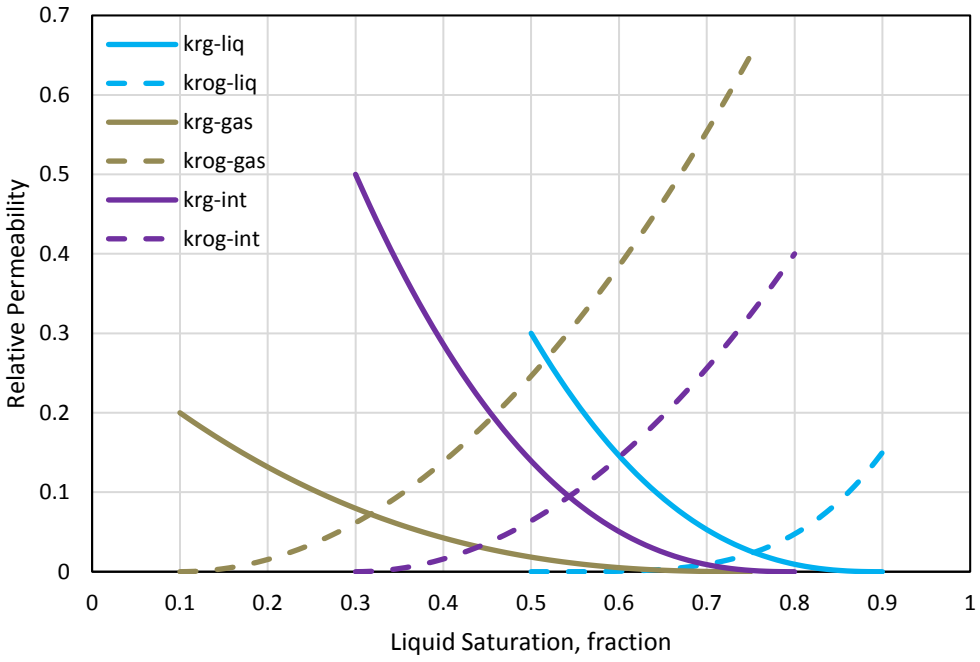

Figure 8. Relative permeability curves used in the study (adapted from Zoghbi et al. 2010)

3.1.2 Fluid Models

Zoghbi et al. (2010) utilizes one example of condensate fluid composition, which is based on a template included in the CMG software. This work expands on past studies by comparing two additional fluid compositions with the intermediate condensate examined in Zoghbi et al. (2010).

Condensate reservoir fluids may be classified quantitatively by API gravity (above 45° API), gas-oil ratio (GOR of 5,000 to 100,000 scf/STB), the weight fraction of components heavier than hexane (C_{7+} fraction), or even qualitatively by the color of the produced fluids (Coskuner 1999). The criterion used as the basis for the creation of the fluid models in this study was the yield, which is expressed in units of the number of barrels of condensate produced per million cubic feet of gas. A rich condensate will typically have a yield in excess of 150 STB/MMcf while a very lean condensate generally displays a yield of less than 50 STB/MMcf. Nevertheless, there is no set rule for this classification scheme and the yield of a condensate reservoir may range anywhere from 7 to 333 STB/MMcf (Shi 2009).

Figure 9 compares the relative proportions of each component included in the three reservoir fluid models. **Table 6A** includes these same values as well as other information pertinent to the thermodynamic properties of the fluid combinations. The bar chart may appear to suggest that the values are quite similar, but small changes in the relative proportions of each of these hydrocarbons can result in massive changes in the phase behavior of the overall system. In addition to the CMG condensate template used in Zoghbi et al. (2010), two other fluid sample compositions were pulled from literature and modified to produce the best comparison and demonstrate the widest range of

behavior. Key differences between these compositions include the amount of methane, which decreases as the fluids become richer, and the C_{7+} fraction, which tends to be lower and lighter in terms of molecular weight for lean fluids. The properties of the C_{7+} fractions are included in **Table 7A**, with the rich case predictably having the heaviest fraction and the lean case containing the lightest fraction composition.

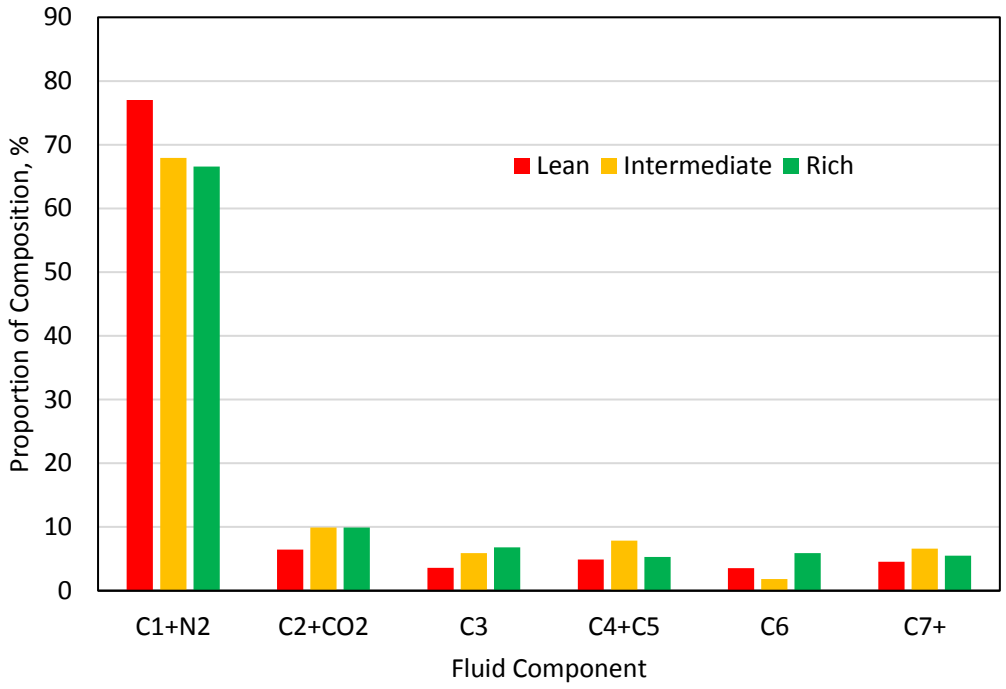

Figure 9. Comparison of composition of three reservoir fluids used in study

Figure 10 displays the two-phase envelopes for the three fluid compositions, which may, perhaps, display the differences in the fluid properties more clearly. As expected, the rich composition in green has the highest cricondentherm, cricondenbar and critical temperature and pressure of the three types, while the lean phase envelope in red has the lowest values for these properties. The reservoir temperature of 220°F is also included on the diagram to show that isothermal pressure depletion path that the model

undergoes before it reaches the minimum bottomhole pressure constraint of 2,000 psi. Due to the fact that all three of the fluid critical points fall to the left of the reservoir temperature line, we can rest assured that the compositions begin in the gaseous phase.

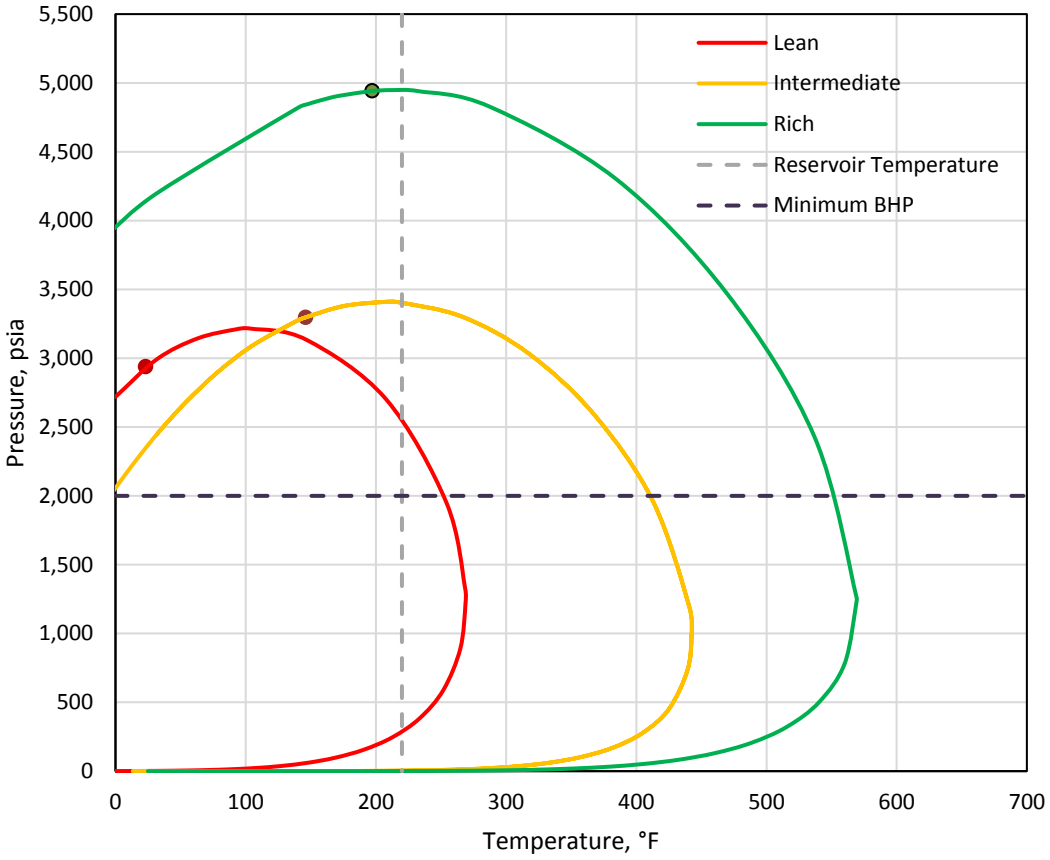

Figure 10. Phase envelopes of the three WINPROP fluid models used in the study

Another important measure to check the validity of the WINPROP models is to assess the liquid dropout curves for each of the fluids. **Figure 11** displays the results of a simulated constant composition expansion (CCE) test at reservoir conditions. In a laboratory CCE test a fluid sample is placed in a cell under high pressure and temperature. Gradually, the pressure in the cell is lowered, usually by the movement of a piston, and the resulting volume fraction of liquid in the cell is recorded. This process is repeated

many times at small pressure increments. If the test is designed to span the range in pressure from reservoir to surface, it will may accurately predict phase volume fractions that can be expected at the surface when the well is produced. The WINPROP software simply models this process. Moving from reservoir pressure at the bottom right of the plot in Fig. 11, the figure shows that the rich composition has the first abrupt introduction of a fluid phase to the mixture, followed by the intermediate case and the lean case. As the pressure continues to fall, the volume fraction of liquid drops to a value near zero, which falls in line with the trends seen in the phase diagrams.

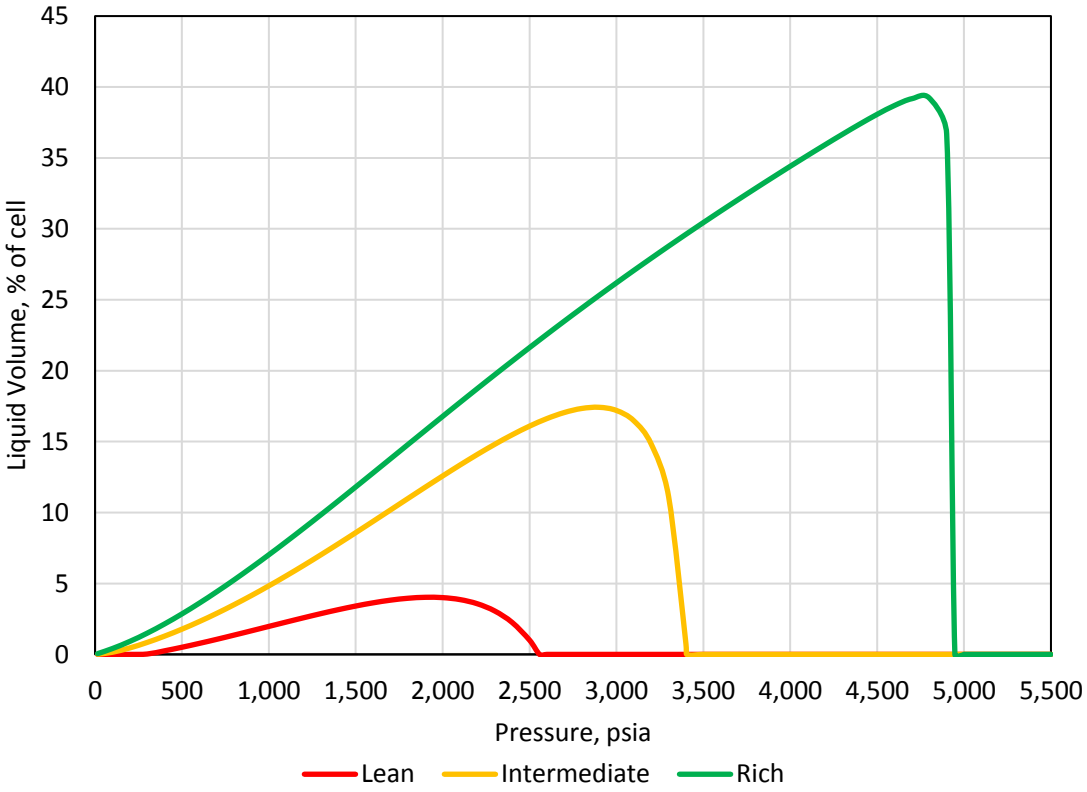

Figure 11. Plot of liquid dropout for three reservoir fluids using simulated CCE test

3.2 Simulation Workflow

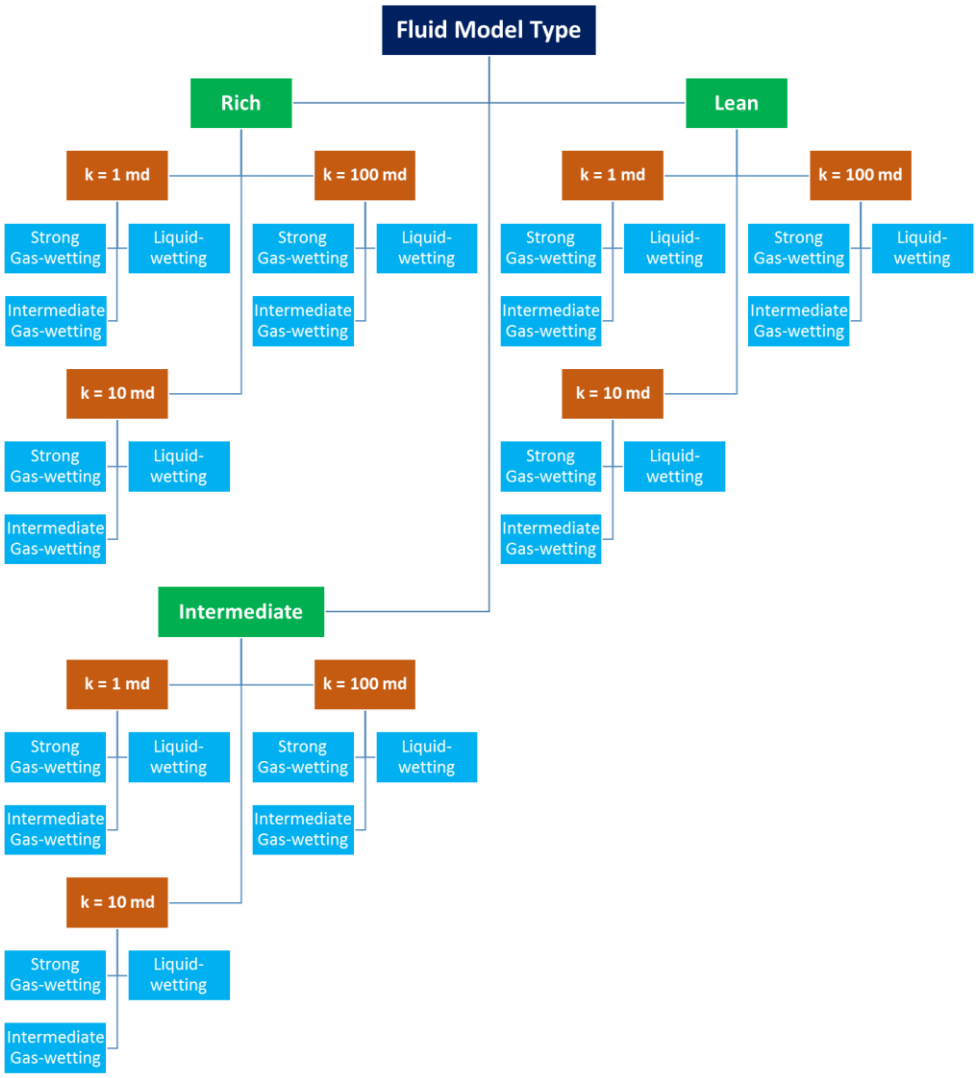

Figure 12. Tree diagram of main simulation cases

Figure 12 displays the general workflow of the simulation process. Three identical CMG models were created, one each for the three reservoir fluid compositions. For each model, three different permeability values were tested: 1 md, 10 md, and 100 md cases. Furthermore, for each of these permeability values, three different relative permeability scenarios were applied to the treatment zone: strong liquid-wetting, strong gas-wetting, and intermediate gas-wetting. This results in a total of 27 primary cases.

The first obstacle encountered for each of the cases was the implementation of a maximum rate constraint on the well's gas production. A well that is initially permitted to flow at full capacity will typically experience a sharper decline in production and lower overall ultimate recovery. The excessively high rate produces a large drawdown that may kill production before the near-wellbore area has time to recharge with gas. This effect can be particularly evident in high permeability reservoirs.

Typically, a well is choked back to a level that results in constant production for the first several months or years, at which time the production will begin to decline at a modest rate. Once a reasonable rate constraint was achieved for a certain absolute permeability case, a good rule of thumb was to increase the maximum rate constraint by a factor of 10 if the permeability was increased by a factor of 10, say transitioning from the 1 md case to the 10 md case, or the 10 md case to the 100 md case. However, it is important to note that this rule of thumb did not apply to every case and was adjusted for different fluids with the goal of an initial rate-plateau period of 2-3 years.

After the maximum rate constraint was set for a certain case, the only remaining step was to attempt to run the model. In some cases, the first attempt would work, in other cases the model would fail due to compositional variations or pressure drops that were too large for the program to compute. When a program encounters a problem like this it will reduce the time step size to a value no less than the minimum time step size defined by the user and try the run again. If this action is required for too many time steps, which means that the program is continually rerunning time steps to achieve stability, the program will simply end before the duration of the simulation has ended. In these situations, the maximum time step would be reduced by the user and another attempt

would be made. The starting maximum time step for each run was 1 day while the smallest maximum time step required for a run was 0.1 days. Reducing the maximum time step size has a greater success rate and reduces running time more than reducing the minimum run time step size. The total simulation duration for each case was 20 years.

3.3 Assumptions Explained

The most basic assumptions that went into the reservoir model used in the study were the conditions of homogeneousness and isotropy, which is to say that static reservoir properties were constant at every point in the model and tensor properties were consistent in every direction. This includes the assumption of equal vertical and horizontal permeability. Typically, the ratio of vertical to horizontal permeability does not exceed 0.1, but for the lateral flow purposes of these simulations this assumption had no impact on the outcomes. An assumption of zero capillary pressure was also factored into the model because the difference in phase pressures at a permeability of 1 md (the lowest permeability considered in the study) would have a negligible impact on the model results. Capillary pressure would only need to be taken into account if the pore throats, and thus permeability, were so small that the interconnected pores or "capillary tubes" in the reservoir resulted in a capillary rise effect.

Finally, though the simulation software ensures that the treatment is 100% effective for every part of the treatment zone, in the field there is often no way of directly measuring how effectively a treatment has been executed. This suggests that, in a practical application of this study, some sort of 'correction factor' would need to be applied to the treatment radius to match the production results to model predictions.

Chapter 4: Results and Analysis

Before the primary focus of the simulation study could begin, significant headway had to be made in understanding the CMG software utilities and limitations. Needless to say, in lieu of a class, trial and error proved a very effective teacher. Great care was taken in creating each of the reservoir and fluid models because, as the saying goes, "garbage in, garbage out". A model that is fundamentally flawed from its inception has no hope of producing anything of value to the engineer and may lead to seriously costly errors in decision making.

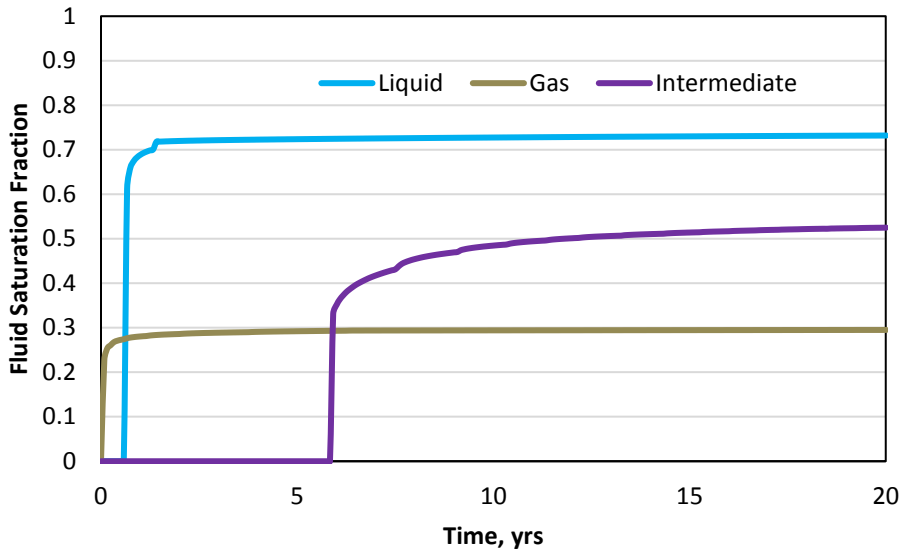

Figure 13. Liquid saturation profile versus time for different wettability treatments (intermediate condensate fluid at 10 md and 0.6 ft from wellbore)

Mistakes can easily be made in simulation studies if proper care is not taken to make sense of each of the model outputs. Even if the majority of data supports the original hypothesis, the presence of a small amount of seemingly bizarre data can call into question the reliability of the results. Take **Fig. 13** for example, where the liquid

saturation was plotted versus time at a constant distance from the wellbore (0.6 ft) for each of the three wettability cases. The researcher must question whether or not it makes sense that the gas-wetting case would develop a liquid saturation before the other two scenarios and that the saturation it maintains is lower than the other two cases. We can conclude that it is appropriate that the liquid-wetting curve in blue maintains the highest saturation because the liquid is being trapped by the mineral grain surfaces. This also explains why the gas-wetting curve maintains the lowest saturation (about 30%), because the liquid is the most mobile in a strong gas-wetting setting. And finally, the early occurrence of liquid saturation in the gas-wetting case can be explained by the fact that it is the first case to fall below the dew point of the fluid at this particular radius. The high fluid velocity in this case is the likely culprit of the higher pressure drop. So, as we have seen, these results can be explained thoroughly by the simulation outputs.

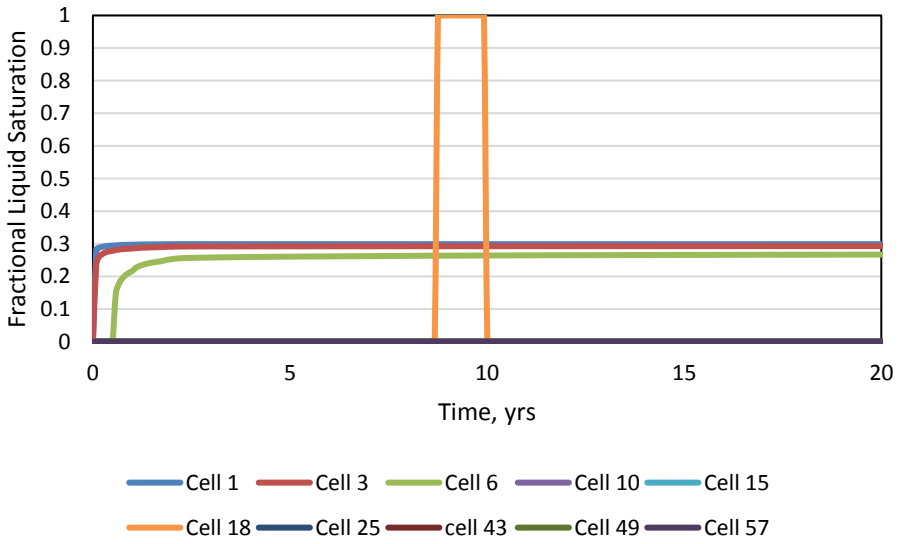

Figure 14. Liquid saturation as a function of time for multiple radii (or cells) for the intermediate condensate fluid with the strong gas-wetting treatment at 1 md

Now let us take a look at another set of simulation data, this time **Fig. 14** shows that cells 1, 3, and 6 develop some liquid saturation in quick succession for the

intermediate fluid model with strong gas-wettability and 1 md permeability. At no point in time do cells 10 or 15 develop any water saturation, but the liquid saturation in cell 18 inexplicably jumps to 100% for a few years before falling back to zero. It should be obvious to the engineer that something is amiss. By looking at the pressure profiles over time for each of the cells in this case in **Fig. 15**, it is clear that the pressure in cell 18 never falls below roughly 3900 psia. The phase envelope for the intermediate fluid tells us that the dew point pressure for the fluid at reservoir temperature is 3400 psia, which suggests that the jump in saturation for the curve of cell 18 is an artifact of the simulation. Indeed, GEM has been known to mistake a 100% gas saturation for a 100% liquid saturation in variable compositions such as this. These examples attempt to illustrate the importance of logic and sound reasoning in the realm of simulations to ensure that erroneous results are not treated as indisputably correct, simply because they come from a computer program. Figure 14 is not the only example of an insensible simulation response, more will follow.

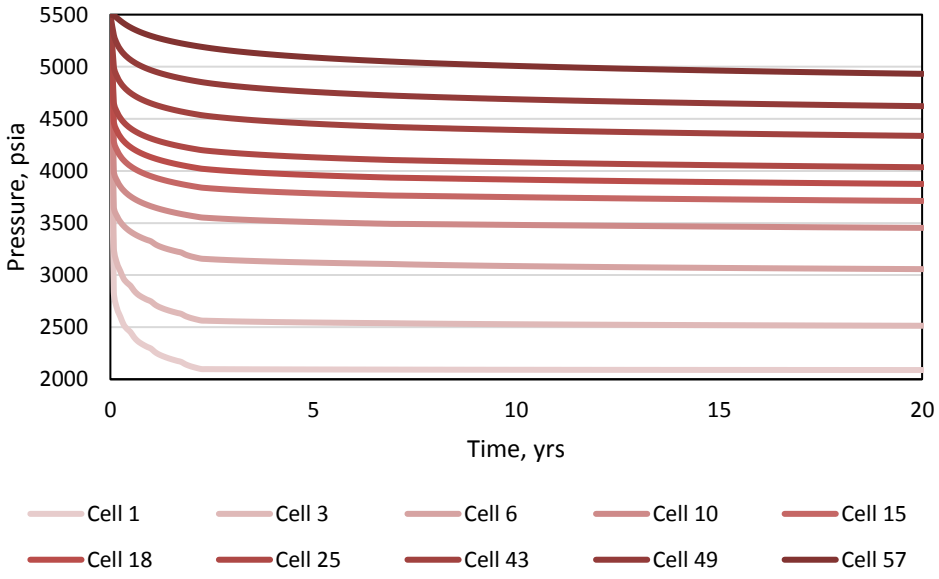

Figure 15. Pressure as a function of time for multiple radii (or cells) for the intermediate condensate fluid with the strong gas-wetting treatment at 1 md

4.1 The Effect of Time Step Size

Even after a simulation model has been fully built, the user may experience some difficulty in persuading the case to run. Often times a simulation software will have built-in conditions to monitor the stability of the mathematical solutions. Even after a time step has been completed, a program may "check" this solution by inputting a value slightly higher than the original input. If this minor adjustment causes a disproportionately large change in the solution, the model is likely unstable. In the early stages of this study, certain case runs would terminate prior to finishing the full run duration, leading to some manipulation of the numerical defaults of the program. A simulation may exhibit instability at a maximum time step of 0.5 days but not at 0.1 days, purely based on the checks and balances of the (often proprietary) algorithms.

Figure 16 illustrates some of the unique challenges that face the engineer involved in simulation work. The 20-year daily gas rate curve of three different maximum time step sizes, 0.5, 0.25, and 0.1 days, were compared for a single reservoir-fluid couplet (intermediate fluid composition, intermediate gas-wettability alteration, and 100 md reservoir permeability). Though the greatest discrepancy in cumulative production over this period is less than 1.7%, there are some clear trends between these trials. Visually, one can see that the run with the smallest time step displays the smoothest curve. Recovery also increases slightly as the time step size decreases. This is likely due to the fact that the large "zig-zag" patterns present in the 0.5 and 0.25 day cases correspond to near-vertical changes (typically drops) in production; this phenomenon corresponds to the abrupt transition of one grid cell from one phase to another. Since each cell, regardless of volume, is held to a single value of pressure, saturation or composition, this creates

dramatic boundaries of pressure differential at the interface of the last liquid cell and the first gas cell.

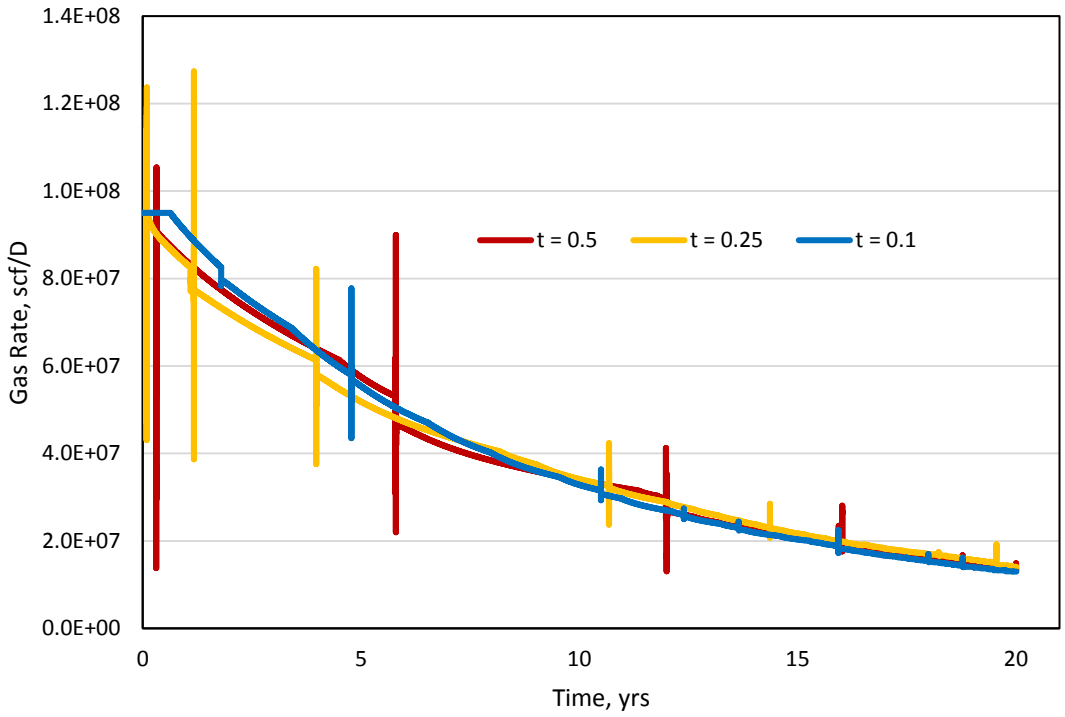

Figure 16. Impact of maximum time step size on intermediate gas-wetting case of intermediate fluid at 100 md

Figure 17 illustrates this boundary with a dark blue line. Outside of the blue circle, the reservoir is entirely in the gas phase, but as the program steps from the red cell on the outside to the orange cell on the inside, there occurs a jarring, step-wise jump in liquid saturation. This jump may or may not cause instability within the simulation; understanding this possibility is just one of many ways the engineer can be alert to the fact that a simulation of a condensate fluid may behave differently than a simple, single-phase dry gas or black oil simulation.

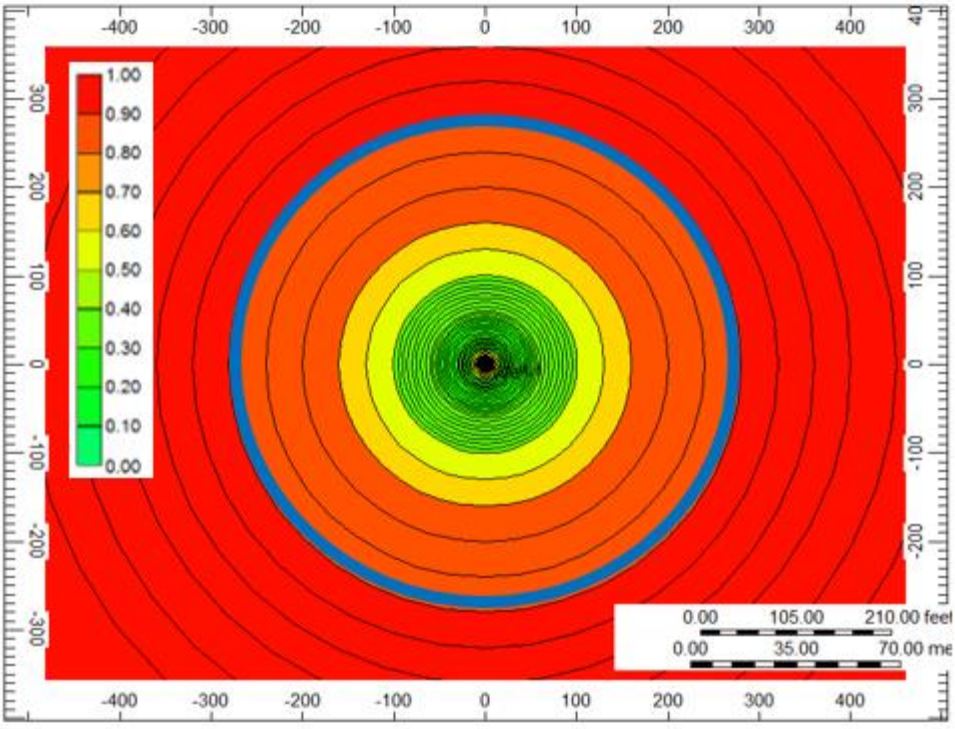

Figure 17. Gas saturation profile of simulation case which highlights the boundary between liquid and gas phases in blue

4.2 The Effect of Fluid Composition

The economic value of each of the fluid compositions examined can easily be summarized in the GOR plots that follow, which are grouped by fluid model, because liquid and gas prices differ dramatocally. GOR values differed slightly depending on the wettability treatment, but only one curve (the intermediate gas-wetting curve) was taken from each of the permeability cases to represent the system as a whole since the variation from case to case for each fluid was minimal. **Figure 18** is another excellent example of a simulation output that must be taken with a grain of salt. The rich condensate case proved to be the most difficult case to work with from a modeling standpoint, by far. A cursory examination of **Fig. 59A** helps to explain this erratic phenomenon in some of the data collected from the rich cases. Figure 59A contains the same phase envelope included

in Fig. 10, but this example also happens to include some curves within the phase envelope that represent different molar volume fractions of vapor inside the two-phase boundary. The isothermal pressure depletion path of the reservoir crosses the dew point line and enters the 2-phase region at nearly 40% liquid saturation, but by the time it reaches the minimum BHP of 2000 psi, the liquid saturation is only about 13%. Compare this change of approximately 27% liquid saturation to the saturation changes of the intermediate and lean condensate fluids in **Fig. 60B and 61B** respectively, each of which show a saturation change of no greater than 10%. The pressure depletion path of the rich case simply traverses more of the 2-phase region than is seen in the other two fluid cases.

For this reason, the numerical simulator sometimes runs into a problem when saturations between cells are changing wildly from one time step to another. With these large gradations, the iterations for different parameters often wildly overshoot, and then undershoot (or vice versa) the "correct" value in an attempt to get back on track. This explains the appearance of the near-vertical lines in all three permeability cases in Fig. 18. Each jump occurs when a new cell suddenly develops a liquid saturation when before it was 100% gas. As explained previously, simulations cannot perfectly mimic real reservoirs because entire cells are given the same properties when in the real world the appearance would be of a smooth, trend rather than a step-wise function. Some grid refinement was attempted to alleviate this problem, which will be explored in later works.

The anomalous 100 md curve in Fig. 18 actually shows an increase in the GOR over time (as opposed to the other consistently flat cases). Further examination of the CCE simulation in Fig. 11 helps to explain this occurrence. Due to the high permeability, the average pressure drop in this case for the entire reservoir is much larger than the other

two permeability cases. It is so large in fact that the reservoir fluid actually starts to become more gaseous over time, just as Fig. 59B predicted. The CCE simulation shows that, for the majority of the intermediate and lean fluid cases, because of the imposed minimum BHP limit, the fluid saturation is increasing or staying the same. However, for the rich case in green, the fluid saturation increases and begins to decrease for quite some time before the minimum BHP limit is reached. This phenomenon is witnessed in the 100 md case for the intermediate reservoir fluid to a much smaller extent.

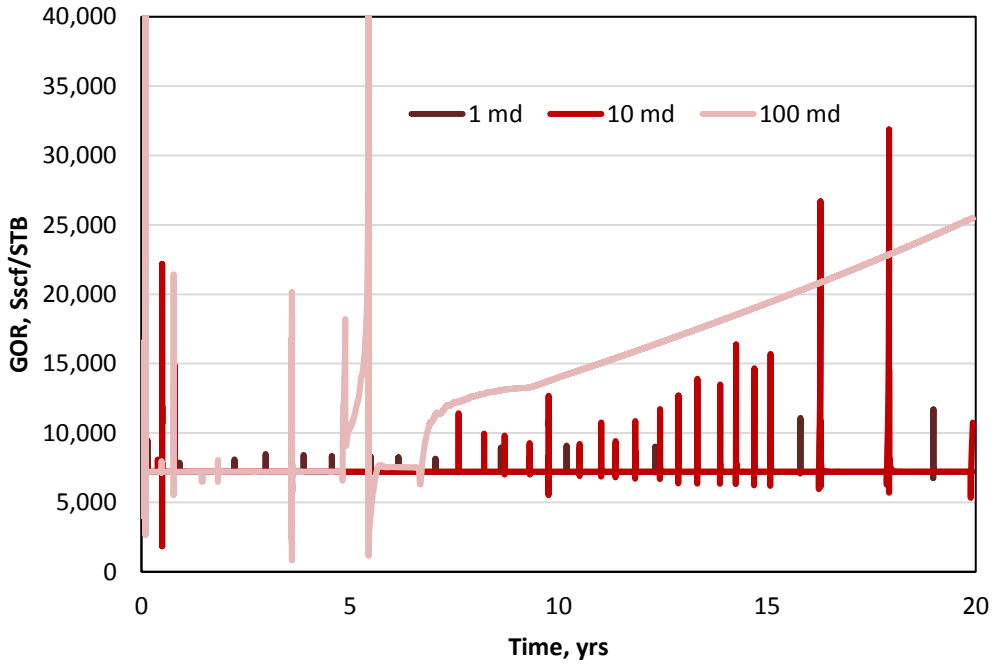

Figure 18. GOR plot at different permeabilities for liquid-wetting cases of rich condensate fluid

Figures 18, 19 and 20 depict approximately constant GOR values of 7200 scf/STB, 10,400 scf/ STB and 25,500 scf/STB for the rich, intermediate and lean condensate fluids respectively. These correspond to yields of roughly 140 MMscf/STB, 95 MMscf/STB and 40 MMscf/STB. The intermediate case was taken from a CMG template as explained previously, but the rich and lean cases were specifically created to

assume these values so that the maximum range of potential condensate yields might be explored. Depending on the prices of oil and gas, one yield value may prove more valuable than another. This theme will be explored in a later section.

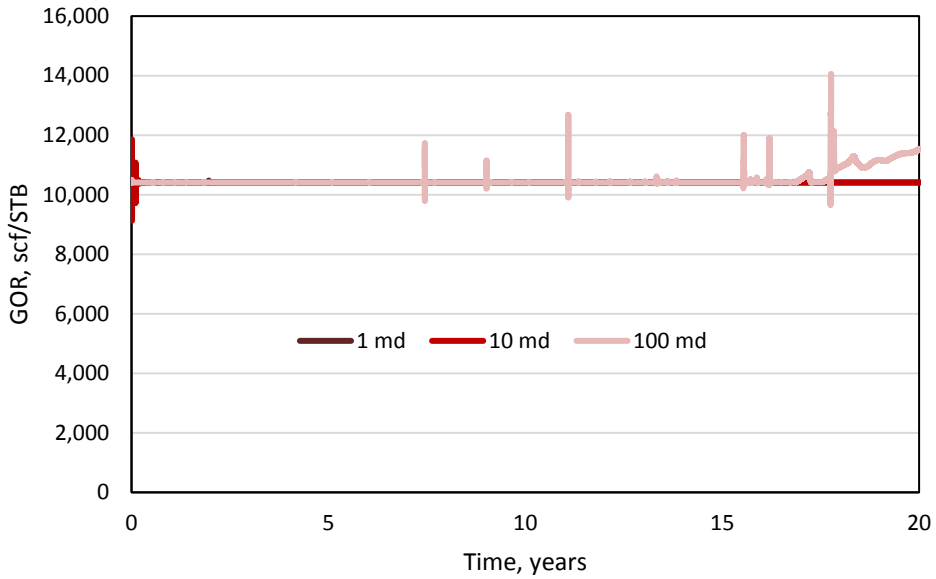

Figure 19. GOR plot at different permeabilities for liquid-wetting cases of intermediate condensate fluid

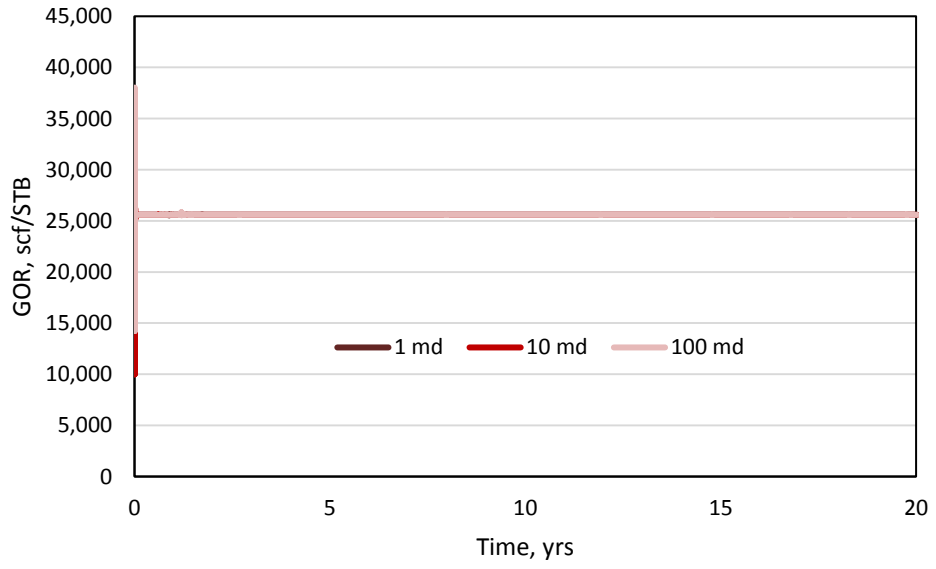

Figure 20. GOR plot at different permeabilities for liquid-wetting cases of lean condensate fluid

4.1.1 Rich Fluid Overview

The effectiveness of one relative permeability set over another was tested according to absolute permeability so that cases could be compared that were run at the same maximum gas rate. In most cases, care was taken to ensure that the rate restriction did not result in more than one flat-lined outcome. **Figure 21** is the only exception. The imposed maximum daily gas rate of 470 Mcf resulted in a production plateau for both the intermediate gas-wetting and fully gas-wetting cases, which suggest that either treatment would result in an improvement over the natural liquid-wetting case. However, based on the bottomhole pressure profiles detailed in **Fig. 22**, the intermediate treatment results in a slower BHP decline than the strongly gas-wetting case, which implies that its production plateau will last longer. The liquid-wetting case production was not stable at a higher rate but both of the modified cases were re-run at a higher rate. These runs confirmed the belief that the intermediate-wetting scenario is more optimal.

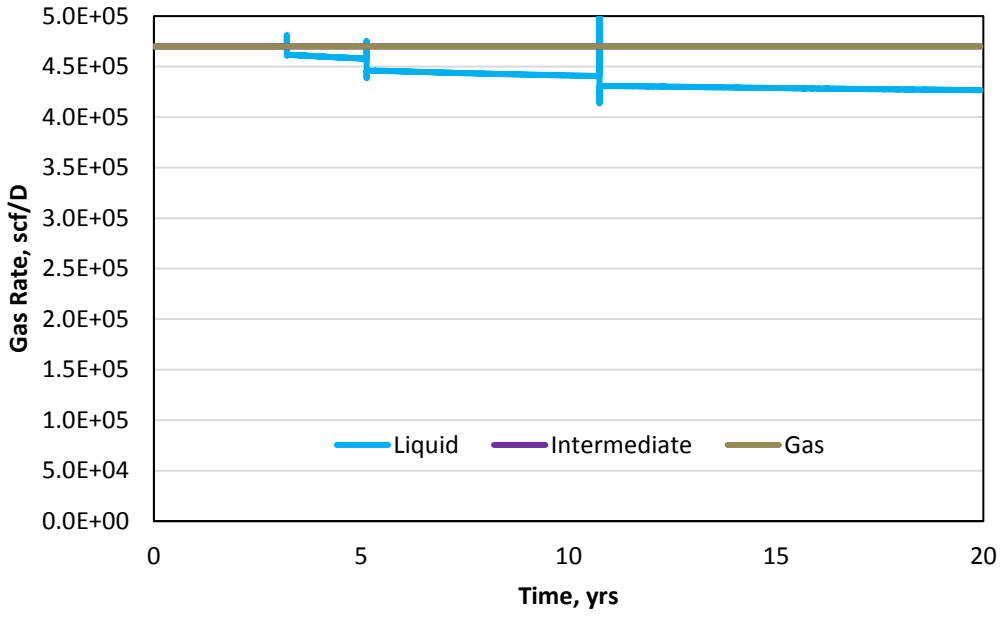

Figure 21. Gas production plot of 1 md permeability case for various wettability scenarios with rich fluid composition

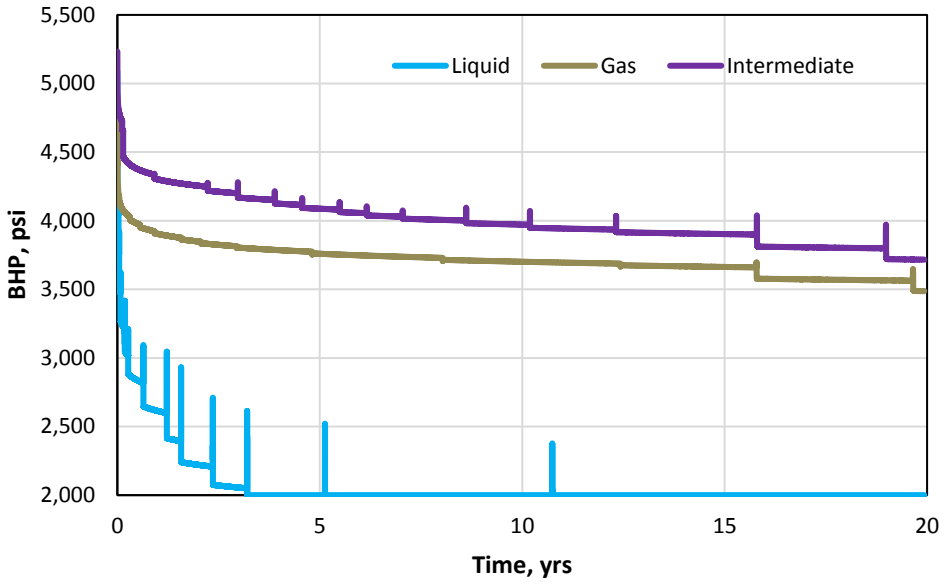

Figure 22. Bottomhole pressure plot of 1 md permeability case for various wettability scenarios with rich fluid composition

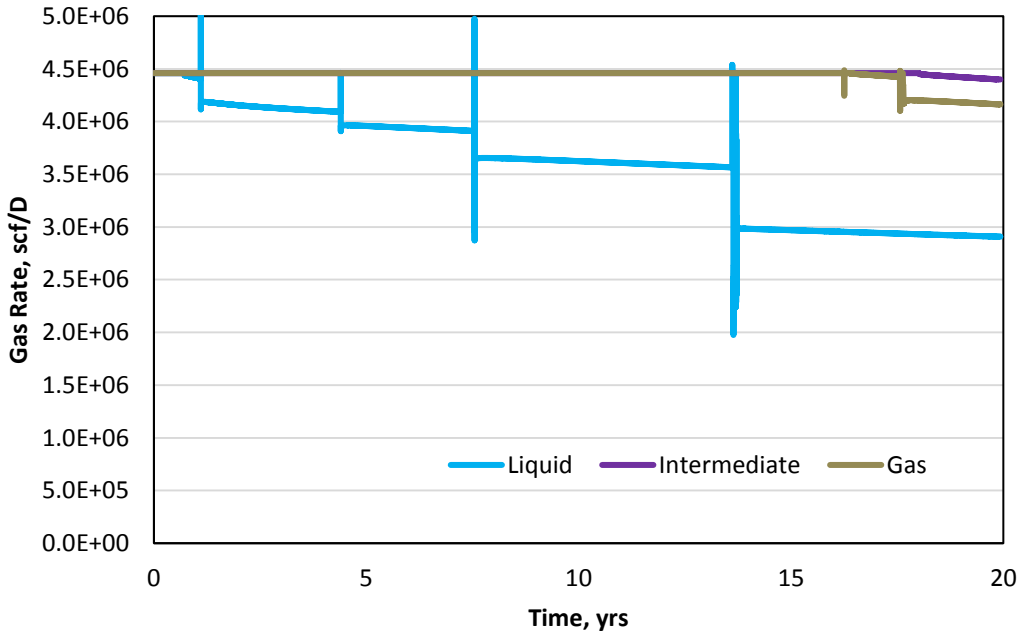

Figure 23. Gas production plot of 10 md permeability case for various wettability scenarios with rich fluid composition

The 1 md case demonstrates that the intermediate treatment is superior to the gas-wetting treatment for the rich fluid, but Zoghbi et al. (2010) demonstrated that this case was superior independent of absolute permeability. In addition to determining whether or not it is superior independent of fluid composition, this study likewise aims to examine the impact of permeability. This means that the rich case was run at 10 md (**Fig. 23**) and 100 md (**Fig. 24**) as well. Both of these figures support the conclusion that the intermediate-wetting case is more optimal than the strong gas-wetting case. The fall and subsequent rise of gas production in the liquid and gas-wetting curves of Fig. 24 can be attributed to the re-vaporization of the liquid previously described.

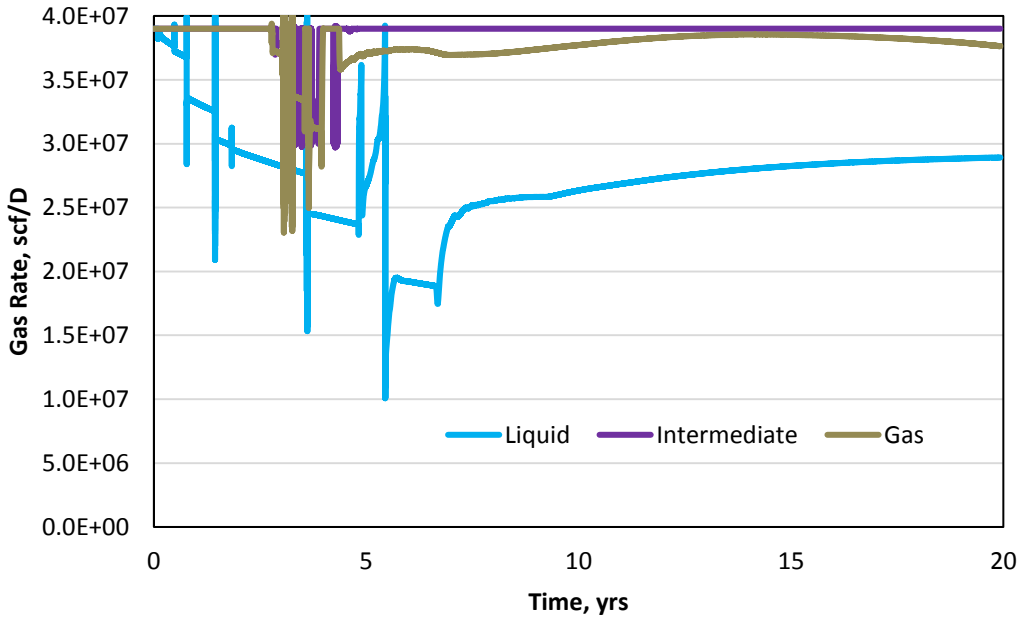

Figure 24. Gas production plot of 100 md permeability case for various wettability scenarios with rich fluid composition

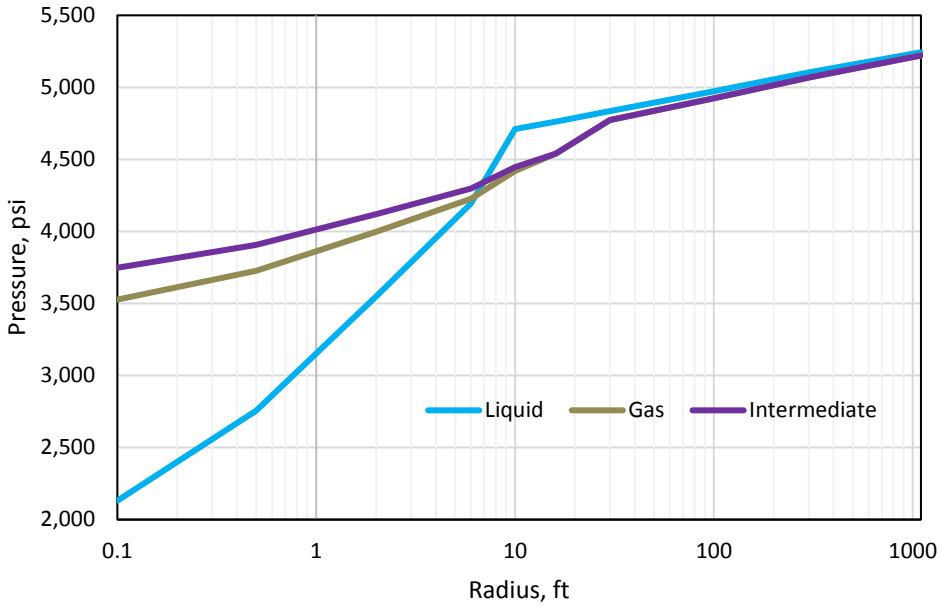

Figure 25. Pressure as a function of radial distance from wellbore for 1 md case of rich fluid composition at year 20

Figures 25, 26 and 27 contain the pressure profiles as a function of distance for a single point in time (year 20 of production). The curves are plotted on a log scale to highlight the impact of the treatment on the pressure within the treatment zone, which is 32 ft in diameter. The convergence of the pressures in the 1 md case shown in Figure 25 at great distances from the wellbore is to be expected given the minimal pressure drop exhibited in reservoirs with low permeability. In this case, the impact of the treatment is limited to the near-wellbore region. As the curves approach the wellbore moving from right to left along the horizontal axis, both the gas-wetting and intermediate-wetting states display a lower pressure drop, or pseudo-skin so to speak, because there is less constriction in the pore passages. When liquid begins to drop out of the gaseous phase it effectively reduces the size of the pore throats, leading to a greater drop in pressure. As the production curves demonstrated previously, the intermediate case is the most effective at diminishing the pressure drop from the edge of the drainage area to the wellbore.

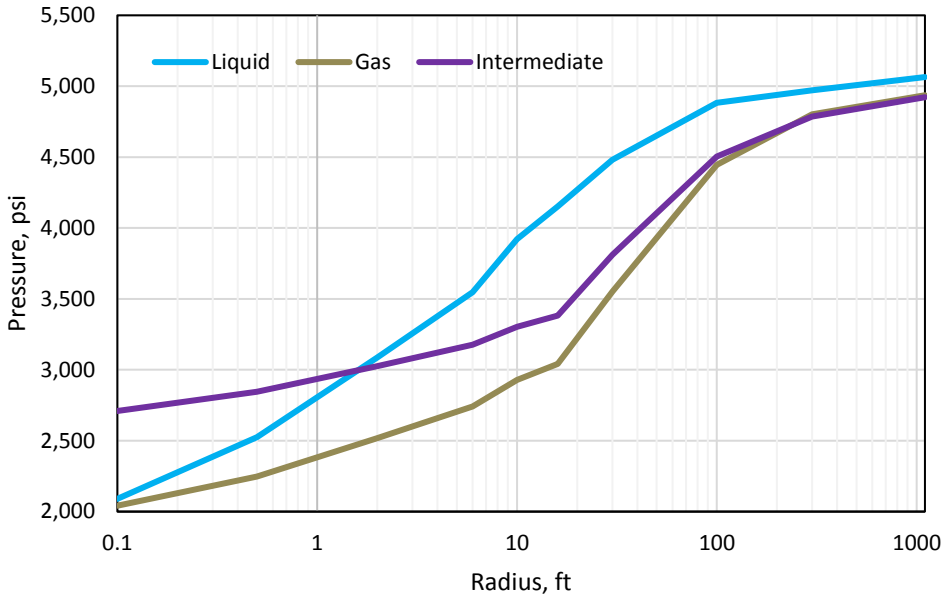

Figure 26. Pressure as a function of radial distance from wellbore for 10 md case of rich fluid composition at year 20

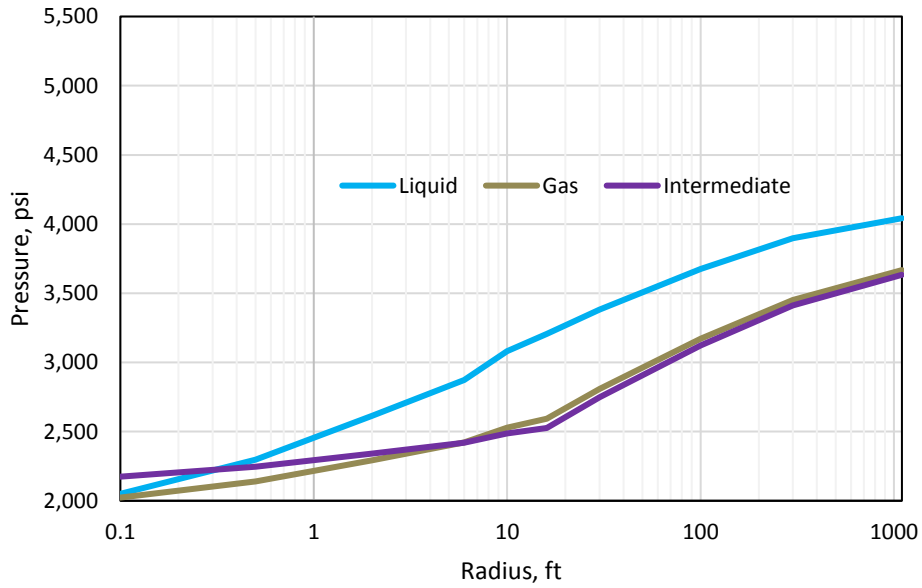

Figure 27. Pressure as a function of radial distance from wellbore for 100 md case of rich fluid composition at year 20

We begin to see some divergence in the curves at the end of the 20-year period for the 10 md and 100 md pressure profiles in Figs. 26 and 27 because the higher

permeability leads to a wider affected radius and overall average pressure drop in the reservoir. In these cases, the effect of the wettability-altering treatments is "felt" beyond the treatment radius, rather unlike the 1 md case in Fig. 25. There is another significant difference in these two higher permeability case. Unlike Fig. 25, the near-wellbore pressures of the liquid-wetting and strong gas-wetting cases are actually closer to one another than the strong and intermediate gas-wetting cases. In fact, the near-wellbore pressure is lower in the gas-wetting case than in the liquid-wetting case. The likely explanation for this observation is that the higher permeability has generated such a high liquid velocity in the gas-wetting case that the pressure drop is even greater than that generated by the gas trying to squeeze through the liquid-lined pores in the liquid-wetting cases.

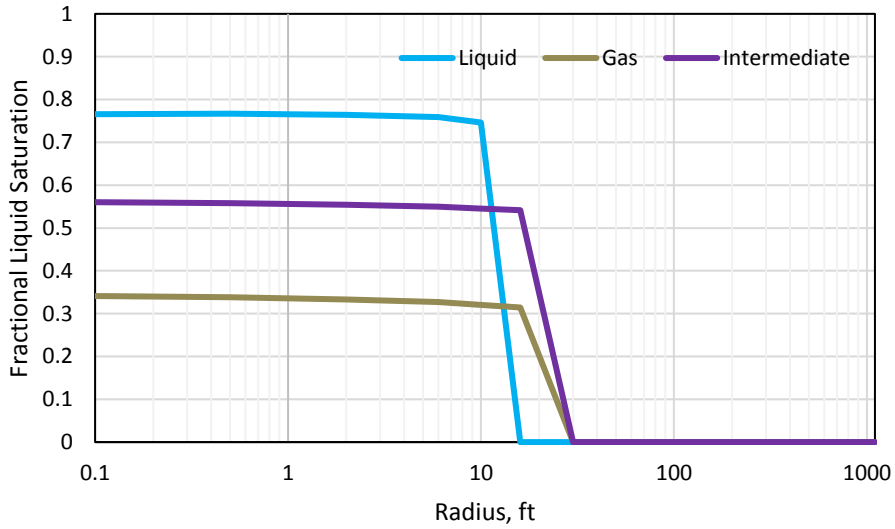

Figure 28. Liquid saturation as a function of radial distance from wellbore for 1 md case of rich fluid composition at year 20

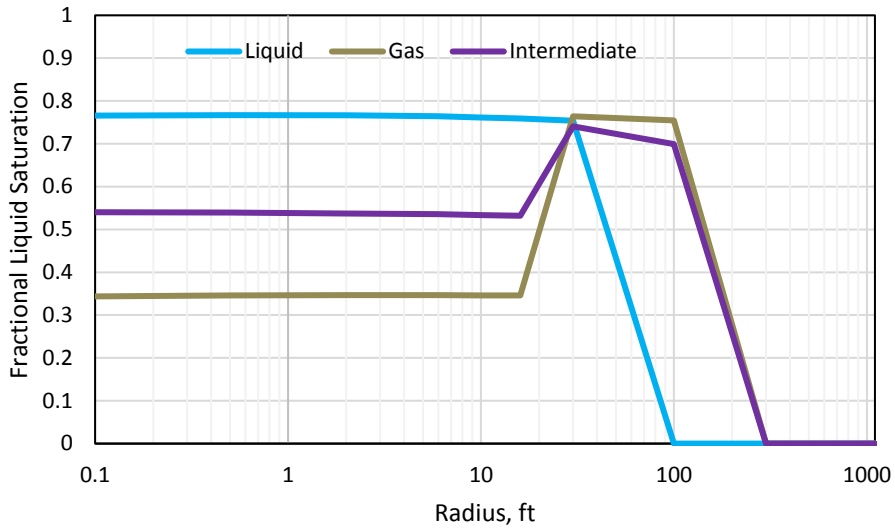

Figure 29. Liquid saturation as a function of radial distance from wellbore for 10 md case of rich fluid composition at year 20

The fluid saturation profiles as a function of distance from the wellbore are closely tied to the pressure profiles because the saturations are related to the proximity of the pressure to the dew point, but this is not the only factor. Close proximity to the wellbore generates high velocities that tend to sweep the fluids collected there. **Figures 28, 29 and 30** are also useful in that they give an approximation of the degree of condensate banking present at the end of the 20-year production life. As one might expect, the succession of increasing permeability from Fig. 28 to Fig. 30 coincides with the greater degree of pressure drop in the reservoir. This is why we see a trend of increasing condensate diameter as the permeability increases.

Several other interesting trends are also present in these graphs, though more in Figs. 29 and 30 because the low permeability in Fig. 28 has prevented the formation of a condensate bank of sufficient size. As expected, we see the smallest liquid saturation near the wellbore for the gas-wetting case and the largest for the liquid-wetting case, however it would appear that the condensate bank for the intermediate- and gas-wetting cases

forms a larger ring around the treated zone. This seems counter-productive to the goal of this study, which is to show the positive effect of wettability alteration on condensate production, which should be hindered rather than helped by a greater degree of condensate banking. However, when one considers that these saturation profiles were taken at the 20-year mark, and considering the greater production volume for these altered cases as seen in Figs. 21, 23 and 24, this makes perfect sense. A higher production volume would result in lower pressures that extend further into the reservoir, dropping more cells below the dew point and resulting in a greater overall degree of liquid drop out when compared to the liquid-wetting case.

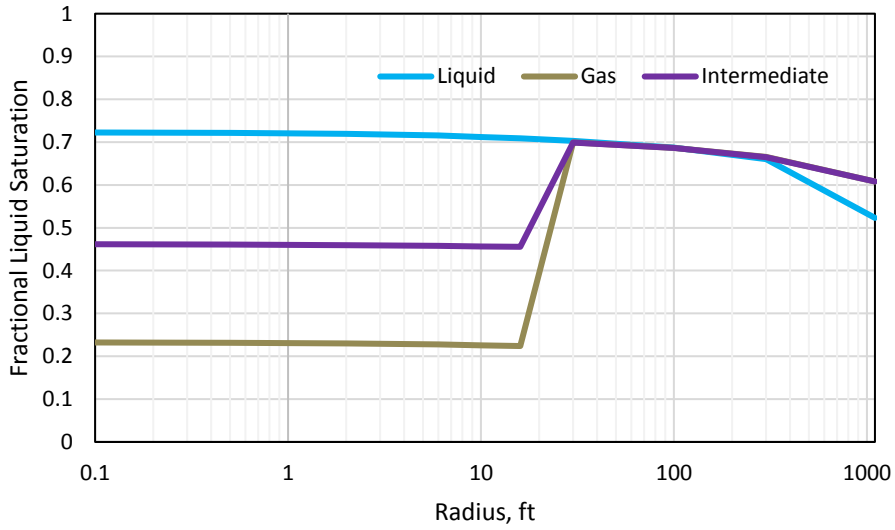

Figure 30. Liquid saturation as a function of radial distance from wellbore for 100 md case of rich fluid composition at year 20

Based on these results, it can be concluded that the intermediate-wetting case is the most effective treatment in terms of production increase for the rich condensate composition, independent of changes in absolute permeability. It accomplishes this by towing the line between a high near-wellbore fluid saturation that would constrict flow,

and a very low residual near-wellbore liquid saturation that would result in high liquid velocities, both of which cause greater pressure drops in the affected areas.

4.1.2 Intermediate Fluid Overview

Overall, the gas production graphs for the intermediate fluid composition follow the results of Zoghbi et al. (2010), which used this fluid as the basis for the entire paper. Intermediate gas wettability demonstrates its greater influence over production than both the strong gas-wetting and liquid-wetting scenarios, though the extent of this improvement appears to diminish with increasing permeability because the production profiles are much closer together in **Fig. 33** than they are in **Figs. 31 and 32**. We also see some instability in the 100 md case of Fig. 33 that isn't present in the other two cases, most likely because the high flow rate generated by the high permeability has led to a state of potentially unstable simulation. The rate of production decline is also much greater here which is typical of higher permeability and a very relevant factor in any discussion of economics.

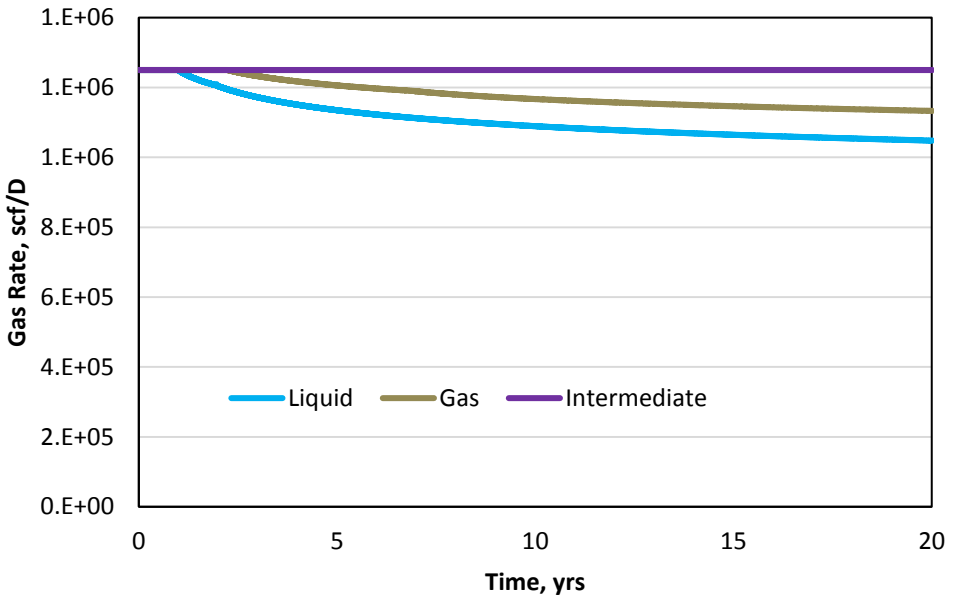

Figure 31. Gas production plot of 1 md permeability case for various wettability scenarios with intermediate fluid composition

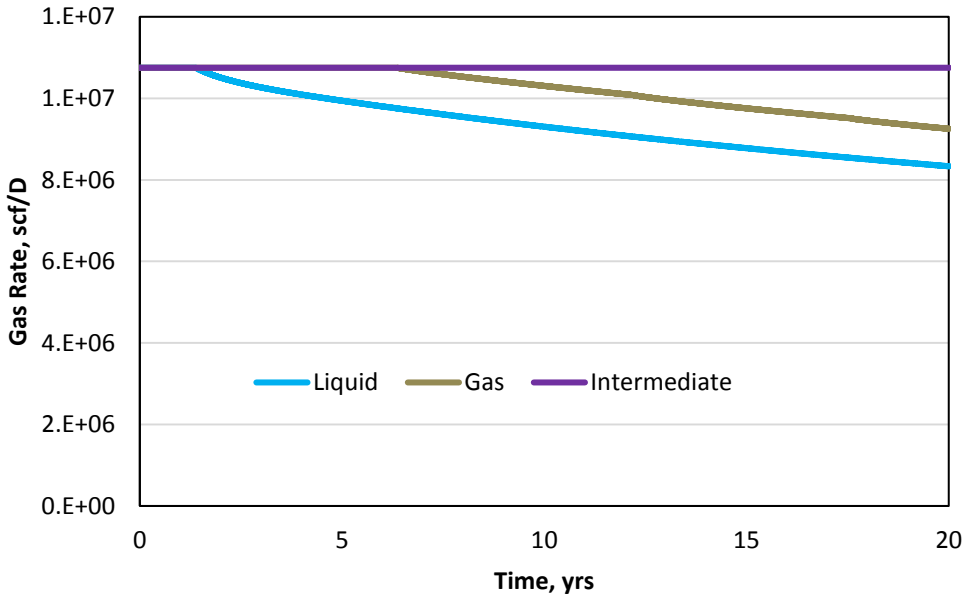

Figure 32. Gas production plot of 10 md permeability case for various wettability scenarios with intermediate fluid composition

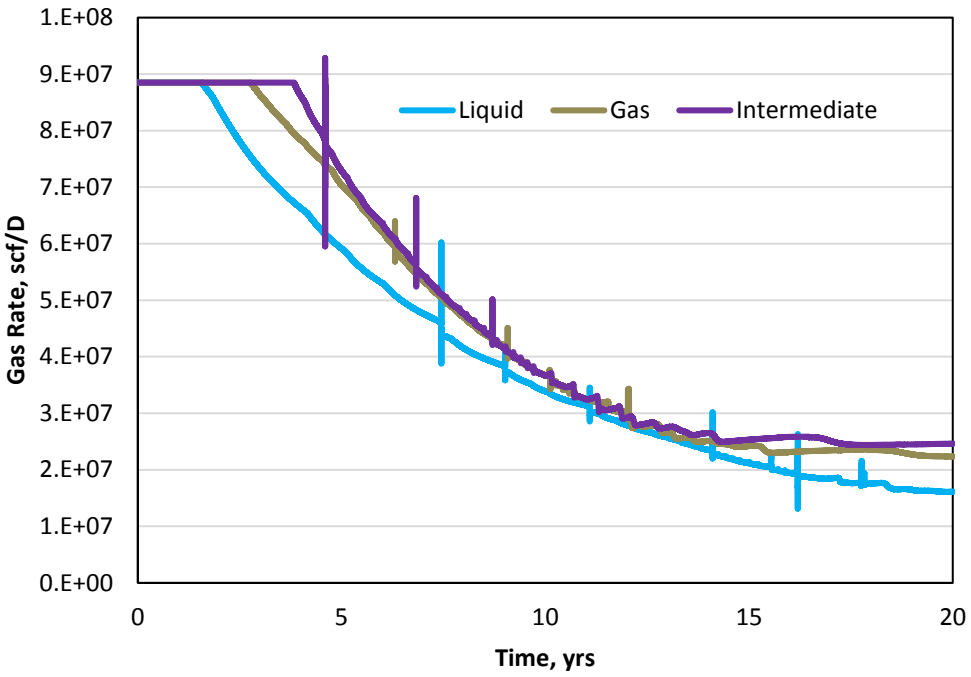

Figure 33. Gas production plot of 100 md permeability case for various wettability scenarios with intermediate fluid composition

Likewise, the pressure profiles in **Figs. 34-36** for the intermediate fluid are very similar to those found for the rich condensate case. For the 1 md case in Fig. 34, the pressure drop for the intermediate-wetting scenario is the least severe, but for permeabilities greater than this, the high velocities in the treated cases actually lead to a greater pressure drop than is found in the liquid-wetting case. For these higher permeability cases (Fig. 35 and 36), the pressure in the liquid-wetting reservoir is greater at every point than the pressures in the other two cases because the cumulative production for these two cases is greater than the liquid-wetting case. The greater production leads to greater pressure depletion by the end of the 20-year period. The main difference between these profiles and those from the rich fluid case is that both the intermediate- and gas-wetting case pressures are lower than the liquid-wetting case, whereas before

only the gas-wetting case pressure was lower than the liquid-wetting pressure near the wellbore. This is likely due to the higher gas velocities in these cases.

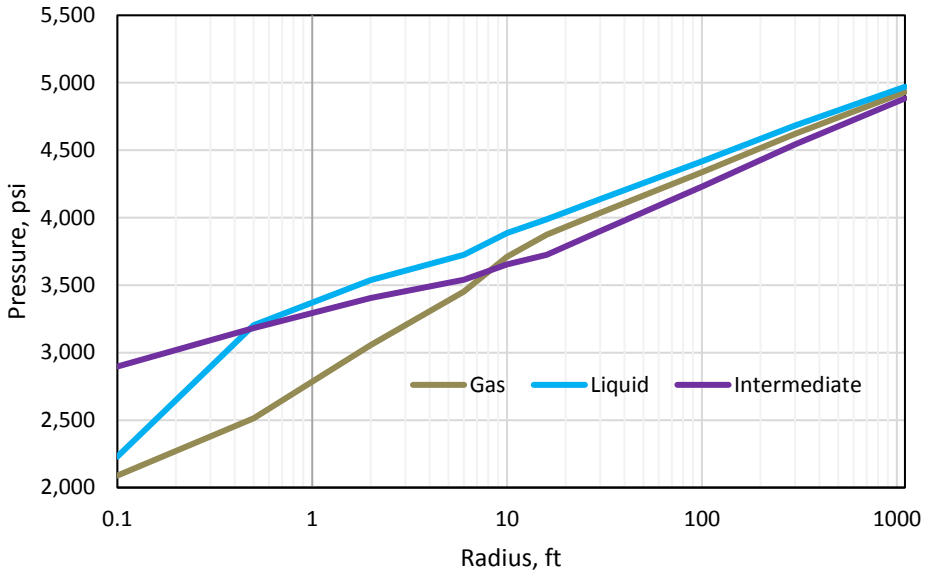

Figure 34. Pressure as a function of radial distance from wellbore for 1 md case of intermediate fluid composition at year 20

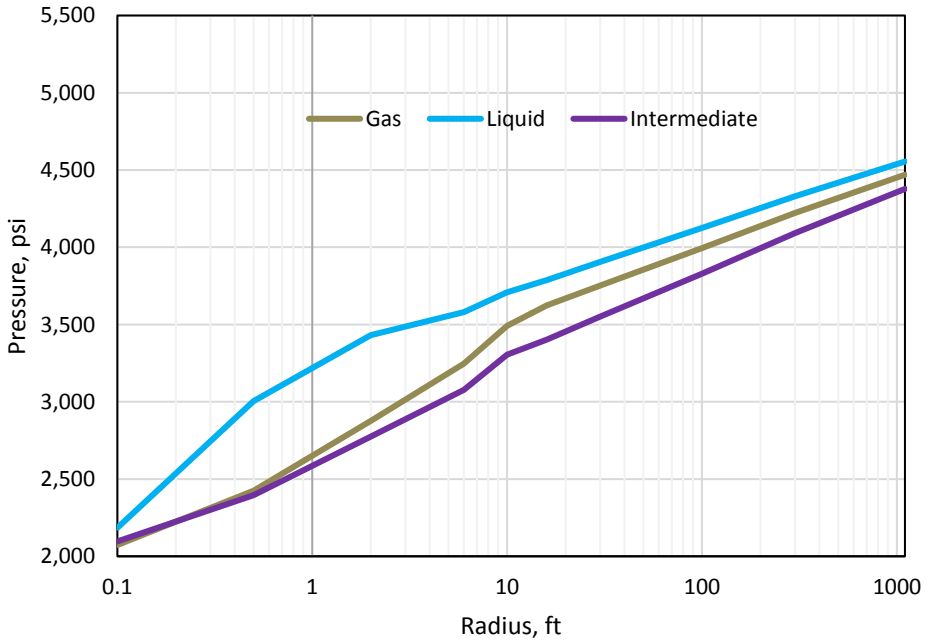

Figure 35. Pressure as a function of radial distance from wellbore for 10 md case of intermediate fluid composition at year 20

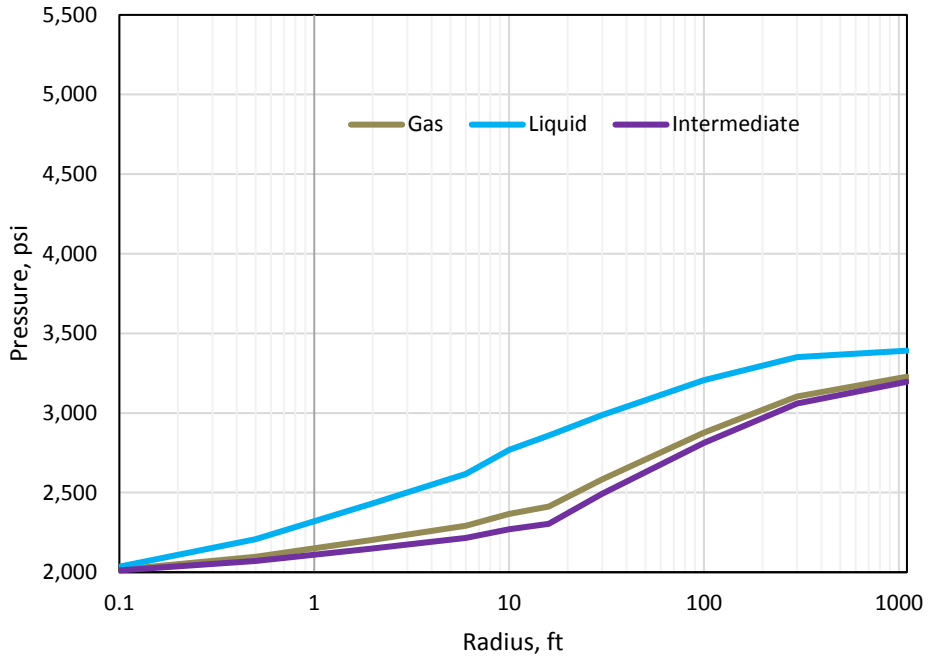

Figure 36. Pressure as a function of radial distance from wellbore for 100 md case of intermediate fluid composition at year 20

Just as in the saturation profiles for the rich condensate composition, the residual saturations near the wellbore in **Figs. 37-39** follow the predictable pattern of the liquid-wetting case having the highest and the gas-wetting having the lowest. One important point to note is that, while these values are fairly close to their values in the rich cases, they are not exactly the same. This is likely because, though the saturations are a function of the relative permeability curves, the velocity of the fluid near the wellbore has a variable ability to draw the saturation closer to the irreducible value. However, since this velocity is a function of the production rates, which were chosen fairly arbitrarily, they cannot be directly compared from one fluid type to another. We also see, in Fig. 38 for example, that the intermediate-wetting case has a much wider condensate bank than the

other two cases. This is a qualitative way of comparing the relative production improvement garnered from the treatment.

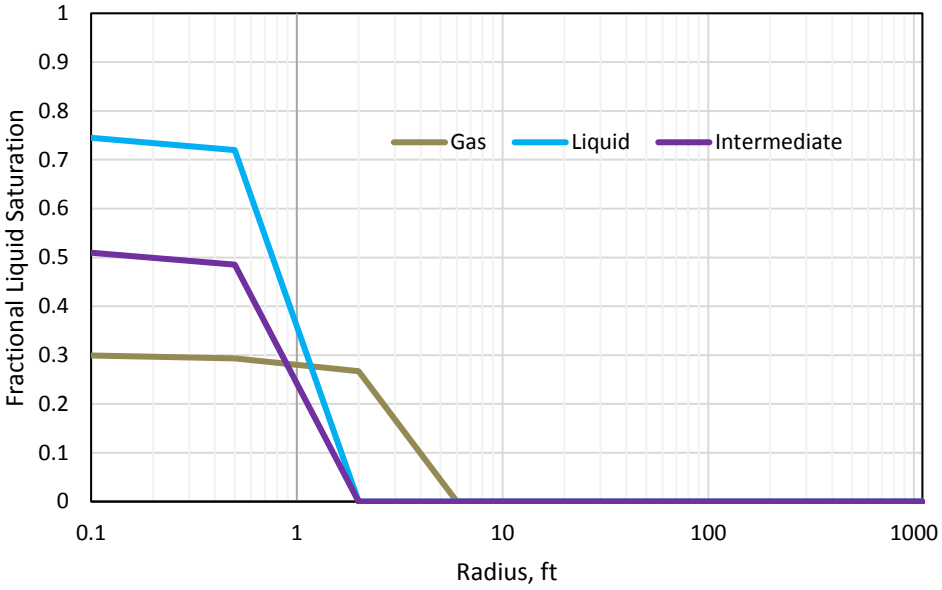

Figure 37. Liquid saturation as a function of radial distance from wellbore for 1 md case of intermediate fluid composition at year 20

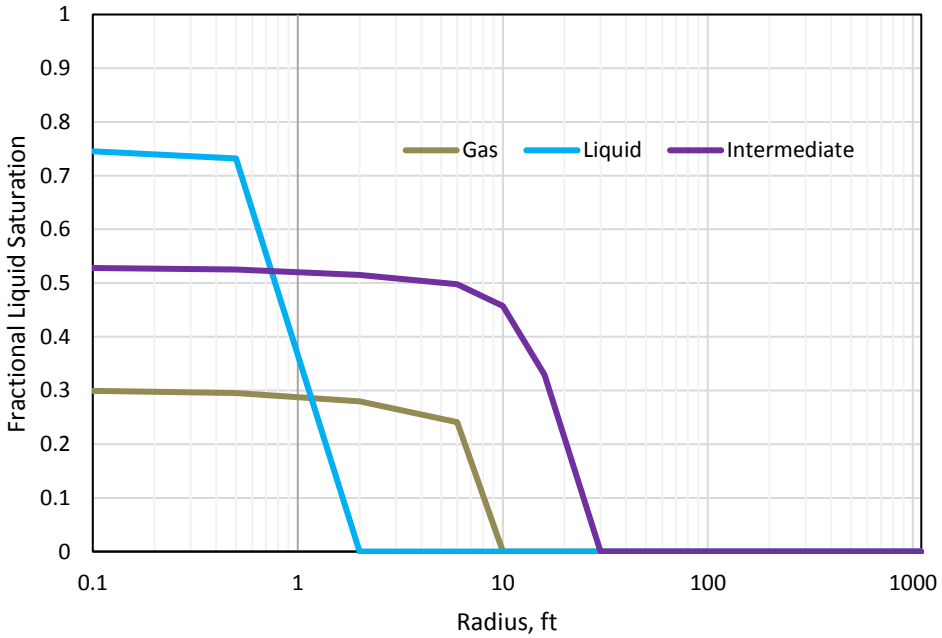

Figure 38. Liquid saturation as a function of radial distance from wellbore for 10 md case of intermediate fluid composition at year 20

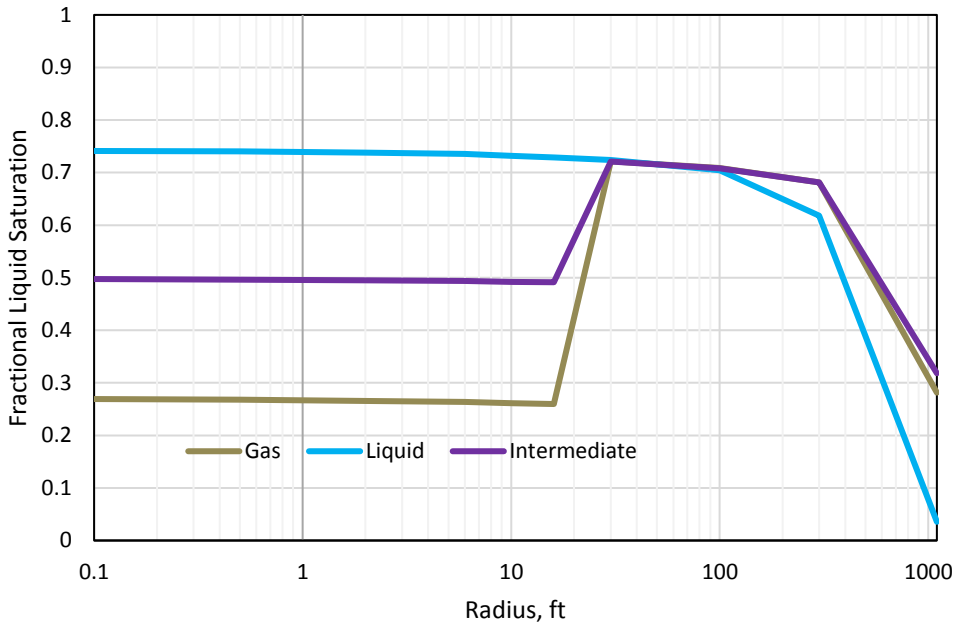

Figure 39. Liquid saturation as a function of radial distance from wellbore for 100 md case of intermediate fluid composition at year 20

4.1.3 Lean Fluid Overview

Observing the production from the lean fluid brought about the first real revelation in this study of wettability optimization. Though the intermediate-wetting scenario still seems to be the most effective method at maintaining the maximum production rate for the well, regardless of permeability, for the first time the liquid-wetting, natural case is not the least productive. The gas-wetting case actually has a lower recovery factor than the other two cases in the 1 md and 10 md cases in **Figs. 40 and 41** respectively. We can rationalize this outcome because it makes sense that a strong gas-wetting treatment would hinder the production of a very lean condensate fluid. This fact underscores the notion that it is possible to over-treat a reservoir, resulting not only in a production situation that is less favorable than it would have been untouched, but the cost of such a treatment

would only exacerbate the negative economic outcome. In **Fig. 42** the gas-wetting case is only slightly more productive than the liquid-wetting case.

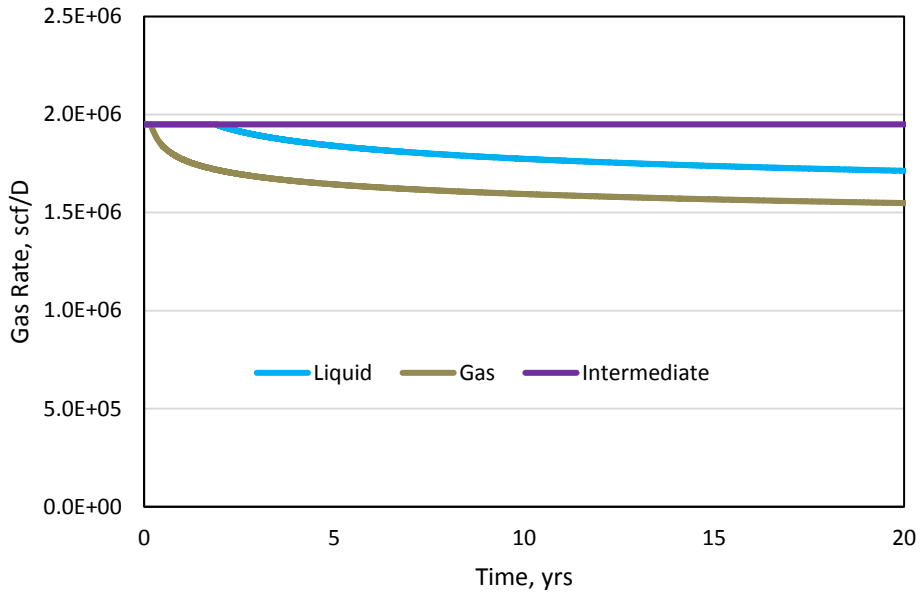

Figure 40. Gas production plot of 1 md permeability case for various wettability scenarios with lean fluid composition

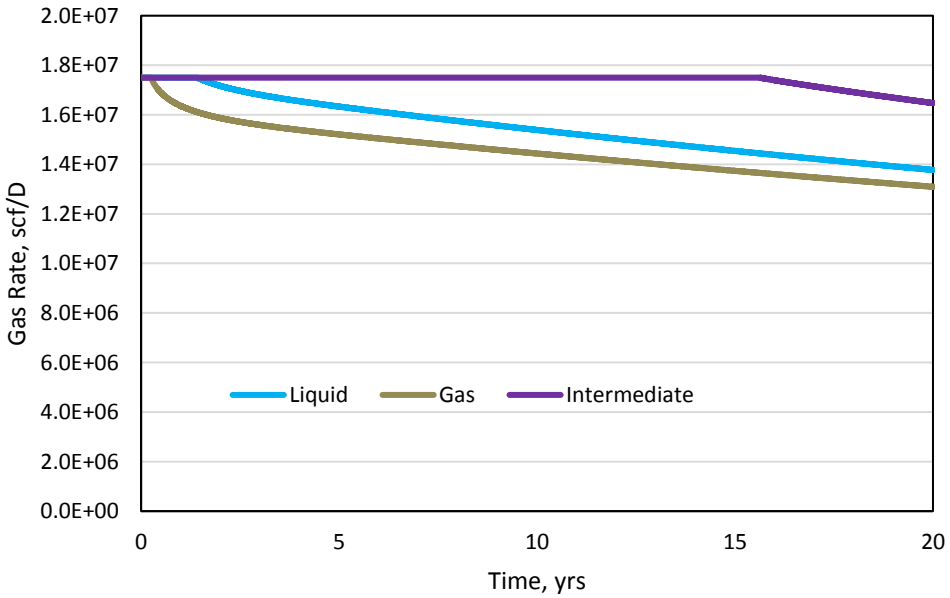

Figure 41. Gas production plot of 10 md permeability case for various wettability scenarios with lean fluid composition

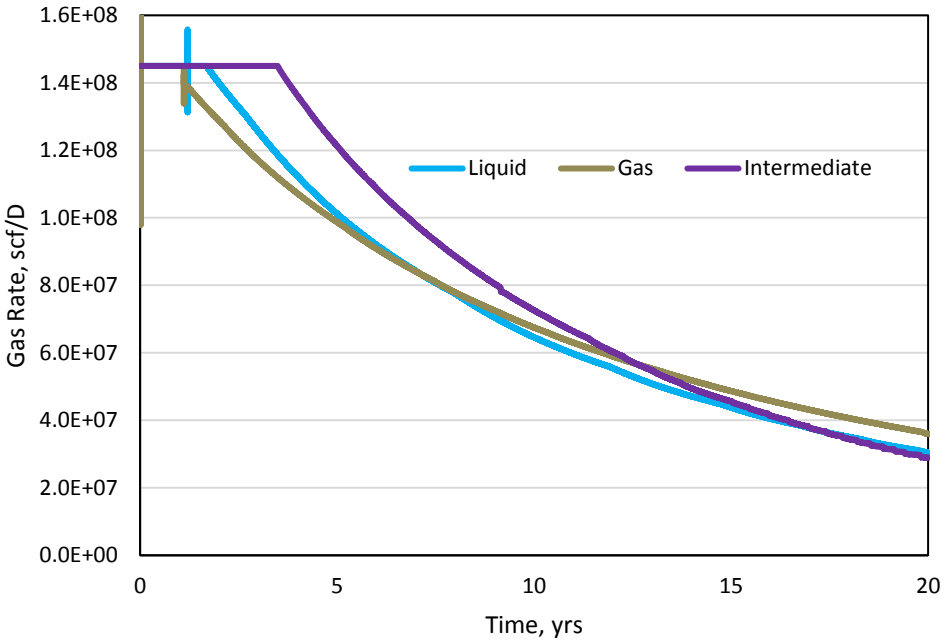

Figure 42. Gas production plot of 100 md permeability case for various wettability scenarios with lean fluid composition

The pressure profiles for the lean cases are quite similar to the other two fluid compositions when comparisons are made for like-permeability cases. We can see the relatively poorer performance of the gas-wetting case in **Figs. 43 ad 44** because the curve (olive-green) is at a higher pressure than the other two curves at distances beyond the treatment radius. Overall, we see lower pressures across the board for every permeability case of the lean composition because the lighter components of the lean fluid make it more compressible (and thus pressure-dependent) than the other two fluids types. The faster depletion of reservoir pressure may have a slight impact on the relative performance of the wettability cases because there is less reservoir energy to contribute to the production; as a lighter fluid, the lean composition might be lacking that extra assistance

that was provided by the reservoir to the other fluid types to overcome the strong gas-wettability.

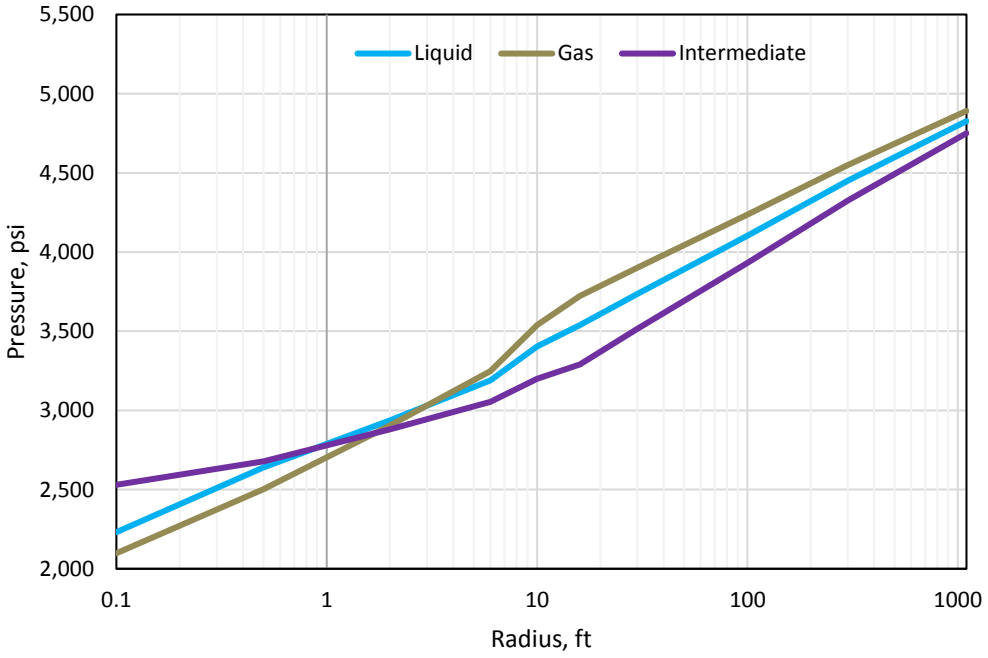

Figure 43. Pressure as a function of radial distance from wellbore for 1 md case of lean fluid composition at year 20

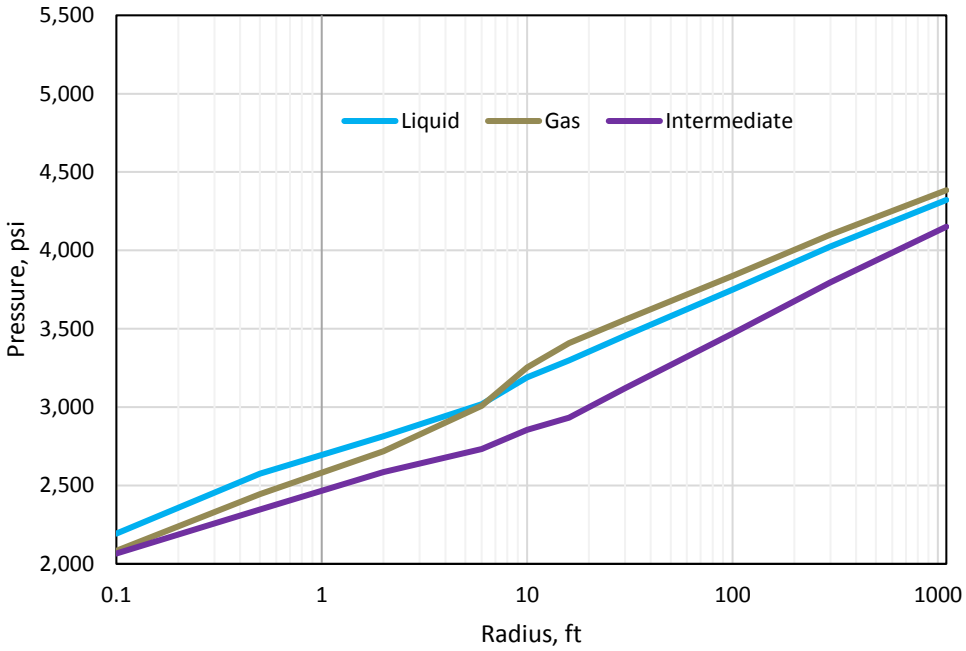

Figure 44. Pressure as a function of radial distance from wellbore for 10 md case of lean fluid composition at year 20

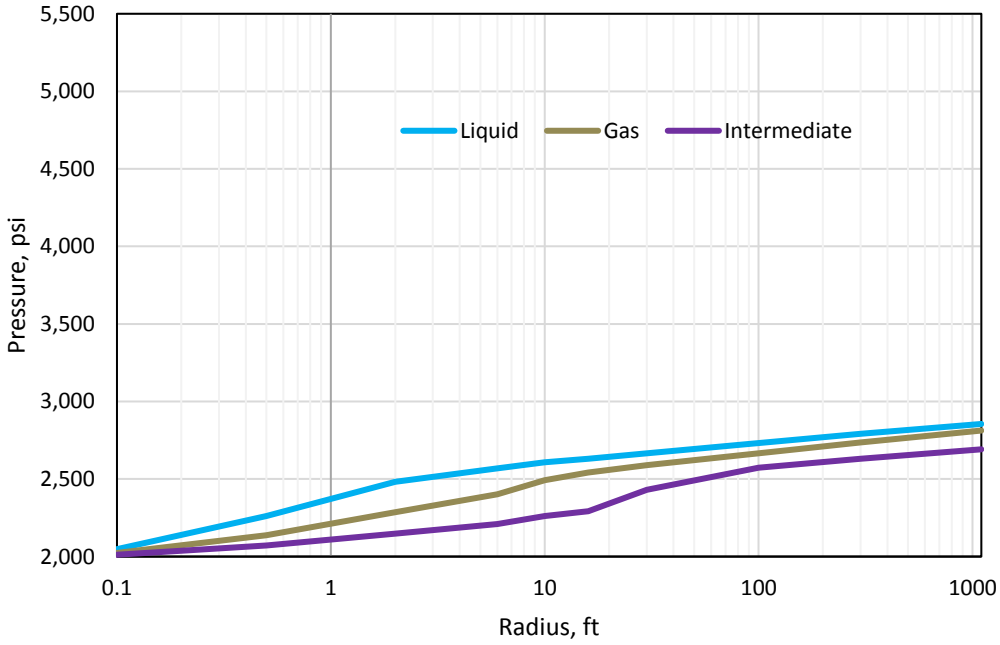

Figure 45. Pressure as a function of radial distance from wellbore for 100 md case of lean fluid composition at year 20

In terms of the saturation profiles, the first obvious point to note was the relative lack of condensate banking in the curves (**Figs. 46-48**) of the lean fluid. This lower level of blockage likely contributed to the lack of pressure drop disparity near the wellbore in Figs. 43-45. The residual saturations near the wellbore are akin to those seen in the other two fluid cases.

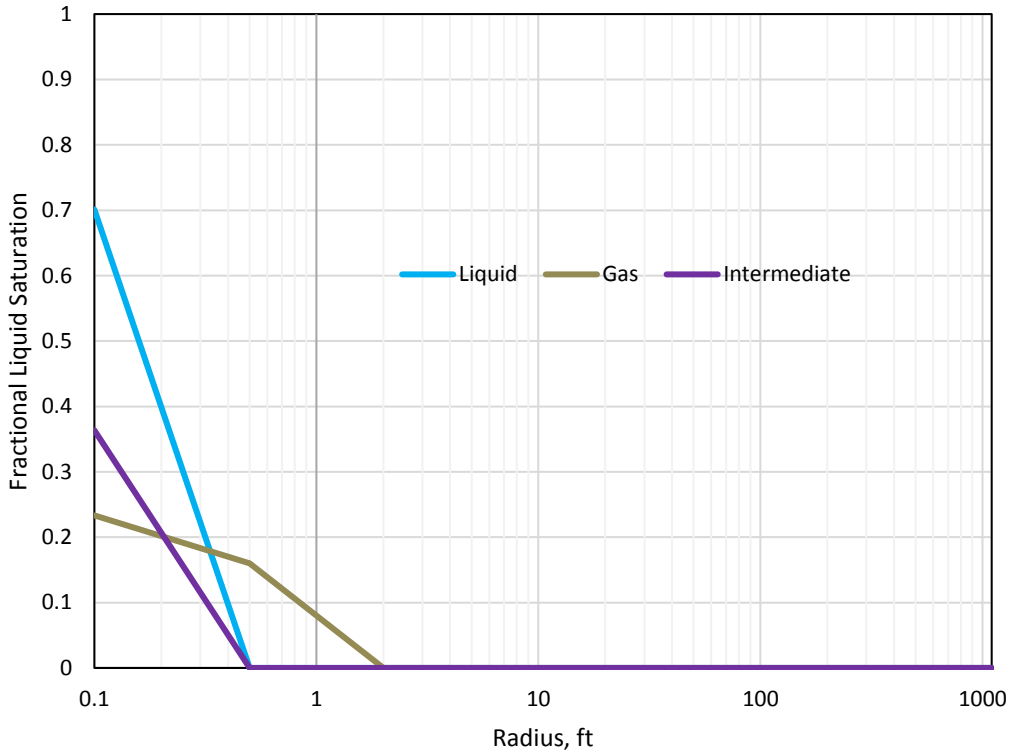

Figure 46. Liquid saturation as a function of radial distance from wellbore for 1 md case of intermediate fluid composition at year 20

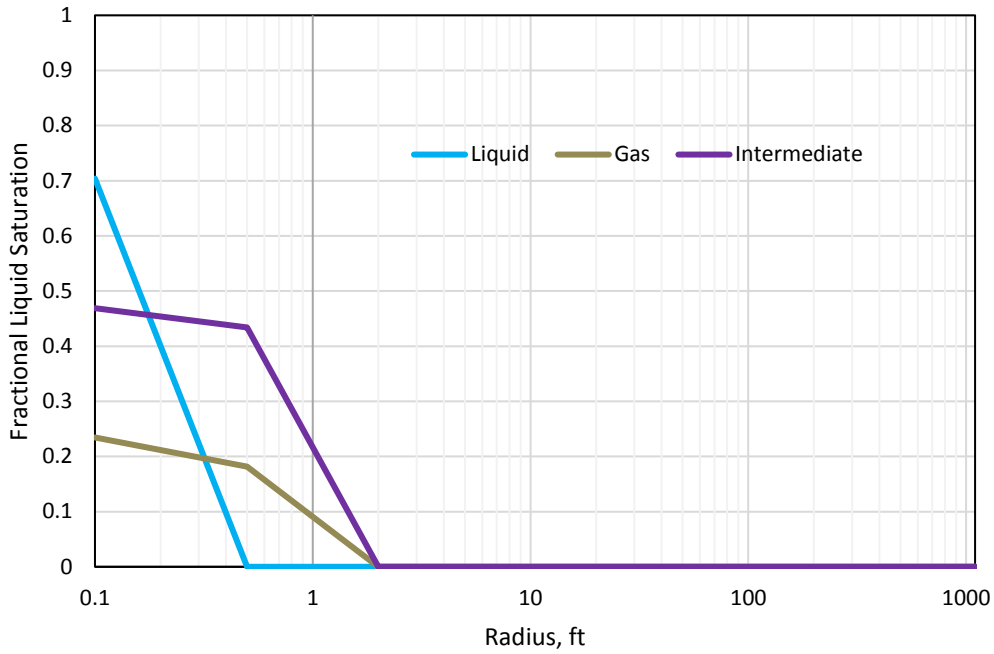

Figure 47. Liquid saturation as a function of radial distance from wellbore for 10 md case of intermediate fluid composition at year 20

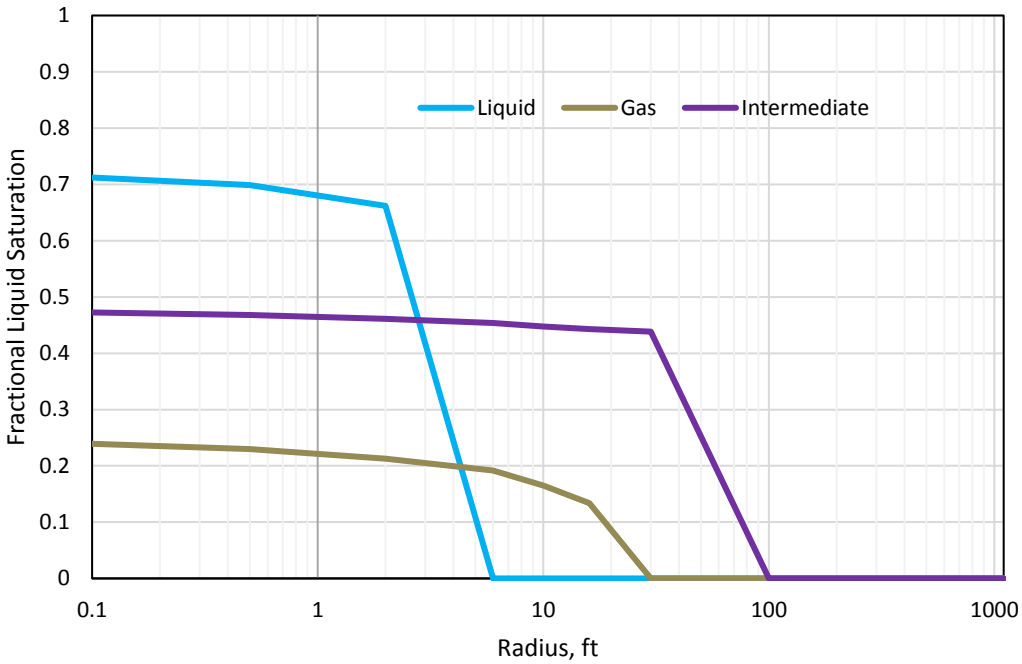

Figure 48. Liquid saturation as a function of radial distance from wellbore for 100 md case of intermediate fluid composition at year 20

4.1.4 Production Comparison of Fluid Cases

While analyzing the shapes of the production curves for the various cases is a very telling exercise, analytically comparing the production improvements across the various cases will help to determine whether or not production improvement can be predicted based on the fluid type and permeability of the system. The cases in **Figs. 49-51** are compared for like permeabilities because their cumulative production values were along the same order of magnitude. Cumulative liquid production values are included in **Figs. 62B-64B** but are not discussed further because the wells operated on a gas production constraint at relatively fixed values of GOR. This means that the intermediate fluid actually has higher liquid production than the rich fluid because the gas rate is so high as to overcome the higher GOR of the intermediate case. It is important to note however, that since many of the intermediate-wetting cases plateaued, we have no way of knowing exactly by how much the production was improved. If production were to continue until depletion or the economic limit was reached, the effect may be more or less pronounced.

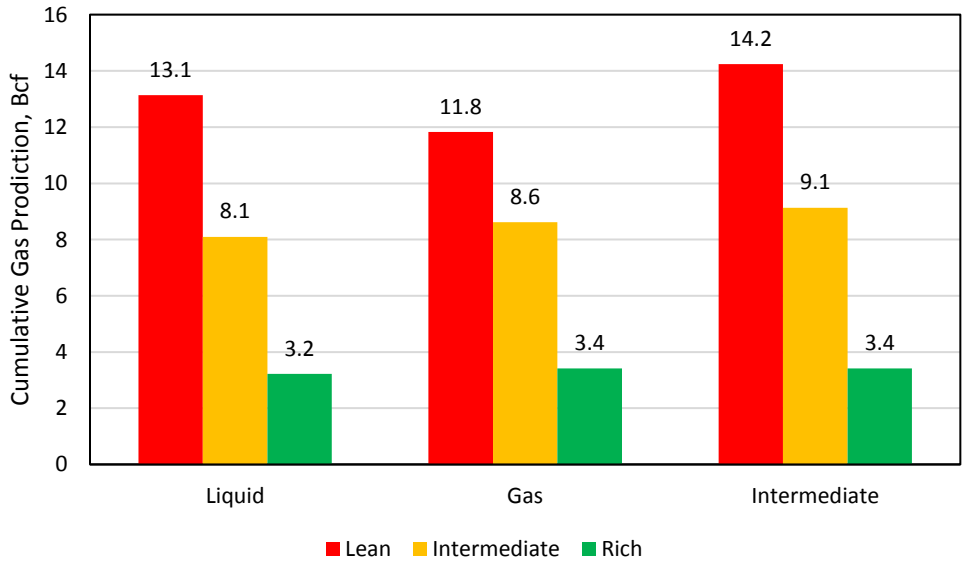

Figure 49. Comparison of 20-year cumulative gas production between fluid compositions and relative permeability curves for all 1 md permeability cases

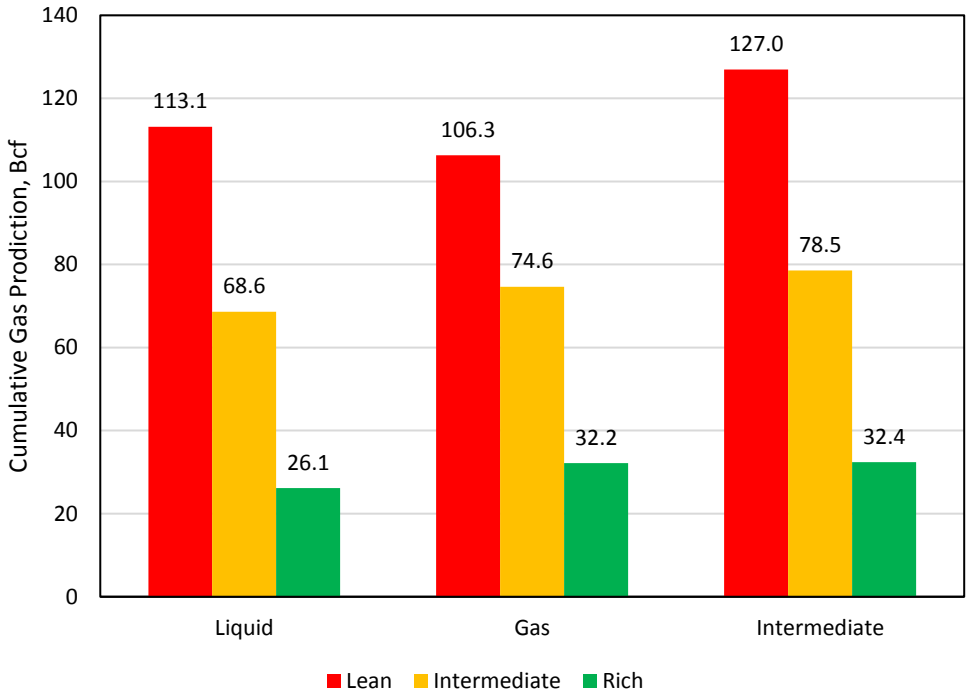

Figure 50. Comparison of 20-year cumulative gas production between fluid compositions and relative permeability curves for all 10 md permeability cases

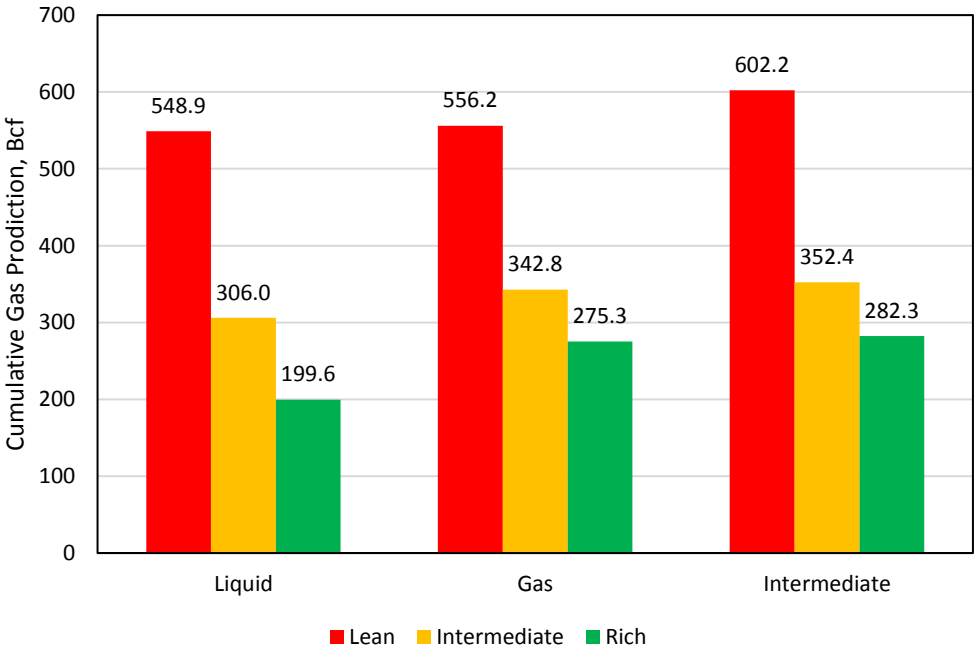

Figure 51. Comparison of 20-year cumulative gas production between fluid compositions and relative permeability curves for all 100 md permeability cases

Table 3. Percentage of gas production improvement of wettability treatments over liquid-wetting base cases

Permeability	Fluid Type	
	Lean Fluid	
	Gas-Wetting Improvement, %	Intermediate-Wetting Improvement, %
1 md	-9.94	8.46
10 md	-6.03	12.24
100 md	1.32	9.71
Mean	-4.89	10.14
	Rich Fluid	
	Gas-Wetting Improvement, %	Intermediate-Wetting Improvement, %
1 md	6.23	6.23
10 md	23.23	24.04
100 md	37.94	41.46
Mean	22.47	23.91
	Intermediate Fluid	
	Gas-Wetting Improvement, %	Intermediate-Wetting Improvement, %
1 md	6.36	12.78
10 md	8.71	14.40
100 md	12.03	15.17
Mean	9.03	14.12

Based on the data in **Table 3**, several generalizations about the outcomes of these simulation runs can be made. First, with only a few rare exceptions, the treatments are more effective in high permeability cases than in low permeability cases, with the caveat that the decline was much more gradual in the 1 md and 10 md cases, so a longer simulation run time may have resulted in proportionally more improvement at lower permeabilities. Next, we see that the proportional increase in production for both wettability cases increases as the fluid composition becomes richer. A possible explanation for this is that the pressure drops in richer fluids are greater, so the alleviation of this effect with fluorosurfactant treatments produces the best result.

4.3 The Effect of Treatment Radius

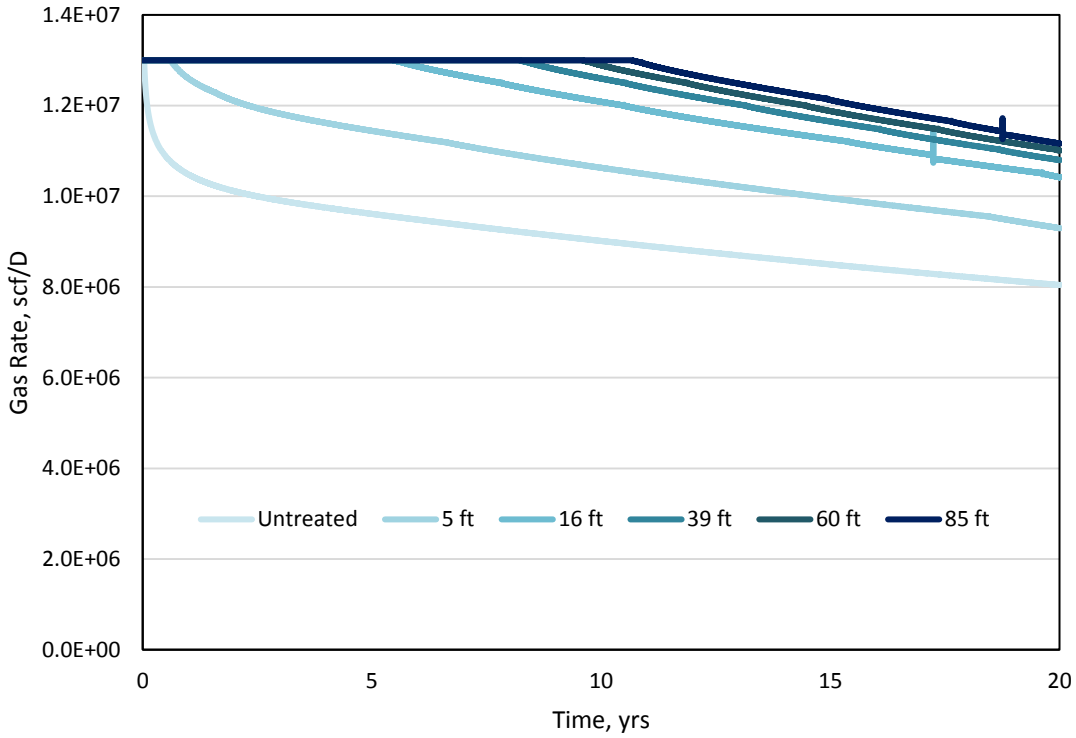

Figure 52. Impact of radius of intermediate gas-wetting treatment on intermediate fluid composition at 10 md

Determining the required volume of chemical to inject into the well in order to gain the desired wettability-altering response is at the heart of this study. It would be critical for an engineer to know whether or not a treatment zone of 16 ft will perform nearly as well as a treatment zone of 39 ft because the cost difference between the two can be astronomical. A typical treatment of this nature may vary in volume anywhere from about 500 bbls to just over 10,000 bbls (Fan et al. 2005). These volumes and several in between were converted to equivalent radii in the model using the thickness and porosity to calculate the equivalent pore volume and examine the effect of increasing the model's assumed treatment radius of 16 ft to the largest possible value obtained from literature; a 5 ft radius was also tested with the 10 md, intermediate gas-wetting,

intermediate fluid composition used as the base case. While the 5 ft radius is clearly a large improvement over the base case (18% higher cumulative production), each successive case contributes less of an increase than the one before, despite the massively large volumes required to stimulate those areas. The 16, 39, 60 and 85 ft cases only add an additional net percentage of 14, 3, 2 and 1% respectively.

This is most probably guided by the fact that the reservoir radius is so large that the cells at those distances do not fall below the dew point for a significant portion of the simulation run time. However, without a tremendous production increase between a treatment radius of 16 ft and 85 ft, the engineer has no reason to select a larger treatment volume, the cost of which would likely exceed the net production that could be gained from the expanded radius.

4.4 The Impact of Economics

While the acquisition of knowledge for the sake of knowledge is very noble and essential, researchers find that they have a hard time acquiring funds from industry if there is no practical application for the new method or theory in the office or field. For this reason, it was determined that a discussion of the potential economic superiority of the treatments should be assessed. When economics were run for the 27 primary cases discussed previously, it was quickly determined that the production values were too large to be of any real use to a practical engineer. It is simply unrealistic to imagine that one well would be left in isolation to produce a field that was nearly six miles in diameter.

Therefore, the next logical step was to restrict the reservoir radius to 2000 ft instead of 15000 ft. Instead of creating a new model to accomplish this, a sector was

simply assigned to a single grid at a radius of 2000 ft in the initial models. A permeability of zero was then applied to this cell, and the net effect was essentially a reservoir with a much smaller effective radius bounded by a "wall" of impermeable rock on the outside. The permeability for all cases was set at 10 md, and for each reservoir fluid, the three wettability cases were run, and the results differed quite distinctly from those of the essentially "infinite" reservoir radius. Because the acreage was reduced so dramatically and the run time was kept at 20 years, the ultimate, cumulative recovery for each fluid case was roughly the same for each wettability scenario as seen in **Figs. 53-55**. One might think that this would make each case equally as economically desirable as the other, but because the curvature and rate at which they reach the ultimate recovery is different for each wettability case, the scenario with the highest rate of return would the one that produces the most quickly rather than the most total. Based on Figs. 53-55, the intermediate-wetting case is actually the best at producing quickly for every fluid, and the liquid-wetting case is the worst, even for the lean fluid.

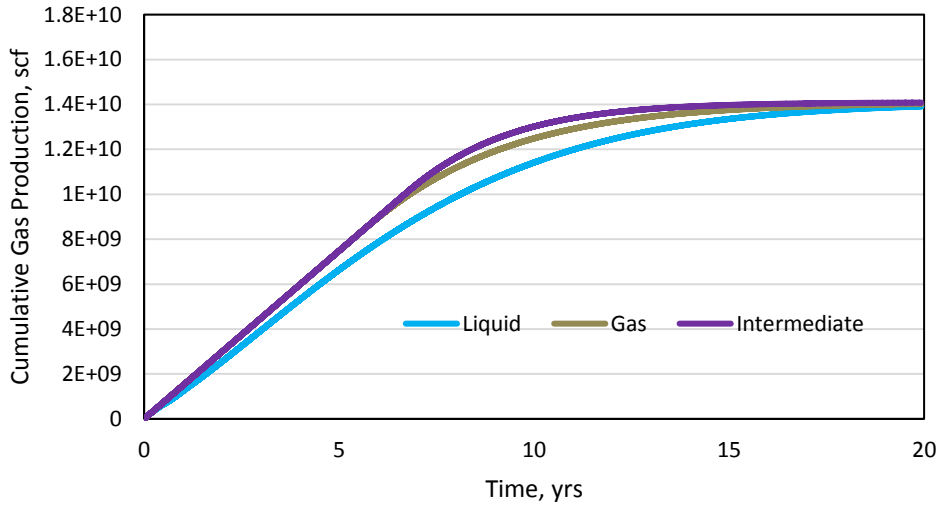

Figure 53. Cumulative gas production (G_p) curves for 10 md case of rich condensate composition

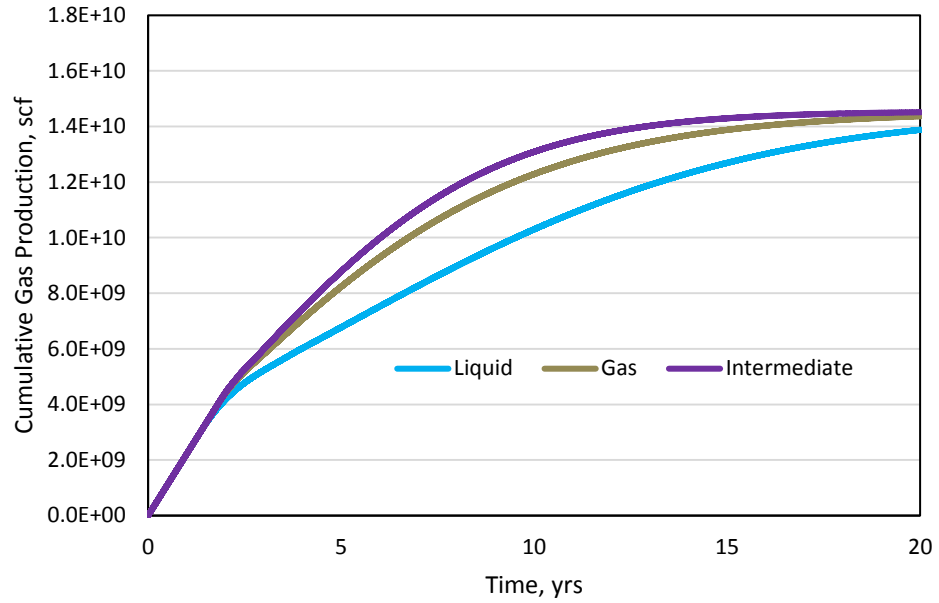

Figure 54. Cumulative gas production (G_p) curves for 10 md case of intermediate condensate composition

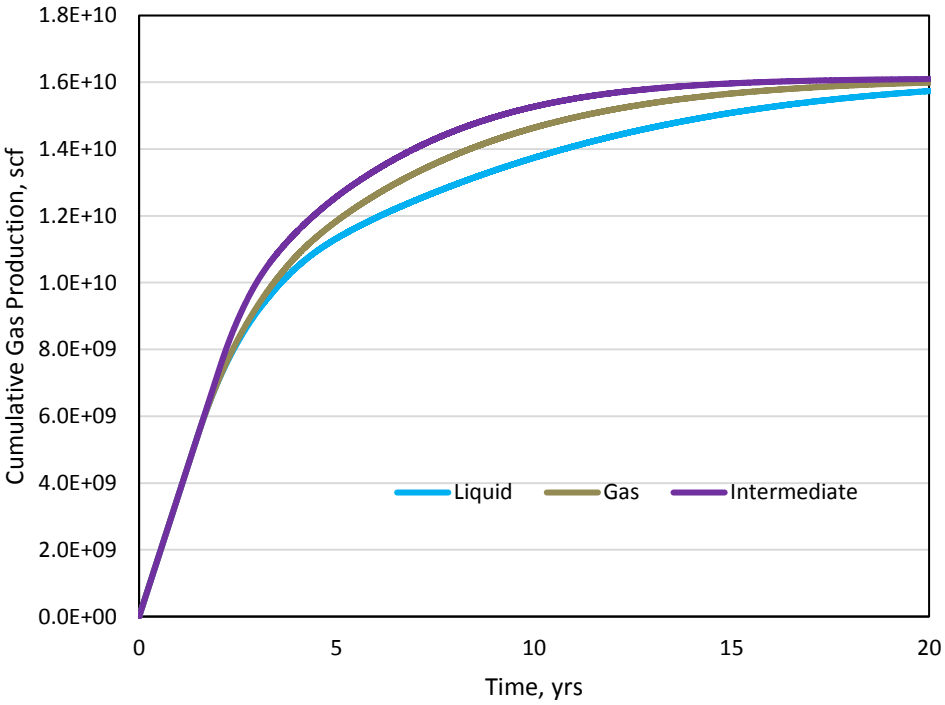

Figure 55. Cumulative gas production (G_p) curves for 10 md case of lean condensate composition

Table 4. Sample economic workflow for rich fluid case with gas-wetting treatment, 10 md permeability and reservoir radius of 2,000 ft

Yearly Gas Volume, scf	Yearly Liquid Volume, STB	Cash Flow, USD	Present Value Factor	Discounted Cash Flow, USD	Cumulative Discounted Cash Flow, USD
0	0	$(15,601,716)	1.000	$(15,601,716)	$ (15,601,716)
1,496,500	162,968	$8,563,703	0.893	$7,646,163	$(7,955,553)
1,496,500	83,505	$6,577,127	0.797	$5,243,246	$(2,712,307)
1,496,500	52,930	$5,812,753	0.712	$4,137,403	$1,425,095
1,500,600	35,399	$5,386,768	0.636	$3,423,389	$4,848,484
1,496,500	24,002	$5,089,561	0.567	$2,887,953	$7,736,437
1,482,927	16,338	$4,857,242	0.507	$2,460,830	$10,197,267
1,247,265	10,079	$3,993,781	0.452	$1,806,584	$12,003,851
973,149	6,166	$3,073,598	0.404	$1,241,375	$13,245,226
742,557	3,915	$2,325,555	0.361	$838,619	$14,083,844
561,478	2,585	$1,749,051	0.322	$563,148	$14,646,992
420,745	1,752	$1,306,030	0.287	$375,452	$15,022,444
314,017	1,214	$972,403	0.257	$249,592	$15,272,036
231,449	848	$715,540	0.229	$163,983	$15,436,019
170,257	601	$525,792	0.205	$107,587	$15,543,607
124,909	430	$385,463	0.183	$70,423	$15,614,030
91,717	310	$282,892	0.163	$46,146	$15,660,175
66,911	223	$206,312	0.146	$30,048	$ 15,690,224
48,937	162	$150,852	0.130	$19,617	$15,709,840
35,766	117	$110,233	0.116	$12,799	$15,722,639
24,270	79	$74,790	0.104	$7,753	$15,730,392

Table 4 includes the values from one of the nine cases run included in Figs. 53-55. The basic outline of the economic procedure involved: determining yearly production of liquid and gas, determining the yearly cash flow based on natural gas and liquids (NGL) prices of $3/Mcf and $25/STB respectively, calculating the present value factor for each year at an industry-standard discount rate of 12%, applying this factor to the cash flow and calculating the cumulative discounted cash flow (Midstream Business 2017).

A drilling cost of $3 million USD and monthly lease operating expense (LOE) of $7,000 USD was assumed for each well. The costs of the intermediate gas-wetting and strong gas-wetting treatments were based on the current price of ethanol (the solvent for the surfactant, which is $1.55/gal) and an assumed chemical cost of $0.50/g (Midstream Business 2017). The gas-wetting treatment was composed of 96% ethanol and 4% chemical while the intermediate treatment was 98% ethanol and 2% wettability-altering chemical. Unfortunately, based on these economic inputs, the liquid-wetting case has the highest net present value (NVP) and rate of return (ROR) of all the wettability scenarios, though the intermediate-wetting case is very close to being economically superior in the case of the rich condensate fluid. This is a regrettable illustration of the fact that an effective process determined through research may never get put into practice if the economics are unfavorable.

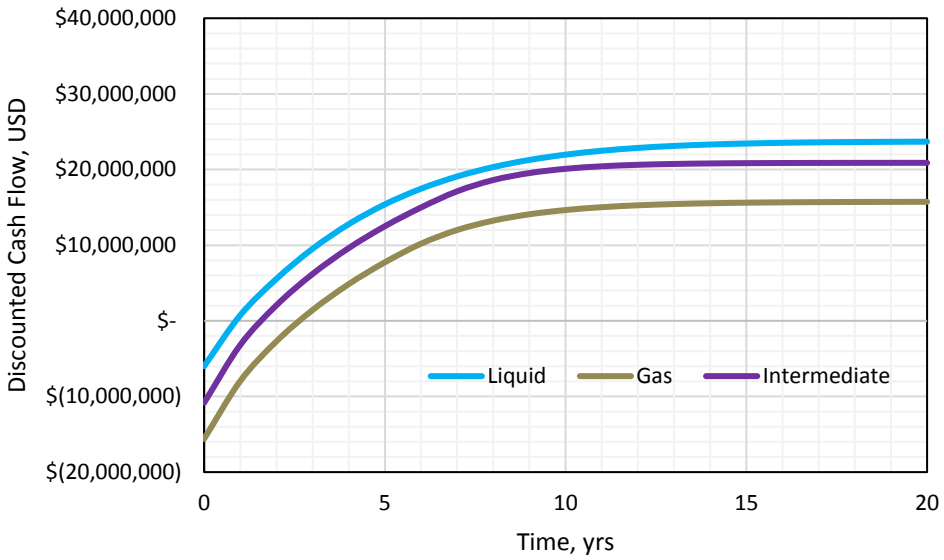

Figure 56. Cumulative discounted cash flow curves for three relative permeability cases with rich condensate fluid at 10 md

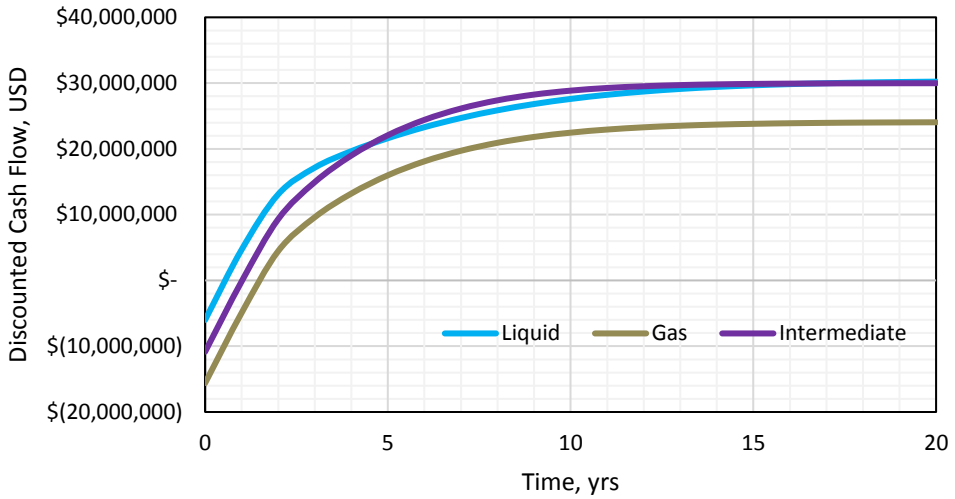

Figure 57. Cumulative discounted cash flow curves for three relative permeability cases with intermediate condensate fluid at 10 md

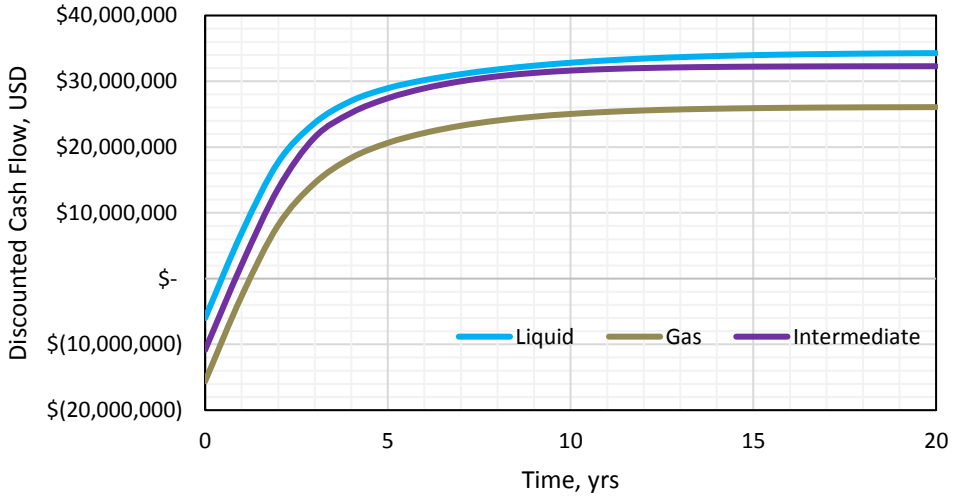

Figure 58. Cumulative discounted cash flow curves for three relative permeability cases with lean condensate fluid at 10 md

Figures 56-58 depict the cumulative discounted cash flow for each of the 9 cases according to permeability. The final point at the end of the 20-year production period represents the net present value of each case. Although the net present value of the strong gas-wetting case is still quite high in most cases, the cost of the treatment is so large that the rate of return (ROR) is quite low. Companies typically don't invest in projects where

the rate of return is below 50%, which disqualifies some of these cases from consideration. The cost of the gas-wetting and intermediate-wetting treatments came to approximately $11.6 million USD and $5.8 million USD respectively. This explains the average rates of return for the liquid-, gas-, and intermediate-wetting cases: 928%, 48% and 221% respectively. The ROR values further prove that the treatments are economically sub-optimal. In general, the lean fluid proved the most valuable of the three.

4.5 Error and Uncertainty

Although some forms of error can be eliminated from a simulation study, simply because they don't involve human error in the form of sample contamination or machine malfunction, that does not mean that the results of this study are not without their limitations. The numerical solutions determined in simulations are distinct from analytical solutions to equations in that they have no one correct value, which is why the examination of different time step sizes revealed different recoveries for the well. Assuming every input value that the engineer has incorporated into the model has at least entered-in correctly, there is still the possibility that some of those input values were obtained through inaccurate assumptions. For example, if an engineer were to input values obtained from a log interpretation into a model, there would likely be a significant source of uncertainty with the model because it is based on parameters that are impossible to verify because log measurements are indirect forms of data acquisition. For these reasons, and likely numerous more, in a business setting some sort of sensitivity analysis should be conducted to assess the possible error associated with recommendations based on simulations.

Chapter 5: Conclusions

5.1 Key Takeaways

This study was able to draw six significant conclusions from the 40+ simulation runs that were carried out on the three reservoir fluids, absolute and relative permeability scenarios, and treatment and reservoir radii. These findings may prove to be an invaluable addition to the engineering workflow of evaluating a condensate well through simulation.

1. The selection of numerical simulation parameters, such as maximum time step size, was shown to have a visual effect on the production curve but only a negligible effect on the quantitative outcome of the runs
2. Simulation results demonstrated that a state of intermediate gas-wettability is more beneficial to the production enhancement of a well than strong gas-wettability for a wide range of fluid compositions
3. The superiority of intermediate gas-wettability was also consistent with each value of absolute reservoir permeability that was examined
4. The significance of avoiding over-treatment of reservoir rock was noted in the lean fluid composition model when the strong gas-wetting case led to even lower production than the natural liquid-wetting state
5. The incremental increase in the positive production impact of a larger treatment radius was shown to diminish as the treatment radius approached the maximum treatment volume taken from literature
6. The economics at play become very important when realistic drilling and production costs and drainage areas are assumed because the natural liquid-wetting state had the highest NPV and ROR for each run

In addition to validating the results of Zoghbi et al. (2010), this simulation approach to wettability optimization has clearly resulted in several conclusions that would prove useful in the evaluation of a condensate asset and the treatment thereof. As the price of oil and chemical treatments shifts in the coming years, ideally to the convergence of a higher oil price with a lower chemical treatment cost, the cost-benefit approach utilized here will continue to be relevant.

5.2 Suggestions for Future Study

As with any research study, the outcome of gaining the answer to a sought-after question is often a series of new questions. While this work presents a thorough description and analysis of the relationship between various reservoir properties and model parameters, it is not all-encompassing. The subject of retrograde production optimization through wettability alteration would benefit from the scrutiny of several other properties summarized in the following paragraphs.

A lack of any water saturation in the reservoir was a significant design choice in this study. It is rare to find a reservoir with low water content, let alone the absence of water altogether, therefore it would be beneficial to run multiple cases for the initial and connate water saturations of the reservoir in any future modeling work on this subject. In addition to providing a sounder and more realistic scenario, the significant cost of processing the produced water could be factored into the overall net present value. In a business with characteristically narrow margins, this added cost would be crucial to the execution of a stimulation treatment.

For a single-well model of a vertical wellbore, a radial grid is generally the most appropriate choice, but depending on the permeability of the formation, a horizontal well and Cartesian grid may be essential to the economics of a development strategy. This theme is closely tied to geography as domestic plays can be quite tight, requiring the added surface area of a horizontal well, while the high permeability of the Middle East would not require such an expense, meaning a vertical well would suffice. Given the abundance of horizontal well designs in the United States, it would be valuable to assess the impact of different wettability treatments on the radically different geometry of a horizontal well.

The lack of smoothness exhibited in some of the graphical trends presented in this study, particularly those of the rich condensate composition, suggest that a finer grid might provide a more accurate depiction of the actual production depletion curves. The selection of the proper grid size must be balanced between the need for thrift and efficiency and the desire for reliable forecasting. Though the grid in this study was intentionally kept constant to match Zoghbi et al. (2010), a more precise picture of production improvement in rich condensates may be obtained from the use of a finer grid.

Lastly, with the introduction of several more fluid compositions ranging from intermediate-lean to intermediate-rich, a more holistic conclusion on the effect of condensate composition on the magnitude of production improvement from permanent wettability modification might be drawn. Statistical analysis, such as principal components, could then be used to determine which aspect of the fluid composition, from the ratio of methane to heptane to the critical point or yield, is the most valid predictor of performance enhancement.

References

Box, G. 1976. Science and Statistics. *Journal of the American Statistical Association* **71**(356): 791-799. http://links.jstor.org/sici?sici=0162-1459%28197612%2971%3A356%3C791%3ASAS%3E2.0.CO%3B2-W.

Corey, A.T. 1954. The Interrelation Between Gas and Oil Relative Permeabilities. Producers Monthly. 19 (November): 38–41. http://www.discovery-group.com/pdfs/Corey_1954.pdf.

Coskuner, G. 1999. Performance Prediction in Gas Condensate Reservoirs. *J Can Pet Technol* **38**(08): 32-36. PETSOC-99-08-DA. https://doi.org/10.2118/99-08-DA.

Delavarmoghaddam, A., Mirhaj, S. A., and Zitha, P. L. J. 2009. Gas Condensate Productivity Improvement by Chemical Wettability Alteration. Presented at the 8th European Formation Damage Conference, Scheveningen, The Netherlands, 27-29 May. SPE-122225-MS. https://doi.org/10.2118/122225-MS.

EIA. 2010. Published by Shale Gas International. EIA Releases new Eagle Ford Shale Maps. (Accessed 2017). http://www.shalegas.international/2015/01/26/eia-releases-new-eagle-ford-shale-maps/.

Egypt Data Portal. 2017. Natural Gas Prices Forecast: Long Term 2017 to 2030. (Accessed 2017). Sponsored by the African Development Bank. http://egypt.opendataforafrica.org/ncszerf/natural-gas-prices-forecast-long-term-2017-to-2030-data-and-charts.

Fahes, M. M., and Firoozabadi, A. 2007. Wettability Alteration to Intermediate Gas-Wetting in Gas-Condensate Reservoirs at High Temperatures. *SPE J.* **12**(04): 397-407. SPE-96184-PA. https://doi.org/10.2118/96184-PA.

Fahimpour, J., Jamiolahmady, M., Sohrabi, M., and Mills, J. 2013. Dependency of Wettability Alteration on Hydrocarbon Composition and Interfacial Tension in Gas/Condensate Systems. Presented at the EAGE Annual Conference & Exhibition, London, UK, 10-13 June. SPE-164802-MS. https://doi.org/10.2118/164802-MS.

Fahimpour, J., and Jamiolahmady, M. 2015. Optimization of Fluorinated Wettability Modifiers for Gas/Condensate Carbonate Reservoirs. *SPE J.* **20**(04): 729-742. SPE-154522-PA. https://doi.org/10.2118/154522-PA.

Fan, L., Harris, B., Jamaluddin, A., Kamath, J., Mott, R., Pope, G., Shadrygin, A., and Whitson, C. 2005. Understanding Gas-Condensate Reservoirs. *Oilfield Review* **Winter**(05/06): 14-27. https://www.slb.com/~/media/Files/resources/oilfield_review/ors05/win05/02_understanding_gas_condensate.pdf.

Ganjdanesh, R., Rezaveisi, M., Pope, G. A., and Sepehrnoori, K. 2016. Treatment of Condensate and Water Blocks in Hydraulic-Fractured Shale-Gas/Condensate Reservoirs. *SPE J.* **21**(02): 665-674. SPE-175145-PA. https://doi.org/10.2118/175145-PA.

Gilani, S. F. H., Sharma, M. M., Torres, D. E., Ahmadi, M., Pope, G., and Linnemeyer, H. 2011. Correlating Wettability Alteration with Changes in Gas Relative Permeability in Gas Condensate/ Volatile Oil Reservoirs. Presented at the SPE International Symposium on Oilfield Chemistry, The Woodlands, TX, USA, 11-13 April. SPE-141419-MS. https://doi.org/10.2118/141419-MS.

Hamoodi, A., Abed, A.F., and Firoozabadi, A. 2001. Compositional Modelling of Two-Phase Hydrocarbon Reservoirs. *J Can Pet Technol* **40**(04): 49-60. PETSOC-01-04-03. https://doi-org.ezproxy.lib.ou.edu/10.2118/01-04-03.

IHS Inc. 2014. Flowing Material Balance (FMB) Analysis Theory. (Accessed 2016) http://www.fekete.com/SAN/WebHelp/FeketeHarmony/Harmony_WebHelp/Content/HTML_Files/Reference_Material/Analysis_Method_Theory/FMB_Theory.htm

IHS Inc. 2014. Relative Permeability. (Accessed 2016). http://www.fekete.com/SAN/WebHelp/FeketeHarmony/Harmony_WebHelp/Content/HTML_Files/Reference_Material/General_Concepts/Relative_Permeability.htm

Jin, J., Wang, Y., Wang, L., Zhang, X., and Ren, J. 2016. The Influence of Gas-Wetting Nanofluid on the Liquid-Blocking Effect of Condensate Reservoir. Presented at the SPE Asia Pacific Oil & Gas Conference and Exhibition, Perth, Australia, 25-27 October. SPE-182350-MS. https://doi.org/10.2118/182350-MS.

Jahanbakhsh, A., Shahverdi, H., and Sohrabi, M. 2016. Gas/Oil Relative Permeability Normalization: Effects of Permeability, Wettability, and Interfacial Tension. *SPE Res Eval & Eng* **19**(04): 673-682. SPE-170796-PA. https://doi.org/10.2118/170796-PA.

Kamath, J. 2007. Deliverability of Gas-Condensate Reservoirs — Field Experiences and Prediction Techniques. *J Pet Technol* **59**(04): 94-99. SPE-103433-JPT. https://doi.org/10.2118/103433-JPT.

Labed, I., Oyeneyin, B., and Oluyemi, G. 2015. Hydraulic Fracture Spacing Optimisation for Shale Gas-Condensate Reservoirs Development. Presented at the SPE Offshore Europe Conference and Exhibition, Aberdeen, Scotland, UK, 8-11 September. SPE-175475. https://doi.org/10.2118/175475-MS.

McCain, W. D. 1990. *The Properties of Petroleum Fluids*, second edition. Tulsa, OK: Pennwell Books. http://civil.gisland.org/wpcontent/uploads/Properties_of_Petroleum_Fluids_2ed.pdf.

Midstream Business. 2017. Prices of Natural Gas Liquids. (Accessed 2017). Published by Hart Energy. http://www.midstreambusiness.com/prices-natural-gas-liquids.

Natural Gas Intel. 2017. U.S. NGL Prices Recovering Faster Than Crude, Report Finds. (Accessed 2017). http://www.naturalgasintel.com/articles/105667-us-ngl-prices-recovering-faster-than-crude-report-finds.

Niemstschik, G.E., Poettmann, F.H., and Thompson, R.S. 1993. Correlation for Determining Gas Condensate Composition. Presented at the SPE Gas Technology Symposium, Calgary, Alberta, Canada, 28-30 June. SPE-26183-MS. https://doi-org.ezproxy.lib.ou.edu/10.2118/26183-MS.

Nobunjenwu, A. Oboho, E. and Gumus, R. (Accessed 2016). Determination of Contact Angle from Contact Area of Liquid Droplet Spreading on Solid Substrate. Rivers State University of Science and Technology. Port Harcourt, Nigeria. http://lejpt.academicdirect.org/A10/get_htm.php?htm=029_038

Noh, M. H., and Firoozabadi, A. 2008. Effect of Wettability on High-Velocity Coefficient in Two-Phase Gas/Liquid Flow. *SPE J.* **13**(03): 298-304. SPE-102773-PA. https://doi.org/10.2118/102773-PA.

Odusina, E. O., Sondergeld, C. H., and Rai, C. S. 2011. NMR Study of Shale Wettability. Presented at the Canadian Unconventional Resources Conference, Calgary, Alberta, Canada, 15-17 November. SPE-147371-MS. https://doi.org/10.2118/147371-MS.

Rahimzadeh, A., Bazargan, M., Darvishi, R., and Mohammadi, A. 2016. Condensate Blockage Study in Gas Condensate Reservoir. *Journal of Natural Gas Science and Engineering*. **33**(2016): 634-643. https://www.researchgate.net/publication/299410809_Condensate_blockage_study_in_gas_condensate_reservoir.

Salager, J. 2002. *Surfactants: Types and Uses*, second edition. Merida, Venezuela: Universidad de Los Andes. http://www.nanoparticles.org/pdf/Salager-E300A.pdf.

Sayed, M. A., and Al-Muntasheri, G. A. 2016. Mitigation of the Effects of Condensate Banking: A Critical Review. *SPE Prod & Oper* **31**(02): 85-102. SPE-168153-PA. https://doi.org/10.2118/168153-PA.

Shell. 2015. What Is LNG and How Can We Use It? (Accessed 2017). Published by Royal Dutch Shell. http://www.shell.com/energy-and-innovation/natural-gas/liquefied-natural-gas-lng.html.

Shi, C. 2009. *Flow Behavior of Gas-Condensate Wells*. PhD dissertation, Stanford University, Stanford, California (March 2009). https://pangea.stanford.edu/ERE/pdf/pereports/PhD/Shi09.pdf.

Udosen, E. O., Ahiaba, O. O., and Aderemi, S. B. 2010. Optimization of Gas Condensate Reservoir Using Compositional Reservoir Simulator. Presented at the Nigeria Annual International Conference and Exhibition, Tinapa, Calabar, Nigeria, 31 July – 7 August. SPE-136964-MS. https://doi.org/10.2118/136964-MS.

Zheng, Y., and Rao, D. N. 2010. Surfactant-Induced Spreading and Wettability Effects in Condensate Reservoirs. Presented at the SPE Improved Recovery Symposium, Tulsa, OK, USA, 24-28 April. SPE-129668-MS. https://doi.org/10.2118/129668-MS.

Zoghbi, B., Fahes, M. M., and Nasrabadi, H. 2010. Identifying the Optimum Wettability Conditions for the Near-Wellbore Region in Gas-Condensate Reservoirs. Presented at the Tight Gas Completions Conference, San Antonia, TX, USA, 2-3 November. SPE-134966-MS. https://doi.org/10.2118/134966-MS.

Appendix A: Tables

Table 5A. Relative permeability curve values for each wettability case

Strong Liquid-Wetting			Strong Gas-Wetting			Intermediate Gas-Wetting		
So	**krg**	**kro**	**So**	**krg**	**kro**	**So**	**krg**	**kro**
0.5	0.3	0	**0.1**	0.2	0	**0.3**	0.5	0
0.5160	0.2709	0.0000	**0.1159**	0.1880	0.0004	**0.3161**	0.4606	0.0004
0.5320	0.2436	0.0000	**0.1317**	0.1765	0.0015	**0.3323**	0.4232	0.0017
0.5480	0.2179	0.0000	**0.1476**	0.1654	0.0035	**0.3484**	0.3877	0.0037
0.5640	0.1940	0.0001	**0.1634**	0.1547	0.0062	**0.3645**	0.3540	0.0067
0.5800	0.1717	0.0002	**0.1793**	0.1445	0.0097	**0.3806**	0.3221	0.0104
0.5960	0.1511	0.0005	**0.1951**	0.1347	0.0139	**0.3968**	0.2920	0.0150
0.6120	0.1320	0.0009	**0.2110**	0.1252	0.0189	**0.4129**	0.2637	0.0204
0.6280	0.1144	0.0016	**0.2268**	0.1162	0.0247	**0.4290**	0.2371	0.0266
0.6440	0.0983	0.0025	**0.2427**	0.1076	0.0313	**0.4452**	0.2121	0.0337
0.6600	0.0837	0.0038	**0.2585**	0.0994	0.0387	**0.4613**	0.1888	0.0416
0.6760	0.0704	0.0056	**0.2744**	0.0916	0.0468	**0.4774**	0.1672	0.0504
0.6920	0.0585	0.0080	**0.2902**	0.0842	0.0557	**0.4935**	0.1470	0.0599
0.7080	0.0479	0.0110	**0.3061**	0.0771	0.0653	**0.5097**	0.1285	0.0703
0.7240	0.0385	0.0148	**0.3220**	0.0704	0.0758	**0.5258**	0.1113	0.0816
0.7400	0.0304	0.0194	**0.3378**	0.0640	0.0870	**0.5419**	0.0957	0.0937
0.7560	0.0233	0.0252	**0.3537**	0.0581	0.0990	**0.5581**	0.0814	0.1066
0.7720	0.0174	0.0321	**0.3695**	0.0524	0.1117	**0.5742**	0.0685	0.1203
0.7880	0.0124	0.0403	**0.3854**	0.0471	0.1253	**0.5903**	0.0569	0.1349
0.8040	0.0085	0.0500	**0.4012**	0.0422	0.1396	**0.6065**	0.0466	0.1503
0.8200	0.0054	0.0614	**0.4171**	0.0376	0.1547	**0.6226**	0.0375	0.1665
0.8360	0.0031	0.0747	**0.4329**	0.0332	0.1705	**0.6387**	0.0296	0.1836
0.8520	0.0015	0.0900	**0.4488**	0.0292	0.1872	**0.6548**	0.0227	0.2015
0.8680	0.0005	0.1075	**0.4646**	0.0255	0.2046	**0.6710**	0.0169	0.2202
0.8840	0.0001	0.1274	**0.4805**	0.0221	0.2227	**0.6871**	0.0121	0.2398
0.9	0	0.15	**0.4963**	0.0190	0.2417	**0.7032**	0.0082	0.2601
			0.5122	0.0162	0.2614	**0.7194**	0.0052	0.2814
			0.5280	0.0136	0.2819	**0.7355**	0.0030	0.3034
			0.5439	0.0113	0.3032	**0.7516**	0.0015	0.3263
			0.5598	0.0093	0.3252	**0.7677**	0.0005	0.3501
			0.5756	0.0075	0.3480	**0.7839**	0.0001	0.3746
			0.5915	0.0059	0.3716	**0.8**	0	0.4
			0.6073	0.0045	0.3960			
			0.6232	0.0034	0.4211			
			0.6390	0.0024	0.4470			
			0.6549	0.0016	0.4737			
			0.6707	0.0010	0.5011			
			0.6866	0.0006	0.5294			
			0.7024	0.0003	0.5584			
			0.7183	0.0001	0.5881			
			0.7341	0.0000	0.6187			
			0.75	0	0.65			

Table 6A. Fluid compositions and thermodynamic properties of components

Component	Lean Composition, wt%	Intermediate Composition, wt%	Rich Composition, wt%	Pc, atm	Tc, K
N2	1.19	1.96	1.01	33.5	126.2
CO2	1.58	1.21	1.01	72.8	304.2
C1	75.82	65.97	65.58	45.4	190.6
C2	4.85	8.69	8.90	48.2	305.4
C3	3.57	5.91	6.78	41.9	369.8
i-C4	0.96	0.00	0.00	36.0	408.1
nC4	0.93	5.17	3.28	37.5	425.2
i-C5	1.01	0.00	0.00	33.4	460.4
nC5	2.01	2.69	2.02	33.3	469.6
C6	3.53	1.81	5.89	32.5	507.5
C7+	4.54	6.59	5.52	-	-

Component	Acentric Factor	Molecular Weight, g/mol	Viscosity, cp	Specific Gravity	Parachor
N2	0.040	28.013	0.090	0.809	41.0
CO2	0.225	44.010	0.094	0.818	78.0
C1	0.008	16.043	0.099	0.300	77.0
C2	0.098	30.070	0.148	0.356	108.0
C3	0.152	44.097	0.203	0.507	150.3
i-C4	0.176	58.124	0.263	0.563	181.5
nC4	0.193	58.124	0.255	0.584	189.9
i-C5	0.227	72.151	0.306	0.625	225.0
nC5	0.251	72.151	0.304	0.631	231.5
C6	0.275	86.000	0.344	0.690	250.1

Table 7A. Properties of C7+ fraction for each fluid composition

Property	Lean Case	Intermediate Case	Rich Case
Acentric Factor	0.424	0.597	0.585
Molecular Weight, g/mol	108	217	201
Viscosity, cp	0.490	0.749	0.793
Specific Gravity	0.736	0.867	0.884
Parachor	433.845	586.200	548.945
Pc, atm	31.7	19.3	18.1
Tc, K	554.0	729.3	736.3

Appendix B: Additional Figures

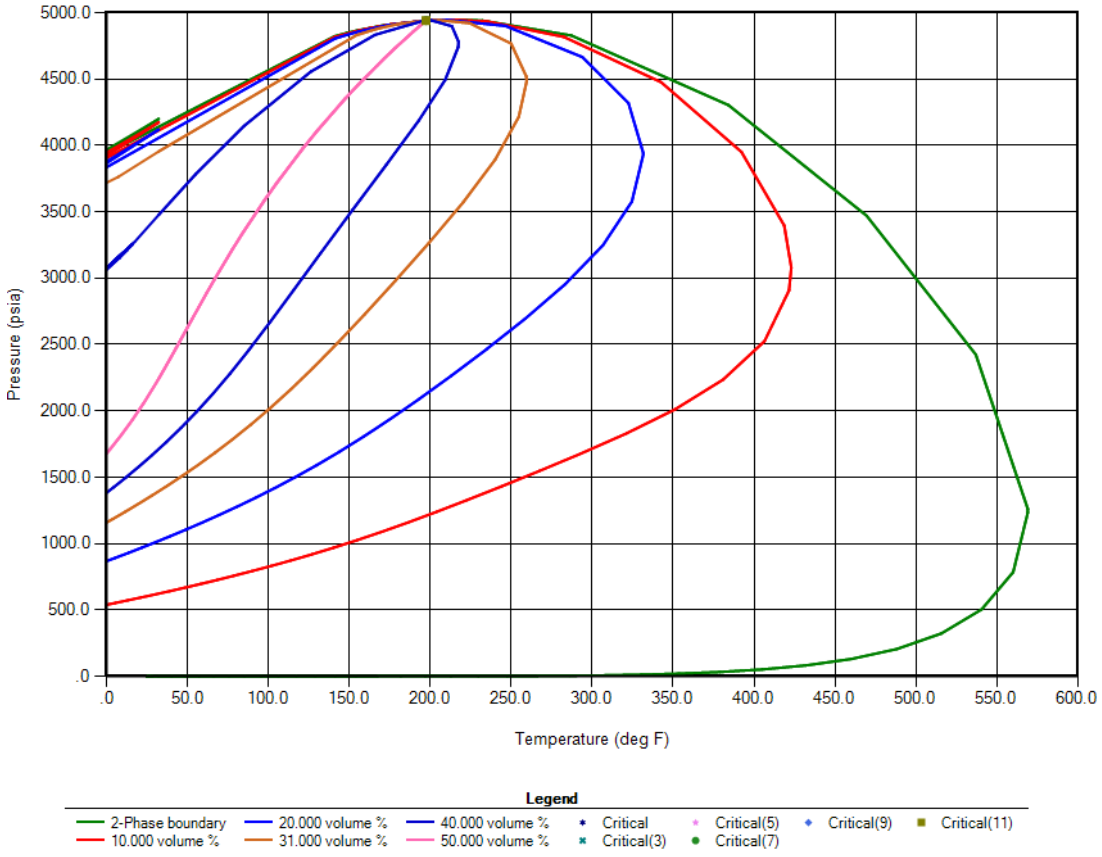

Figure 59B. Phase diagram for rich condensate composition with fractional vapor phase molar volume lines

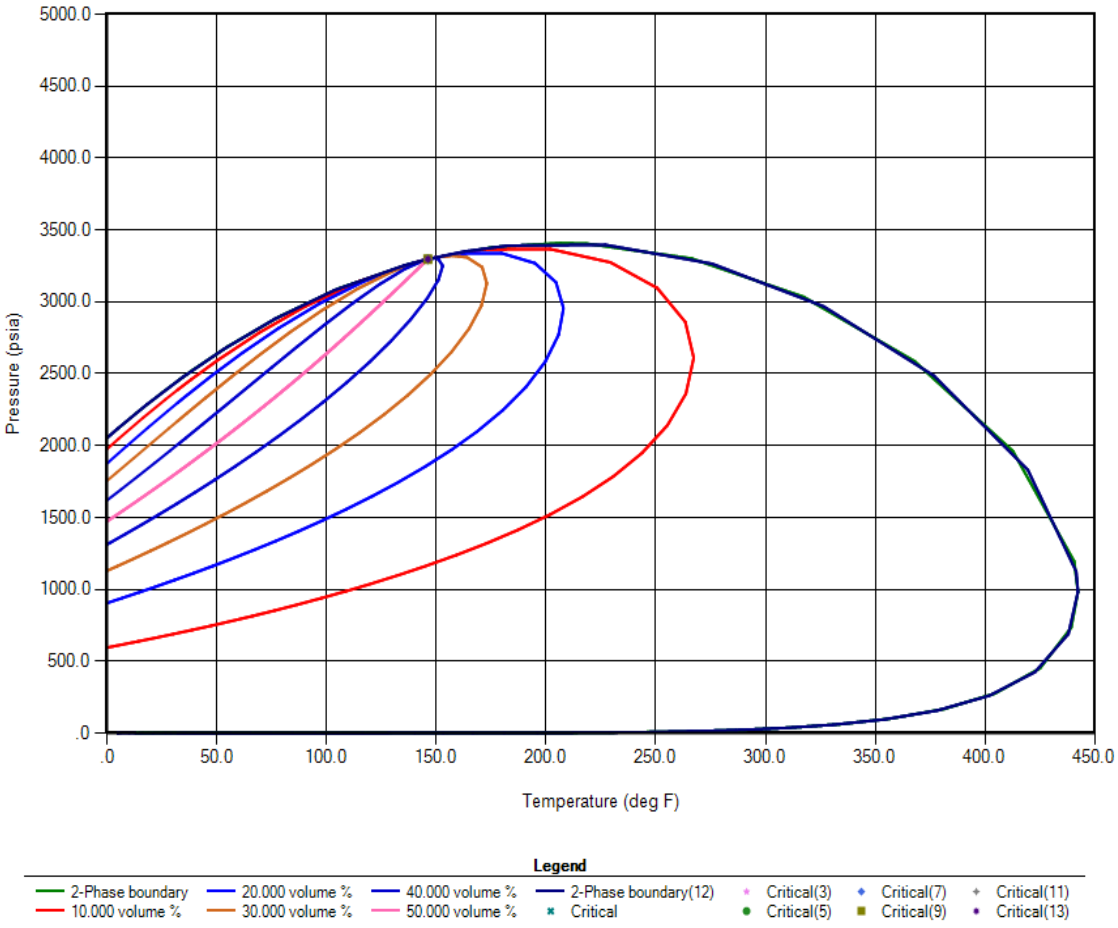

Figure 60B. Phase diagram for intermediate condensate composition with fractional vapor phase molar volume lines

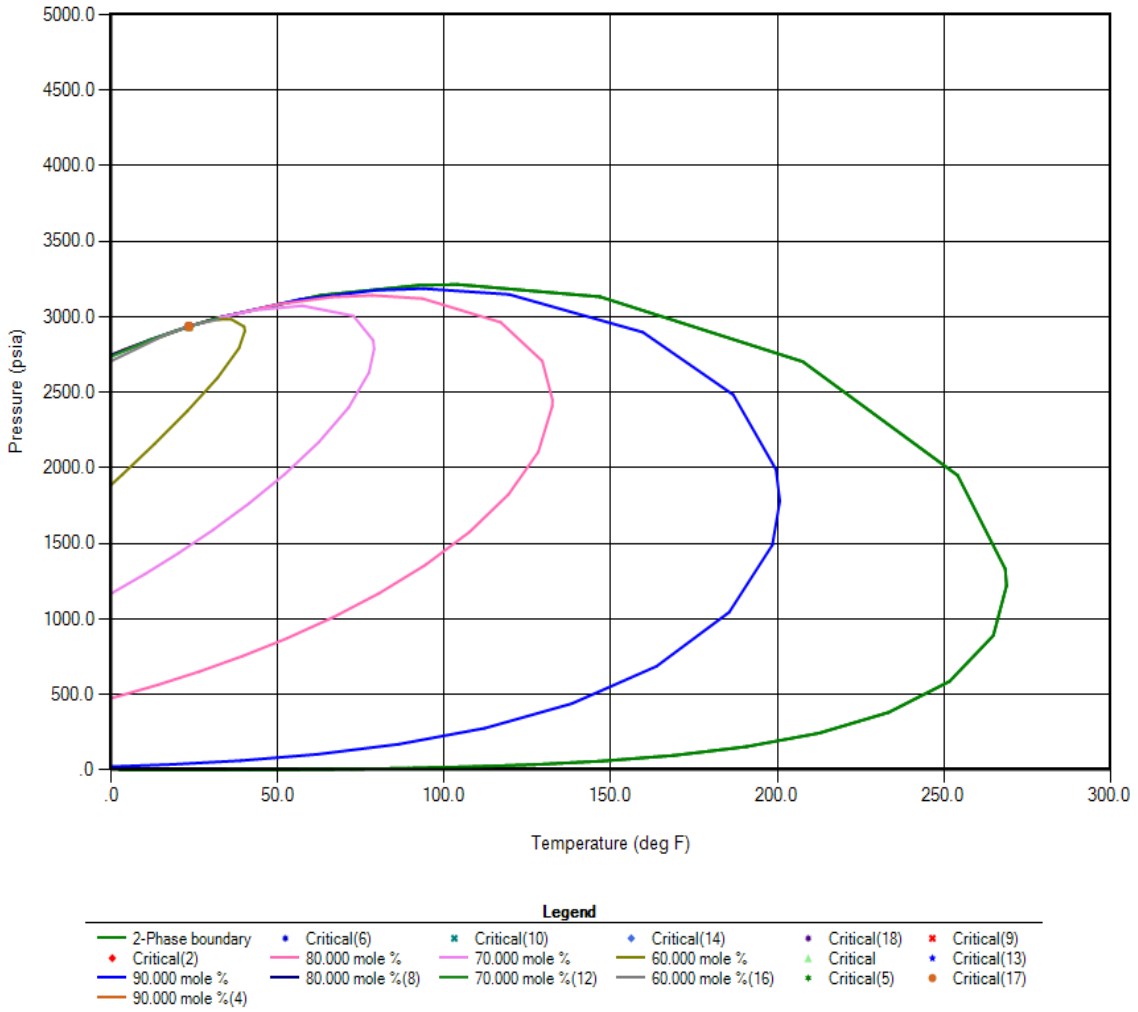

Figure 61B. Phase diagram for lean condensate composition with fractional vapor phase molar volume lines

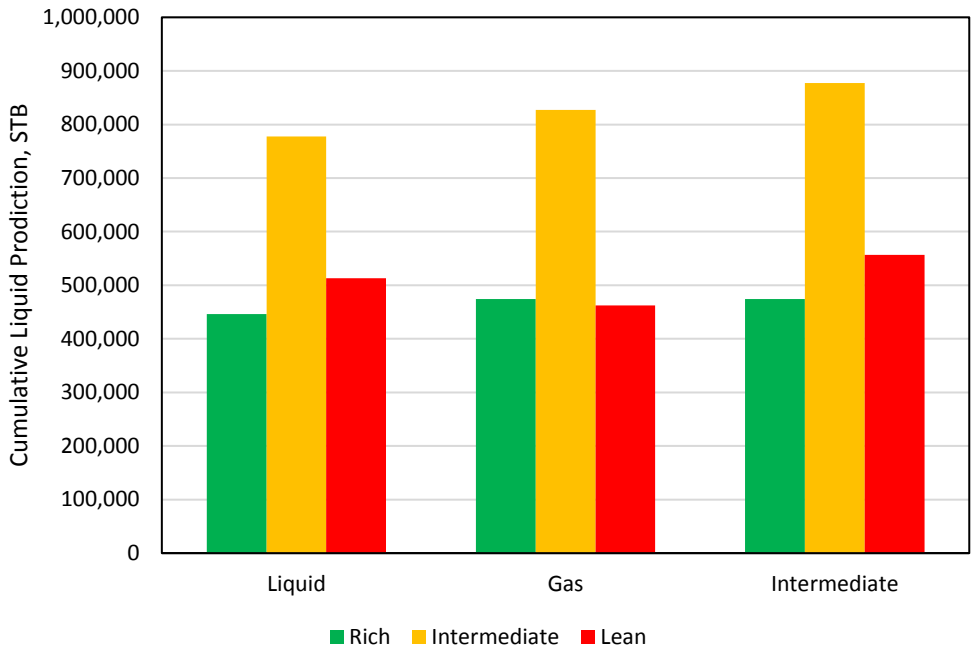

Figure 62B. Comparison of 20-year cumulative liquid production between fluid compositions and relative permeability curves for all 1 md permeability cases

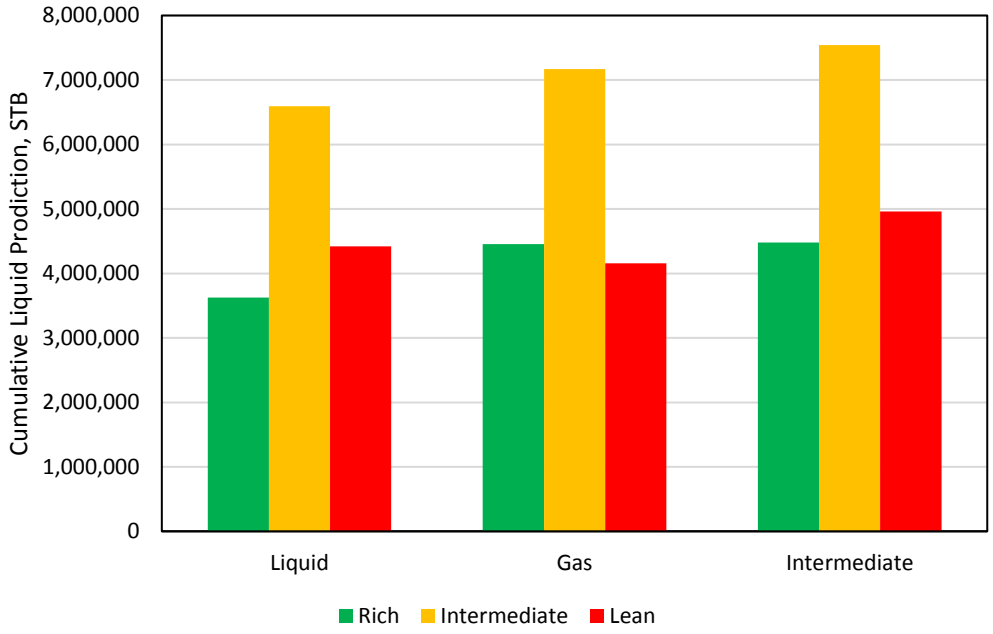

Figure 63B. Comparison of 20-year cumulative liquid production between fluid compositions and relative permeability curves for all 10 md permeability cases

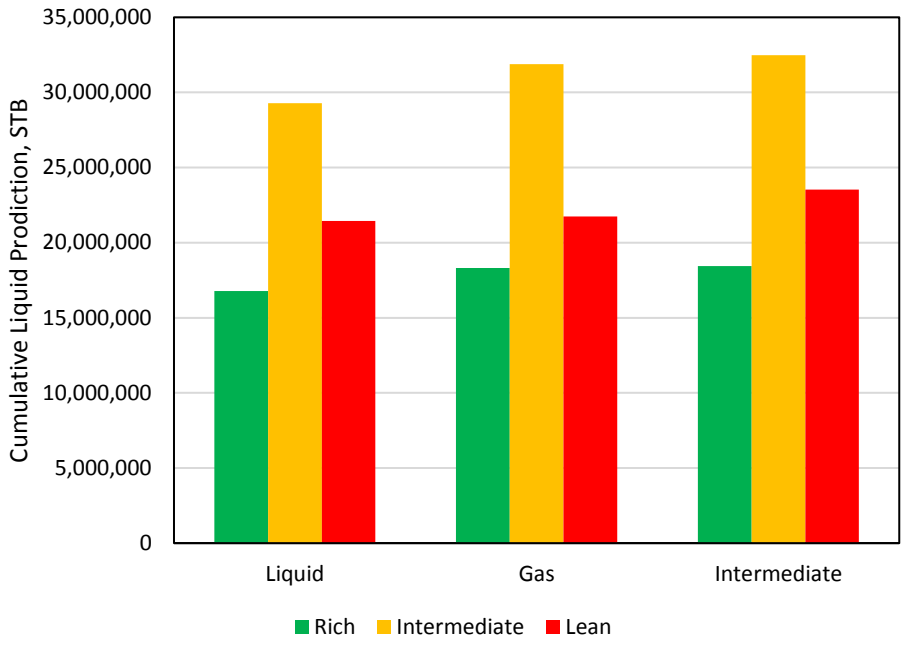

Figure 64B. Comparison of 20-year cumulative liquid production between fluid compositions and relative permeability curves for all 100 md permeability cases

Appendix C: Nomenclature

A	Cross-sectional area, cm^2
dl	Change in length, cm
dP	Change in pressure, psi
G_p	Cumulative gas production, scf or Bcf
i	Discount rate (interest rate), fraction
k	Permeability, darcy
k_{rg}	Relative permeability to gas
k_{ro}	Relative permeability to oil
N_p	Cumulative oil production, STB
n_g	Corey exponent for gas relative permeability
n_o	Corey exponent for oil relative permeability
p_{cog}	Capillary pressure, dynes
p_g	Gas phase pressure, dynes
p_o	Oil phase pressure, dynes
p_{wf}	Bottomhole flowing pressure, psia
$\bar{p}$	Average reservoir pressure, psia
r_c	Radius of capillary tube, cm
r_e	Radius of reservoir, ft
r_w	Radius of the wellbore, ft
S	Spreading coefficient, mNm^{-1}
S_g	Gas saturation

S_{cg}	Critical gas saturation
S_o	Oil saturation
S_{co}	Critical oil saturation
q	Flow rate, cm^3/s or scf/D or bbl/D
v	Velocity, cm/s
β	Two-phase high-velocity coefficient, 10^{-6} cm^{-1}
γ	Interfacial tension, dynes/cm^2
θ	Contact angle, radians
μ	Viscosity, cp

Appendix D: Abbreviations

API	American Petroleum Institute
bbl	Reservoir barrel
Bcf	Billion cubic feet
BHP	Bottomhole pressure
BLPD	Barrels of liquid per day
CCE	Constant composition expansion
CF	Cash flow
CMG	Computer Modelling Group
CVD	Constant volume depletion
D	Day
DME	Dimethyl ether
EOS	Equation of state
EtOH	Ethanol
GOR	Gas-oil ratio
IFT	Interfacial tension
LOE	Lease-operating expenses
LNG	Liquified natural gas
MeOH	Methanol
MMcf	Million cubic feet
MMSTB	Million stock tank barrels
Mcf	Thousand cubic feet

MSTB	Thousand stock tank barrels
NGL	Natural gas liquids
NMR	Nuclear magnetic resonance
NPV	Net present value
OGIP	Original gas in place
OOIP	Original oil in place
PVT	Pressure-volume-temperature
PV12	Present value at discount rate of 12%
ROR	Rate of return
scf	Standard cubic feet
STB	Stock-tank barrel
TOC	Total organic content
USD	United State dollars
WAG	Water-alternating gas
WTI	West Texas Intermediate
XPS	X-ray photoelectron spectroscopy